12-2018

Positive Identification via Frontal Sinus Morphology: A Geographic Information Systems (GIS) Approach

Jenna Mackenzie Watson
University of Tennessee

To the Graduate Council:

I am submitting herewith a thesis written by Jenna Mackenzie Watson entitled "Positive Identification via Frontal Sinus Morphology: A Geographic Information Systems (GIS) Approach." I have examined the final electronic copy of this thesis for form and content and recommend that it be accepted in partial fulfillment of the requirements for the degree of Master of Arts, with a major in Anthropology.

Amy Mundorff, Major Professor

We have read this thesis and recommend its acceptance:

Lee Meadows Jantz, Michael Kenyhercz

Accepted for the Council:
Carolyn R. Hodges

Vice Provost and Dean of the Graduate School

(Original signatures are on file with official student records.)

Positive Identification via Frontal Sinus Morphology: A Geographic Information Systems (GIS) Approach

A Thesis Presented for the
Master of Arts
Degree
The University of Tennessee, Knoxville

Jenna Mackenzie Spears Watson
December 2018

ACKNOWLEDGEMENTS

I would like to thank my advisor, Dr. Amy Mundorff for her constant support, encouragement, and wisdom throughout this journey. I have been blessed with many strong women role models in my life, and I consider myself lucky to have another as an advisor and mentor in my journey through graduate school. When I think of the type of person, teacher, mentor, and anthropologist I want to be, I look to you.

For all of the faculty and staff who assisted with this research: First, thank you to my committee members Drs. Lee Meadows Jantz and Michael Kenyhercz. Dr. Jantz for her helpful comments and feedback during the development of this project. Dr. Kenyhercz for his GIS and statistics expertise, and for helping me through some initial bumps in the development of this project. His insight and knowledge were greatly appreciated and made this research possible. Thank you to Dr. Becky Kelso for welcoming me into her home and assisting me with scanning the radiographs used for this research. Thank you to Dr. Angi Christensen for her comments on my proposal. Her dissertation inspired this research and would not have been possible without the radiograph sample she compiled for her study. Finally, thank you to Dr. Xiaojuan Zhu from the Office of Information Technology for helping me with the statistics for this project. Her patience and expertise were much appreciated.

I would like to give a special thank you to Lindsey Cochran and Martin Walker for their GIS knowledge, endless patience, mentorship, and assistance in developing this project and helping me through many technical difficulties. You are both the epitome of peer mentors and will make incredible mentors and teachers in your future careers. A huge thank you to my dear friends Meg Kleeschulte, Lucia Elgerud, Derek Boyd and Melanie Beasley. Meg, I am so glad we ended up on this journey together. Your friendship and support have been a great source of

strength and comfort over the past two years. We started this journey together, inadvertently wearing the same outfit, and are finishing it together, still inadvertently wearing the same outfit. I don't mind if people continue to confuse us for the rest of our careers. Lucia, your calm, cool, and collected approach to everything is something I aspire to everyday. Thank you for your friendship, mentorship, encouragement, and support throughout this process. Derek Boyd, my Fit buddy, thank you so much for reading many drafts, and for always being a sounding board for ideas, problems, frustrations, and joys. Our runs and conversations have kept me sane, and your constant support and belief in me have been a great source of strength for me. Melanie, our many lunches and adventures to national parks have kept me sane over the past year. Thank you for all of your support, advice, guidance, and of course, great beer. Also, a huge thank you to the members of my cohort, and to all of my fellow graduate students in the department. Seeing all of the amazing work you all do, and the constant support, mentorship, and encouragement you provide is inspiring and heartening.

Thank you to my mom, dad, and my sister Megan for their life-long encouragement, support, and unwavering belief in my ability to do anything I set my mind to. Mom and dad, whether you realize it or not, the way you raised your daughters was quietly radical and revolutionary. Because of you, I did not grow up believing that who I am isn't enough, or that I had to make myself smaller to accommodate others. You never taught me I couldn't do something because of my gender or that I had to be a certain way to make you happy. I wouldn't be where I am or who I am today without you. I love you all. Finally, thank you to all of the individuals who generously donated their bodies to the Forensic Anthropology Center. Without you, this project would not have been possible.

ABSTRACT

Frontal sinus radiographs are frequently used to identify human remains. However, the method of visually comparing antemortem (AM) to postmortem (PM) cranial radiographs has been critiqued for its lack of sufficient error rates and the potential of practitioner training, experience, and education to influence results (Page, et al. 2011). In an effort to provide a more quantifiable method of frontal sinus identification, this thesis explored the use of the ArcGIS mapping software, ArcMap, and its spatial analyst tool, Similarity Search, for identifying frontal sinus matches. AM and PM cranial radiographs for 100 donors from the William M. Bass Donated Skeletal Collection and the Forensic Skeletal Collection at the University of Tennessee, Knoxville were organized into test groups containing one PM radiograph and ten AM radiographs and were uploaded into ArcMap 10.5 (ESRI 2018). Each frontal sinus was digitized using the Create Features tool, and the area and perimeter was calculated for the resulting polygons using the Calculate Geometry tool. For each test group, the Similarity Search tool was instructed to select the AM frontal sinus polygon that was most similar to the PM frontal sinus polygon based on the area and perimeter values. The percentage of correct matches by Similarity Search was calculated and statistical analyses were conducted to assess inter-observer and intra-observer variation, and to establish a threshold of similarity index values for correctly identified polygons. The results indicate that area and perimeter do not capture shape, only size. Based on these results it is concluded that for this method to be usable in forensic casework, more analyses will need to be included that provide Similarity Search with more characteristics than just area and perimeter and provide Similarity Search with information about the shape of the polygons.

TABLE OF CONTENTS

CHAPTER 1: INTRODUCTION 1
Problem Orientation 1
Research Questions 3
Chapter Organization 4
CHAPTER 2: LITERATURE REVIEW 5
Radiographic Identification Methods and GIS 5
Visual Recognition and Radiographic Image Identification Methods 5
Frontal Sinus Radiograph Comparison Methods 8
What is a GIS? 15
Application of GIS to Anthropology and Related Fields 16
Application of GIS to Skeletal Elements 17
Application of GIS to Forensic Anthropology and Crime Scene Investigation 18
CHAPTER 3: MATERIALS AND METHODS 21
Digitizing in ArcMap 21
Sample 22
Radiograph Methodology 24
Methodology Parameters, Sample Organization, and Anonymization 26
Digitizing the Frontal Sinus 28
Calculating Area and Perimeter 39
Similarity Search 44
Analysis 51
Inter-observer Variation 51
Intra-observer Variation 54
Similarity Search Accuracy 56
No True Match vs. True Match 56
Similarity Index Range for Correctly Identified Polygons 57
Each Donor to Entire Sample 58
Summary 58
CHAPTER 4: RESULTS 60
Inter-observer Variation 60
Hierarchical Cluster Analysis 60
Coefficient of Variation (C_v) and Analysis of Variance (ANOVA) 70
Descriptive Statistics and Similarity Search Results 70

Intra-observer Variation 83
Coefficient of Variation 83
Similarity Search Accuracy and Correct Identifications 93
No True Match vs. True Match 93
Similarity Search Threshold 103
Similarity Index Range for Correctly Identified Polygons 103
Each Donor to Entire Sample 103
CHAPTER 5: DISCUSSION 112
Are area and perimeter sufficient for Similarity Search identification? 112
Similarity Search: An accurate tool for identifying a frontal sinus match? 122
Overall Accuracy 122
Similarity Search: A new method for frontal sinus positive identification? 123
Inter-observer and Intra-observer Variation 124
Similarity Index Value Range 132
Additional Limitations 133
Significance and Future Directions 135
Forensic Identification and Uniqueness of Biological Characteristics 137
CHAPTER 6: CONCLUSION 139
REFERENCES CITED 142
APPENDIX 149
Appendix 1 150
Test Group Example 150
Appendix 2 153
Inter-observer Polygons 153
VITA 159

LIST OF TABLES

Table 4.1 Donors present in Cluster 1 for each observer…….....61

Table 4.2 Donors present in Cluster 2 for each observer…….....63

Table 4.3 Donors present in Cluster 3 for each observer……...64

Table 4.4 Donors present in Cluster 4 for each observer……...65

Table 4.5 Tests of Normality for area, perimeter and SIMINDEX by cluster……...66

Table 4.6 Descriptive statistics for Cluster 1……75

Table 4.7 Descriptive statistics for Cluster 2……76

Table 4.8 Descriptive statistics for Cluster 3……77

Table 4.9 Descriptive statistics for Cluster 4……78

Table 4.10 Mean, standard deviation, and C_v of area values for each donor……79

Table 4.11 Mean, standard deviation, and C_v of perimeter values for each donor……80

Table 4.12 Descriptive statistics for all observations…….....81

Table 4.13 Descriptive statistics of area, perimeter, and similarity index values for each observer……...82

Table 4.14 Observers ranked first and last by Similarity Search for each donor…….....84

Table 4.15 Coefficient of Variation of average area for female donors……85

Table 4.16 Coefficient of Variation of average perimeter for female donors……...87

Table 4.17 Coefficient of Variation of average area for male donors……...89

Table 4.18 Coefficient of Variation of average perimeter for male donors……...91

Table 4.19 Similarity ranks for true match polygons not identified as most similar by Similarity Search……...101

Table 4.20 Similarity index values of each donor's true match and match selected by Similarity Search in absence of the true match…….....102

Table 4.21 Area, perimeter, and similarity index values for all correctly identified females……104

Table 4.22 Area, perimeter, and similarity index values for all correctly identified males……105

Table. 4.23 Descriptive statistics for correctly identified male and female polygons……106

Table 4.24 Cluster 1 descriptive statistics of similarity index values for each female donor……108

Table 4.25 Cluster 1 descriptive statistics of similarity index values for each male donor……...110

LIST OF FIGURES

Figure 3.1 Simulated AM radiograph and PM radiograph……....25

Figure 3.2 Creation of shapefiles in ArcCatalog……...29

Figure 3.3 Designating each shapefile as a polygon in ArcCatalog.....30

Figure 3.4 Importing JPEG files into ArcMap……...31

Figure 3.5 Importing shapefiles into ArcMap.....32

Figure 3.6 Create Features tool……..34

Figure 3.7 Digitizing the frontal sinus…….....35

Figure 3.8 Completed frontal sinus polygon……..36

Figure 3.9 Frontal sinus polygon without the radiograph……..37

Figure 3.10 Adding new field to attribute table…….....38

Figure 3.11 Calculate Geometry tool…….40

Figure 3.12 Calculating area……..41

Figure 3.13 Calculating perimeter…….42

Figure 3.14 Final geometry calculation in attribute table……..43

Figure 3.15 Merge tool……..45

Figure 3.16 Attribute table for merged AM polygons……...46

Figure 3.17 Similarity Search tool…….....48

Figure 3.18 Polygons color coded from most similar to least similar……...49

Figure 3.19 Table of Contents displaying color codes……..50

Figure 3.20 Similarity Search results attribute table……..52

Figure 4.1 Normality plot of perimeter values for Cluster 2…….67

Figure 4.2 Normality plot of perimeter values for Cluster 3…….68

Figure 4.3 Normality plot of perimeter values for Cluster 4…….69

Figure 4.4 Normality plot of similarity index values for Cluster 1……...71

Figure 4.5 Normality plot of similarity index values for Cluster 2……...72

Figure 4.6 Normality plot of similarity index values for Cluster 3……...73

Figure 4.7 Normality plot of similarity index values for Cluster 4……...74

Figure 4.8 Distribution of area and perimeter values for donor 48a
coded by similarity rank…….....94

Figure 4.9 Distribution of area and perimeter values for donor 80a
coded by similarity rank…….....95

Figure 4.10 Distribution of area and perimeter values for donor 82a
coded by similarity rank…….....96

Figure 4.11 Distribution of area and perimeter values for donor 105a
coded by similarity rank…….....97

Figure 4.12 Distribution of area and perimeter values for donor 176a
coded by similarity rank…….....98

Figure 4.13 Distribution of area and perimeter values for donor 163a
coded by similarity rank…….....99

Figure 4.14 Distribution of area and perimeter values for donor 132a
coded by similarity rank……...100

Figure 5.1 Group 33 frontal sinus polygons……115

Figure 5.2 Group 33 Similarity Search attribute table…….116

Figure 5.3 Group 48 frontal sinus polygons……117

Figure 5.4 Group 45 frontal sinus polygons……118

Figure 5.5 Group 45 Similarity Search attribute table…….119

Figure 5.6 80a frontal sinus polygons……..126

Figure 5.7 176a frontal sinus polygons……127

Figure 5.8 132a frontal sinus polygons……128

Figure 5.9 Inter-observer polygons for donor 2a……129

Figure 5.10 Inter-observer polygons for donor 41a……130

Figure 5.11 Inter-observer polygons for donor 80a……131

CHAPTER 1: INTRODUCTION

Problem Orientation

Forensic human identification is based on unique characteristics and biological features of the human body. The rapid development of DNA sequencing technology over the past few decades has resulted in an increased reliance on it by the medicolegal community for the identification of human remains. However, DNA identification is not an option without access to sequencing technology, viable postmortem samples, or antemortem comparative samples. When DNA analysis, or other biometric methods such as fingerprints, are not available, radiographic comparison methods can be utilized. Antemortem (AM) and postmortem (PM) radiographs can be used to compare features such as AM fractures, pathologies, and the morphology of skeletal and dental elements. Individuals have been identified through AM and PM radiographic comparison of the chest (sternum, ribs, clavicles, and vertebrae), teeth and surrounding alveoli, and the maxillary and frontal sinuses (Angyal and Dérczy 1998; Derrick, et al. 2015; Kahana, et al. 2002; Mundorff, et al. 2006; Stephan, et al. 2011).

When radiographs of the skull are accessible, comparison of the frontal sinus is a feasible method for positive identification. The current method consists of comparing the PM cranial radiograph of the unidentified individual to the AM radiographs of individuals who are potential matches. While visual matching has shown to be an accurate method that is widely accepted by forensic practitioners, it has been critiqued for lacking reliable error rates and relying on a visual pattern match that can be influenced by practitioner training, experience, and education (Christensen 2005b; Page, et al. 2011). There has been extensive research testing the validity of radiographic frontal sinus identification (Da Silva, et al. 2009; Jablonski and Shum 1989; Kirk,

et al. 2002; Marlin, et al. 1991; Murphy and Gantner 1982; Ubelaker 1984). Researchers have also tested the uniqueness of the frontal sinus among individuals and developed more quantitative methods for assessing frontal sinus morphology that utilize metrics, statistical models, and mathematical methods such as Elliptic Fourier Analyses (Christensen 2003, 2005a; Cox, et al. 2009; Patil, et al. 2012; Yoshino, et al. 1987).

ArcGIS (ESRI 2018) is a tool that has yet to be utilized for frontal sinus identification. A Geographic Information System (GIS) is a database management system that allows the user to store and analyze spatial data. The program ArcGIS and its mapping program, ArcMap, allow the user to import or create maps, and conduct analyses of data with a spatial component. ArcGIS is commonly used in fields like geography, natural resource management, surveying, urban planning, and archaeology. In recent years, ArcGIS has been utilized by biological anthropologists to assess anything from spatial patterns of fossil assemblages to the spatial relationships between the presence of pathogen vectors and skeletal lesions (Benito-Calvo and De la Torre 2011; Gowland and Western 2012). Several researchers have even applied ArcGIS to skeletal elements, including teeth and the pelvis (Beckett, et al. 2014; Jernvall, et al. 2000; Ungar and Williamson 2000). These studies illustrate the potential of ArcGIS as a tool for spatially analyzing the human skeleton to address questions about human variation, human evolutionary history, and potentially aid in forensic human identification.

In this thesis, I explore the use of ArcMap to digitize the frontal sinus as a polygonal shape from radiographs and to calculate the area and perimeter of the polygon. I also test the ability of the spatial analyst tool, Similarity Search, to correctly identify frontal sinus matches based on user-defined attributes. If this method proves accurate, I suggest that ArcMap and its spatial analyst tools can provide a quantitative, user-friendly, and automated method for

identifying a frontal sinus match that can be easily implemented in forensic case work when frontal sinus radiographs are available and accessible. This method will also address the need for more quantitative identification methods in forensic anthropology.

Research Questions

The main objective of this study is to assess the use of ArcMap and its spatial analyst tool, Similarity Search, for identifying a frontal sinus match from radiographs. This objective will be achieved by answering three questions:

1. Are the area and perimeter values of a frontal sinus polygon sufficient variables for Similarity Search to be able to identify a match?
2. Can ArcMap's Similarity Search tool identify a PM to AM radiographic match using the frontal sinus polygon?
3. If ArcMap Similarity Search can match a PM to AM radiograph, is this a quantifiable and reproducible method for positive identification using radiographs?

These questions will be answered by testing the Similarity Search tool on a sample of 100 individuals from the William M. Bass Donated Skeletal Collection and the Forensic Skeletal Collection that each have two cranial radiographs. Overall accuracy of Similarity Search's ability to identify the correct match will be assessed, as well as intra- and inter-observer variation. Statistical analysis will inform the establishment of a range for the similarity index values that are produced by Similarity Search to indicate the most similar and least similar polygons. It is expected that this research will provide preliminary results for how Similarity Search can be leveraged for frontal sinus identification, and with further research can be developed into a practical, quantifiable, and user-friendly method for frontal sinus identification.

Chapter Organization

Chapter two is a literature review to place this study in context. The literature on radiographic identification methods in general, and frontal sinus radiograph identification methods in particular, will be discussed. This chapter will also explain what a GIS is and how the ArcGIS software program functions. The origins of GIS and the applications of GIS to anthropology, forensic anthropology, and the human skeleton will also be reviewed.

Chapter three is the materials and methods chapter. It discusses the study sample composition including the methodology used to obtain the cranial radiographs, and sample organization, and anonymization. Methodology for digitizing the frontal sinus in ArcMap, the calculation of area and perimeter, and function and application of the Similarity Search tool to this study are explained. Chapter three also details the statistical analyses for this study. These include inter and intra-observer variation analyses, the percentage of Similarity Search's correct identifications, and the establishment of a similarity index range.

Chapter four presents the results of the statistical analyses. Chapter five provides an interpretation and discussion of the results and their significance to forensic anthropology and human identification methods. Future directions for this research are addressed in chapter five as well. Chapter six provides concluding remarks, synthesizing the significance of this study and potential ways to develop this method for future implementation.

CHAPTER 2: LITERATURE REVIEW

This chapter provides an introduction to visual and radiographic image identification methods and Geographic Information Systems (GIS). It reviews identification methods that use visual recognition of unique anatomical features, and radiographic images of the post-cranial skeleton and the frontal sinus. The origins and fundamentals of GIS are discussed, as well as its applications to archaeology, biological anthropology, forensic anthropology, and crime scene investigation. The chapter concludes with a discussion of the importance of spatial analytical tools like GIS to forensic science and forensic anthropology.

Radiographic Identification Methods and GIS

Visual Recognition and Radiographic Image Identification Methods

There are several methods available to medical examiners and anthropologists for establishing a positive identification of human remains. Positive identification requires a scientific modality to identify unique biological data that can exclude all other individuals, such as DNA analysis (Caplova, et al. 2017). Examples of methods that utilize unique biological data for identification include: visual identification of unique body features such as scars, tattoos, moles, etc., dermatoglyphics (fingerprint analysis), and dental comparison (Caplova, et al. 2017; Derrick, et al. 2015; Patil, et al. 2012).

Caplova, et al. (2017) reviewed current identification methods based on physical appearance: simple visual recognition, identification based on specific facial and/or body areas, soft biometrics such as tattoos, moles, and scars, and AM/PM dental superimposition. Individual identification by physical characteristics is very subjective and not applicable in every setting, particularly situations that lack antemortem data for comparison such as migrant and refugee

deaths, and mass disasters with open populations (Caplova, et al. 2017). Moreover, few studies have tested the reliability and applicability of visual identification methods, and there are no set standards or studies validating these methods. This lack of standardization, reliability, and applicability is a problem seen throughout identification methodologies (Caplova, et al. 2017). When visual recognition methods, fingerprints, and DNA analysis are not feasible due to decomposition, thermal damage, or the lack of a comparative reference sample radiographic comparison methods may be another option for identification (Derrick, et al. 2015; Kuehn, et al. 2002; Patil, et al. 2012).

When human remains are skeletonized or otherwise visually unrecognizable, forensic anthropologists rely on the morphology of highly variable traits in the human skeleton to assist with identification. Morphological identification is primarily done through the comparison of AM and PM radiographs (Angyal and Dérczy 1998). Skeletal elements most commonly used for radiographic comparison are in the chest region – clavicles, sternum, ribs, and vertebrae – along with the dentition and surrounding alveoli, and the maxillary and frontal sinuses (Angyal and Dérczy 1998; Derrick, et al. 2015; Kahana and Hiss 1997; Mundorff, et al. 2006; Stephan, et al. 2011). The sphenoidal sinus, *sella turcica*, mastoid processes, and shoulder girdle have also been used for positive identification (Quatrehomme, et al. 1996).

Murphy and Gantner (1982) reviewed eight forensic cases that used radiographic images to re-associate body parts or establish identity. Four of the cases involved the use of radiographic images to re-associate human body parts that had been separated from the rest of the body as a result of grave desecration or theft from anatomy labs. The other four cases demonstrated how radiographic images of skeletonized remains can be used to see individualizing features such as fractures, anatomical differences, and pathological features which may help establish identity

(Murphy and Gantner 1982). While Murphy and Gantner (1982) agree that radiographs of human remains can contribute to a forensic investigation, the authors further argue that radiological methods should never replace osteological analysis. Instead, radiographs should be used in conjunction with or as a supplement to osteological analysis and other methods when applicable (Murphy and Gantner 1982).

Adams and Maves (2002) discuss the use of the right clavicle to identify a civilian who went missing during the Vietnam war. Dental records were not available for comparison, but an AM chest radiograph that had been taken five months prior to the victim's disappearance was located. For this case, the authors used superimposition of the AM and PM chest radiograph and found the shape and size of the clavicles matched, allowing them to confirm identity.

Other studies have confirmed the validity of identification using chest radiographs. Kuehn, et al. (2002) aimed to validate the method of comparing AM and PM chest radiographs for human identification by quantifying the method's reliability, identifying individualizing features in chest radiographs, and recognizing potential errors in comparisons. The authors found an 80% accuracy rate and determined that the quality of the radiographs was a major limitation to this method. Building on the work of Kuehn, et al. (2002), Stephan, et al. (2011) addressed the need for known error rates and studies that quantify the accuracy of identification methods. The authors acknowledged that previous chest radiograph studies had been performed on remains that were still fleshed, thus the accuracy rates could not apply to skeletal remains due to the significant postmortem changes in the skeleton from decomposition processes. Using clavicle morphology and the third cervical through the fourth thoracic vertebrae for AM to PM comparison, Stephan, et al. (2011) found that chest radiographs could sufficiently be used for

identification even with poorly preserved skeletal remains and compromised AM radiograph image quality.

In addition to the assessment of AM chest radiographs for identification, the morphology of the spine has been assessed as a feature for AM/PM radiograph comparison. Valenzuela (1997) used lumbar spine morphology to identify human remains found in a cave in Granada, Spain. The author compared PM to AM radiographs of the individual's lumbar spine, and was able to establish a positive identification by matching unique features such as osteophytes on the third, fourth, and fifth lumbar vertebrae, spinous and transverse process morphology, and lumbar spine scoliosis (Valenzuela 1997). Kahana, et al. (2002) used AM and PM radiographs of the spine to identify eight individuals. The authors used normal anatomical variation of the vertebrae, degenerative processes, healed trauma, and congenital malformations to identify radiographic matches (Kahana, et al. 2002). Mundorff, et al. (2006) examined a set of skeletonized remains recovered from the East River in New York City. The biological profile of the remains matched a missing person report, and AM radiographs were obtained from the medical records of this individual. Using AM and PM radiographs, the authors compared the seventh cervical and first thoracic vertebra, showing that the morphology of the spinous processes matched. The positive identification based on AM and PM radiographs was later confirmed with DNA.

Frontal Sinus Radiograph Comparison Methods

The previous studies illustrate how AM and PM radiograph comparison of normal skeletal variation can be used establish a positive identification. One of the most widely accepted and commonly used radiographic identification methods uses frontal sinus morphology (Christensen 2005b). The frontal sinus, which is located inside the frontal bone in the glabellar

region, has been shown to be a reliable feature for comparison due to its morphological stability after age 20, its high rate of preservation due to its location within the cranium, and its highly variable morphology among individuals (Angyal and Dérczy 1998; Cox, et al. 2009). Radiologists, anatomists, and anthropologists have confirmed the significance of the frontal sinus as a highly variable feature that can be used for forensic identification purposes (Nambiar, et al. 1999). The frontal sinus has a known rate of development with the paranasal sinuses developing *in-utero*, and enlargement and definition of the sinus occurring after birth with the initial presentation by age one. The frontal sinus will show up radiographically by about age six, but will not obtain full size until late adolescence, usually age 20 (Nambiar, et al. 1999).

Once fully developed, the sinus is highly variable among individuals. The left and right sides of the sinus develop independently resulting in asymmetry or absence of the sinus on one side or the other. It is estimated that 4-15% of the population is missing one side of the sinus, possibly due to extreme cases of a deviated septum (Nambiar, et al. 1999). The size of the frontal sinus is highly variable, but it has been observed that the sinus tends to be larger in males, and smaller in females with more scalloping on the upper borders. The degree of variability seen in the frontal sinus among individuals, its morphological stability throughout life (barring disease or trauma), and its presentation on radiographs has made it a useful feature of forensic identification (Nambiar, et al. 1999).

Culbert and Law (1927) were the first to show that the comparison of AM and PM radiographs of the frontal sinus could be used to establish identity. They observed that the mastoid processes and cranial sinuses remained constant throughout an individual's life, and the shape and arrangement of these sinuses was different in every individual they observed, making these features ideal for determining identity. This was the first study to show that AM and PM

radiographs could be used to compare the cranial sinuses for the purpose of positive identification (Culbert and Law 1927).

Since Culbert and Law's study in 1927, many other medical professionals and anthropologists have published studies on the use of frontal sinus radiographs to confirm identification. By the 1980s research into the use of cranial sinuses for identification was present in the anthropology and anatomy literature. Ubelaker (1984) used cranial radiographs to identify a set of remains. AM radiographs from the victim's medical records were accessed and compared to the PM radiographs of her skull. The lateral and frontal views of the skull were compared, which showed that the size and shape of the *sella turcica* of the sphenoid, and the frontal sinus was an exact visual match. When the case went to trail, Ubelaker testified in court to the method of comparing AM and PM frontal sinus radiographs for the purpose of determining identity. While Ubelaker testified to the fact that the radiographs belonged to the same individual, this case brought up questions regarding the precedent for making positive identifications based on radiographic comparison, and the probability that two individuals could have identical frontal sinus patterns. As a result, Ubelaker conducted his own study using 35 frontal radiographs of crania from the National Museum of Natural History/National Museum of Man. He compared each radiograph to all the radiographs in the sample to determine the number of differences in the presentation of the frontal sinus, orbits or frontal crest, and to document any relationship to surrounding cranial structures. Each comparison showed at last three differences and the average number of differences in the frontal sinus region between two individuals was eight. Ubelaker concluded that there were enough differences to support the assumption that the frontal sinus is unique to each individual (Ubelaker 1984).

Since the Ubelaker (1984) study, many other researchers have addressed the question of frontal sinus uniqueness and its usefulness for identification, as well as the precedent for the use of radiographs for identification purposes. Yoshino, et al. (1987) used skull radiographs from 35 Japanese individuals to assess the frontal sinus using a quantitative method based on the total area and asymmetry of the sinus. They further used descriptive statistics to analyze the frontal sinus areas and codes to classify the different patterns observed. The authors concluded that the frontal sinus is unique enough among individuals to be a reliable method for identification. The authors implemented their method of using qualitative coding by assessing the area and asymmetry of the frontal sinus from AM and PM radiographs to successfully identify a missing person.

Jablonski and Shum (1989) discuss two forensic cases to demonstrate how radiographic images of anatomically variable skeletal features can aid in identification. First, the authors utilized frontal sinus radiographs to confirm the identity of burned remains. Next, they compared AM and PM radiographs of a torso, specifically the morphology of the spine and the absence of the 12^{th} rib, to confirm an individual's identity. These cases illustrate the significance of using radiographs to compare anatomically variable features in order to determine identity, but also show that radiographic comparison is not a method to be used in isolation or as a first option. Both instances used it in conjunction with other methods of analysis, including osteological analysis, and when more traditional identification modalities such as dental comparison were not possible.

Marlin, et al. (1991) established four positive identifications by using frontal sinus radiograph comparisons. The authors found this method to be useful and reliable, but underutilized. They further stressed the importance of accurate record keeping as radiographic

images, particularly of the head, are a valuable forensic tool. Quatrehomme, et al. (1996) use the frontal sinus as a comparative feature for positive identification in two homicide cases. First, both victims were presumptively identified through anthropological methods. Based on these results, radiographs were located and used as a comparison for positive identification. Kirk, et al. (2002) tested the validity of visually matching the frontal sinus for identification. Using the Caldwell and Waters' positions (traditional positions for viewing the sinonasal area in radiographic films) (Hamed, et al. 2016) digital tracings were made for 35 sets of AM and PM radiographs of the frontal sinuses. Superimposition of the radiographs was used to identify a match. In addition to this visual assessment, (Kirk, et al. 2002) also used a quantitative method of measuring the width and length of each sinus from the radiographic image. The authors found sex and age did not affect the examiner's ability to pattern match, and time between when the AM and PM films were taken did not have an effect. The authors confirmed that frontal sinus pattern matching from radiographs is a valid method for human identification (Kirk, et al. 2002).

For the last few decades, this acceptance of frontal sinus uniqueness was anecdotal and based on the reported experiences of many experts reviewing thousands of radiographs over the course of their careers and never seeing two that were alike (Besana and Rogers 2010; Christensen 2005b; Cox, et al. 2009). However, until recently there were no studies that empirically tested this assumption. Christensen (2005a) empirically tested the uniqueness of the frontal sinus using Elliptic Fourier Analysis (EFA), a mathematical method that applies a curve to an ordered set of data points in order to reproduce the outline of a shape, in this case the outline of the frontal sinus from radiographs. By calculating Euclidean distances between pairs of frontal sinus outlines Christensen found that the average distance between the frontal sinus shapes of different individuals was significantly larger than the average distance between

duplicate frontal sinus shapes from the same individual. Christensen's findings empirically prove that the frontal sinus shape of each individual is significantly different, and the probability of two different individuals having the same frontal sinus shape is low.

Christensen (2005b) furthered this research by testing the reliability of frontal sinus identification using EFA to assess frontal sinus variation and identify a match. Using *Bayes Theorem* Christensen calculated the posterior probabilities and likelihood ratios of the comparisons made between frontal sinus outlines. Her results show that using EFA to compare frontal sinus radiographs is a reliable method with a 96% probability of identifying a match correctly. Christensen has shown that the widely-accepted belief that frontal sinus morphology is unique to each individual is supported as it has now been empirically tested, and also mathematically proved that there is a very small probability of any two individuals having identical frontal sinus morphology. This is an important step toward improving existing methods and developing new methods that meet rigorous standards.

Since Christensen's (2005a and 2005b) studies, other researchers have sought to develop quantitative methods for frontal sinus identification, tested qualitative coding methods to assess frontal sinus patterns, and established known error rates for the superimposition method. Cameriere, et al. (2005) developed a similar qualitative method as Kirk, et al. (2002) for assessing frontal sinus morphology for identification, which also builds off of the method described by Yoshino, et al. (1987). The authors aimed to estimate the potential error of the pattern matching method. They digitized radiographs from 98 individuals and assigned a code for each specific frontal sinus pattern identified. They determined that the frontal sinus is a reliable feature for identifying individuals due to its variable morphology and their results indicated a low probability of misidentification.

Da Silva, et al. (2009) affirmed the forensic importance of frontal sinus radiographs in the identification of a male killed in a traffic accident who had remained unidentified for over a year. A presumptive identification was made from postmortem photographs leading investigators to request medical records from the victim's family. The medical records contained two skull radiographs, which after digitization and adjustment for brightness and contrast, allowed for frontal sinus comparison. A match was determined from visual comparison, superimposition in Adobe Photoshop, and through measurements. The authors acknowledge that comparative visual analysis is based on the experience of the observer, rather than on an objective method. Given the need to establish more objective methods many anthropologists have worked to develop new methods for the analysis of frontal sinus morphology (Da Silva, et al. 2009).

Drawing on Christensen's study, Cox, et al. (2009) also sought to quantify the differences between frontal sinus outlines by measuring each sinus from a fixed point and summing the differences between the measurements. The authors calculated the probability that a pair of radiographs came from the same individual or different individuals. They achieved an error rate of 0%. Besana and Rogers (2010) tested the independence of frontal sinus traits and the probability of correctly identifying a match based on combinations of traits. The authors compared this method to superimposition and found that most frontal sinus traits are dependent on other traits and thus cannot be used to calculate probabilities, and discrete traits do not have enough discriminatory power to rule out a match and be useful for positive identification. The authors concluded that superimposition was the most reliable method. Patil, et al. (2012) supported this conclusion. They tested the superimposition method and found that identification by superimposition of radiographs was 100% accurate.

Forensic anthropologists have long recognized that frontal sinus shape is unique to each individual. The above studies confirm this finding and are further able to show that this variability can be leveraged as a reliable method for human identification.

What is a GIS?

A Geographic Information System (GIS) is a database management system (DBMS) that is designed to store and analyze data so that it can be presented geographically or spatially in geospatial software programs such as ArcGIS/ArcMap. A DBMS can store geospatial information where it can then be managed, edited, analyzed, and displayed using a GIS. In a sense, GIS combines cartography, statistical analysis, and database technology in order to display and analyze spatial data (Aldenderfer and Maschner 1996; Dawsen 2011). GIS displays data in layers, with each layer being a distinct phenomenon (roads, forest, buildings, etc.). Data in layers can be represented in two data formats: raster or vector. Raster data is data that has been put into a tessellation, or grid, so that each data point is represented by a cell or pixel. Vector data is represented by some combination of points, lines, and polygons (two dimensional shapes). Both data formats operate on an x, y coordinate system. The decision of which data format to use depends on the project and what the researcher is trying to understand about a set of data (Aldenderfer and Maschner 1996).

The earliest known use of a Geographic Information System was by John Snow, the founder of modern epidemiology, who was able to pinpoint the cause of a massive cholera outbreak in England in 1853 by mapping cases of the disease. The spatial pattern of the cholera cases showed a distinct cluster around a water pump on Broad Street that had been contaminated by sewage and was determined to be the source of the outbreak (Anemone, et al. 2011). This early use of spatial data, and interpreting patterns in those data to problem solve, set the stage for

the later development of GIS computer software and spatial analysis of geospatial data in fields like geography, remote sensing, land surveying, urban planning, natural resource management, and archaeology (Aldenderfer and Maschner 1996; Dawsen 2011).

Application of GIS to Anthropology and Related Fields

GIS has also been utilized by anthropologists to analyze spatial patterns in anthropological data. For example, Anemone, et al. (2011) applied remote sensing technology and GIS to the study of primate and human evolution. The authors acknowledge the ability of spatial analysis technologies like GIS to allow paleoanthropologists and paleontologists to study the spatial patterns of fossils. Anemone, et al. (2011) advocates for the use of geospatial science and spatial technologies like GIS in anthropology as this technology is capable of revealing patterns and relationships in the data that would otherwise not be apparent. This can be seen in several studies that have utilized GIS to better understand spatial relationships in anthropological studies.

Benito-Calvo and De la Torre (2011) used GIS to examine the site formation processes of Bed I of Olduvai Gorge in Tanzania, which is one of the most renowned sites from the African Plio-Pleistocene. The authors hypothesized that natural processes played a more significant role in the site's formation than hominins and carnivores. They imported the original site drawing into ArcMap and conducted spatial analyses of the artifact and bone distribution. The results showed that the assemblage pattern was significantly different from a uniform model, which is the model you would expect to find when an assemblage has not been affected by natural processes. From these results the authors concluded that geological forces were responsible for the post-depositional changes of the artifact and bone assemblages rather than just hominin and carnivore activity (Benito-Calvo and De la Torre 2011).

In addition to paleoanthropology, spatial analysis with ArcGIS software has been used in bioarchaeology and paleo-epidemiology. Gowland and Western (2012) looked at skeletal remains from 27 Anglo-Saxon sites in eastern England and documented the remains that presented with indicators of poor health, specifically cribra orbitalia (CO) and enamel hypoplasia (EH). Using GIS to map the instances of CO and EH, the authors compared these data to the spatial patterns of malarial outbreaks or outbreaks of "ague" during that time period. The authors found that the pattern of CO and EH was similar to historically recorded outbreaks of "ague" (malaria). These hotspots of malaria, CO, and EH also matched the distribution of the mosquito species, A. *atroparvus*, which was responsible for spreading malaria in that region.

Application of GIS to Skeletal Elements

GIS has also been applied to evolutionary studies by examining the relationship between mammalian tooth morphology and diet. Jernvall, et al. (2000) used GIS to quantify the evolutionary changes that impact dental morphology of the first lower molar in two rodent species, mouse and vole. The authors conducted a topographic analysis of the molars using GIS to understand the link between genes and morphological changes. The results of the spatial analysis in GIS indicated different growth patterns between mouse and vole molars, which suggests that at least two hierarchical development processes are responsible for the divergence in molar morphology between Families (Jernvall, et al. 2000).

Ungar and Williamson (2000) also investigated tooth morphology of G. *gorilla*, specifically how tooth wear from diet affects functional efficiency, and whether worn teeth can be used to understand diet of past species. Most studies on the relationship between diet and tooth wear focus on inferring diet from unworn teeth, but Ungar and Williamson aimed to use GIS to analyze the topography of worn teeth. The authors looked at the tooth as a geographic

landscape that can be modeled and analyzed by looking at cusp surface area, aspect, slope, relief and even drainage. Ungar and Williamson concluded that GIS can be used to analyze morphological differences in worn teeth to understand diet (Ungar and Williamson 2000).

Rose, et al. (2012) applied GIS to histological bone samples to understand biomechanical properties of loading and bone remodeling on the human skeleton. The authors used ArcGIS spatial analyst tools to look at directional distribution of bone remodeling sites in the bone microstructure in cross section histological samples. The directional distribution tools produced standard deviation ellipses of all of the points of remodeling in the cross section and allowed the authors to analyze the directional trend of bone remodeling. Rose, et al. refer to this as practicing "bone geography" because using ArcGIS on the skeleton requires viewing the skeleton, features on the skeleton, and bone microstructure as a kind of geographical landscape that can be understood spatially using spatial analysis tools like ArcGIS (Rose, et al. 2012).

Application of GIS to Forensic Anthropology and Crime Scene Investigation

Aldenderfer and Maschner (1996) argue that spatial thinking is key to many fields of anthropology. Cultural anthropology and archaeology both deal with spatial data, whether it be artifact scatters or the movements and geographic locations of modern and archaeological human settlements. The previously reviewed literature shows the many possible applications of spatial analysis to biological anthropology and bioarchaeology research questions regarding morphology, evolution, biomechanics, diet reconstruction, site formation processes, and epidemiology. However, the use of GIS in forensic science, particularly forensic anthropology is still new.

Current research on GIS in forensic anthropology predominantly focuses on the spatial patterns of scattered human remains. Manhein, et al. (2006) used GIS and spatial analysis

technology to study the spatial patterns of dumped and scattered human remains in order to better predict the location of human remains and aid in the effective recovery of those remains in forensic contexts. Spradley, et al. (2012) used GIS and Global Positioning System (GPS) to analyze the spatial patterns of human remains scattered from vulture scavenging. Kolpan and Warren (2017) utilized GIS to study geographic patterns of where human remains were recovered in forensic cases in Florida in order to better understand where human remains were most likely to be found. Gundel (2017) used body disposal data from the Office of the Chief Medical Examiner, Connecticut and ArcGIS to create a predictive model for body disposal sites. Predictive modeling using ArcGIS would allow law enforcement to predict the most likely areas where perpetrators would dispose of their victim's remains, which would drastically reduce the amount time and resources needed to search for a missing individual (Gundel 2017). Carlton, et al. (2018) used Structure from Motion (SfM) and GIS to document and analyze the taphonomic processes that affect human remains and burials.

GIS has also been used by law enforcement to understand spatial relationships between crime scenes. Investigators of the 2002 sniper shootings in Washington, D.C. utilized GIS to create maps of where each shooting took place, and field guides outlining the proper procedure for cataloging data for inventories of each crime scene. This allowed the investigators to spatially analyze the crime scene locations and the evidence found at each crime scene. While the perpetrators were caught before the method could be operationalized, it showed how understanding the spatial relationships between crime scenes and evidence is a vital tool in reconstructing a crime and catching the perpetrators (Wilson 2003).

Bolton applied ArcGIS directly to the skeleton (Beckett, et al. (2014). Using ArcGIS to analyze topographic data on the pubic symphysis from 3D pelvic images, the authors recorded

features like slop, aspect, and valley volume of the pubic symphysis. These features were analyzed as if they were geographical landscapes in order to determine significant differences in these features between age groups (Bolton 2013). The use of ArcGIS to assess age from the pubic symphysis could improve age estimations and provide a new tool for biological profiling.

Each of these studies illustrates the importance of GIS and other spatial technologies to forensic science and forensic anthropology. Spatial analytical technologies like GIS can aid our understanding of patterns and processes that affect human remains post-deposition, whether a body dump site or predator scavenging. In each of these studies GIS was applied to a natural landscape or to a set of human remains in order to understand how human remains interact with a landscape. Given GIS's ability to map landscapes and analyze patterns and specific points on a map, it follows that this same principle can be applied to specific features on the skeleton, particularly the frontal sinus. Additionally, GIS is capable of statistically analyzing patterns, and quantifying the landscapes and patterns it maps. Given the need for more quantifiable methods in forensic anthropology, it is worth exploring the ability of GIS to provide a quantifiable method for analyzing frontal sinus morphology as a landscape for the purpose of positive identification.

CHAPTER 3: MATERIALS AND METHODS

This chapter discusses the method of digitizing the frontal sinus from cranial radiographic images in ArcMap to produce polygons that are representative of the frontal sinus, and the use of the spatial analyst tool, Similarity Search, to identify matches from a pool of frontal sinus polygons. Cranial radiographs of 100 donors (50 males and 50 females) from the Bass Donated and Forensic Skeletal Collections are used to test ArcMap's (ESRI 2018) ability to digitize the frontal sinus, and the ability of Similarity Search to correctly identify a match. This chapter will first explain the digitization process and describe both the study sample and the radiograph methodology. Next, sample organization, frontal sinus digitization, polygon geometry calculation, and the Similarity Search tool are explained. The chapter concludes with an explanation of the statistical analyses used.

Digitizing in ArcMap

Digitizing is the process of translating non-digital information such as hard-copy images and maps into digital format (desktop.arcgis.com 2018b). This process is commonly used in the field of geography because hard copy maps often need to be digitized so that they can be uploaded to websites or imported into mapping software programs like ArcGIS (ESRI 2018). There are two types of digitizing: hard-copy or "heads down" digitizing and on-screen or "heads-up" digitizing. Heads-up digitizing is done in software programs like ArcGIS/ArcMap where digital map images, or raster images, are uploaded into ArcMap and features of the map are digitized using points, lines, and polygons (desktop.arcgis.com 2018b). This process uses two types of data models: raster and vector. Raster data models are for continuous data like air temperature or soil pH and is defined in a grid base. Images, for example aerial images of geographic landscapes, are also examples of raster data as they represent a continuous image

organized in a tessellation, or grid (Burrough 2015). Vector data models are for discrete data that can be precisely defined such as population levels, gross median income, and geographic features like roadways and bodies of water that can be represented with vector graphics such as points, lines, and polygons (Burrough 2015). Vector data is defined mathematically rather than in a grid like raster data. For example, the user can import an aerial map JPEG file of a national park (raster) and create point, line, and polygon shapefiles, and then use the *Create Features* tool to digitize features such as buildings, roads and lakes (vector). The result is a map that is an abstraction of the original map where features like buildings, roads, and lakes are represented by geometric shapes (points, lines, and polygons).

This same "heads-up" digitizing method is used for this study, but instead of using an aerial map of a geographic landscape on Earth and digitizing buildings, roads, and lakes, a raster image of human crania will be imported (JPEG radiograph images) and then the frontal sinus will be digitized as if it is a geographic feature. This process produces a two-dimensional representation of the frontal sinus referred to as a polygon.

Sample

To assess frontal sinus pattern matching with ArcGIS, I utilized a subset of cranial radiographs from the Forensic Anthropology Center (FAC) at the University of Tennessee. The radiographs were taken at the University of Tennessee Student Health Services by Dr. Angi Christensen, for her doctoral dissertation (Christensen 2003). The complete collection includes radiographs of 423 adult crania from the William M. Bass Donated Skeletal Collection (N = 257), the Forensic Skeletal Collection (N = 105), and the historic plains Arikara archaeological collection (N = 61), all housed at the University of Tennessee, Knoxville. The radiograph collection also includes 161 radiographs from the University of Tennessee Student Health Center

that were taken for clinical purposes. The Bass Collection is comprised of individuals that donated their remains to the FAC Body Donation Program, which began in 1981 and continues to receive donations today. All individuals used in the Christensen study, and therefore the current study, were donated between 1981 and 2001. This study sample, which is a subset of the complete Christensen radiograph collection, consists of 50 males and 50 females, each with two separate radiographs to simulate AM and PM images, for a total of 200 radiographs. All of the individuals in the subset are from the Bass Collection except for six females that are from the Forensic Collection, because there were fewer female donors between the years of 1981 and 2001 compared to male donors. In addition, some of the females who were radiographed had too small or unclear frontal sinus outlines rendering them unsuitable for this study. The study sample only includes individuals with the clearest presentation of the frontal sinus because the best examples of frontal sinus radiographs are needed to evaluate ArcMap's ability to create polygons representative of the frontal sinus, and the ability of ArcMap's spatial analyst tools to assess these polygons for the purpose of positive identification.

All of the radiographs used in this study were originally hard copy radiographic images. These radiographs needed to be scanned into digital electronic files so that they could be uploaded into the ArcMap software program. The radiographs were scanned into Digital Imaging and Communication in Medicine (DICOM) files on a Diagnostic Pro Edge scanner at the West Virginia School of Osteopathic Medicine in Lewisburg, WV, with the assistance of Dr. Becky Kelso, and edited with OsiriX Lite viewer software. Editing was limited to contrast and exposure settings to enhance images that were too dark or over-exposed to maximize the visibility of the frontal sinuses. Each radiographic image was exported as a Joint Photographic Experts Group (JPEG) and saved onto an external hard-drive.

Radiograph Methodology

Dr. Angi Christensen and an x-ray technician produced the cranial radiographs used for this study at the University of Tennessee Student Health Center. They used a HoLogic HFP Series 100kHz High Frequency machine with the following parameters: KVP (peak kilovoltage): 48 kV_{peak}, (50kV_{peak} for denser skulls), CM (distance from the tube to film): 40 cm, MA (current in the x-ray tube): 75 mA, SEC (exposure time): 65 ms. Christensen used a standardized methodology to orient all of the crania so that each radiograph would be taken in the same orientation and with the image beam running from posterior to anterior. The crania were oriented facedown with the midsagittal plane perpendicular to the x-ray plate, and the frontal bone closest to the film, which would decrease distortion and increase clarity of the frontal sinus. The skulls were also oriented in the "Caldwell view" which involves positioning the crania so that the machine is perpendicular to a line running from nasion to the superior border of the external auditory meatus (Christensen 2003:66-67).

In order to simulate AM and PM radiographs, each cranium was radiographed twice rather than using a copy of each cranium's radiograph. Each cranium was radiographed using the same methodology, but at separate times so that each cranium would have to be repositioned and the second image would be similar to but not an exact copy of the first image (see Figure 3.1). This was done to introduce error that would be similar in a forensic case where the practitioner must approximate the orientation of the AM radiograph when radiographing the cranium, and it is expected that the practitioner will not be able to perfectly replicate the AM orientation (Christensen 2003:67).

Radiographic images are 2-dimensional (2D) and thus prone to distortion and opacity due to the presence of overlapping structures within the skull. This can inhibit the visibility of the

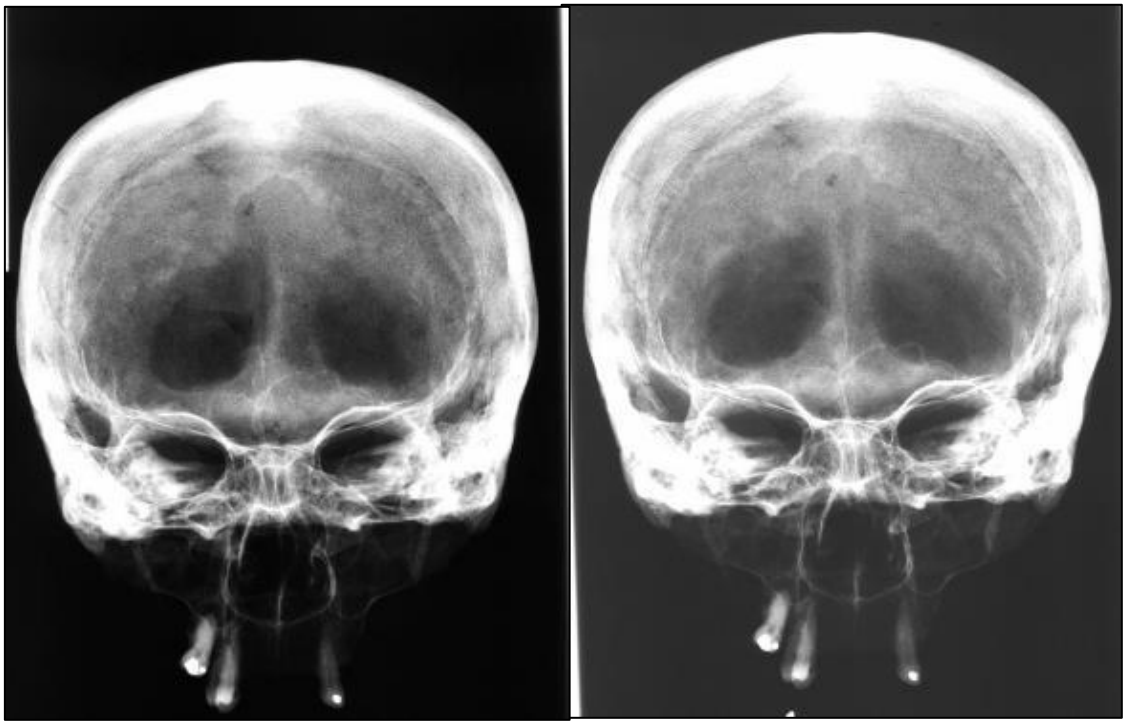

Figure 3.1 *Simulated AM radiograph (left) and PM radiograph (right)*

frontal sinus making frontal sinus matching difficult. Computed Tomography (CT) produces 3-dimensional (3D) images that allow the user to assess features that are not visible with 2D radiographic images, particularly anterior to posterior width and volume. This makes CT a useful tool for positive identification and sex estimation using the frontal sinus (Akhlaghi, et al. 2016; Choi, et al. 2018; Cossellu, et al. 2015; Tatlisumak, et al. 2007). While CT images may provide higher resolution 3D images that are better for frontal sinus visualization, cranial radiographs are still a common procedure for many individuals, and a large radiograph sample was available and readily accessible for study. Sample access and the pervasiveness of radiographs were both important factors in the decision to use radiographs for this study, however, another major factor was the novelty of this method.

Methodology Parameters, Sample Organization, and Anonymization

Methodology parameters were established on a subset of five male and five female radiograph pairs (AM and PM) to identify limitations of the ArcMap software and potential weaknesses in the proposed methodology. One PM radiograph and five comparative AM radiographs, including the corresponding AM match to the PM radiograph, were imported into ArcMap 10.5 (ESRI 2018) and displayed as individual data layers in the table of contents. Radiographs were not anonymized for the preliminary assessment tests. The initial testing of Similarity Search on the subset sample did not reveal any technical limitations given the dataset. This initial testing helped to refine the methodology for successfully digitizing the sinuses, calculating the area and perimeter values, and formatting the data so that it could be read by the Similarity Search tool.

After initial testing of this method with the subset sample, this process was implemented for the complete dataset of 50 males and 50 females. However, prior to implementation, the

sample needed to be anonymized and randomized to prevent any bias based on knowledge of the case information. Dr. Amy Mundorff anonymized the radiographs by assigning a randomly generated number (2018) followed by either an "a" or "b" to denote AM or PM. The randomly generated numbers were recorded in an electronic spreadsheet.

Once the radiographs were anonymized, a fellow graduate student (Megan K. Kleeschulte) organized the data into 100 randomized test groups. Each test group contained one PM radiograph and a comparative group that was comprised of nine randomly selected AM radiographs, as well as the PM radiograph's corresponding AM radiograph (the true match) for a total of 11 radiographs per group (Appendix 1). In addition to the 100 test groups that contained a true match, 20 groups (10 males and 10 females) were created using the same process, but no true match was included in the group as a means to assess how Similarity Search classifies the radiographs when there was not a true match included in the comparative group. In total, the test data consisted of 120 test groups,

The test groups were limited to all male or all female because the sexes were to be assessed separately in this study. There has been limited research into sexual dimorphism of the frontal sinus, but in a recent study Choi, et al. (2018) used Cone-beam Computed Tomography (CBCT) images to assess a new methodology for sex estimation from the frontal sinus. The authors measured several variables on the three-dimensional frontal sinus images and used logistic regression to determine which variables were significant in determining sex. The authors found that volume has a significant influence on the accuracy of their model (an increase of 5%), suggesting that frontal sinus volume has significant power of explanation when it comes to sex estimation from the frontal sinus. These results are consistent with other studies that have found frontal sinus volume to be a distinguishing feature between males and females (Akhlaghi, et al.

2016; Nambiar, et al. 1999). Given the above-mentioned studies and the potential for males to have sinuses with larger volumes than females, the sexes were assessed as separate groups instead of combining them for analysis. This decision was taken in order to minimize the confounding variables that might affect the Similarity Search results.

Additionally, this method is designed to confirm or exclude a potential match, which first requires a presumption of the individual's identity in order to access medical radiographs for comparison. By the time medical records are requested, the practitioner will have already estimated the individual's sex and will only request the medical records of individuals who are consistent with the biological profile of the remains. National databases, such as NamUs and CODIS, work by including genetic information and case details of both male and female missing and unidentified persons so that the user can search a combined pool to find matches. The creation of a national frontal sinus database like NamUs or CODIS is not the purpose of this method; instead it is designed to provide forensic practitioners with a user-friendly, quantitative method for identification when comparative frontal sinus radiographs are available.

Digitizing the Frontal Sinus

Once the radiographs had been anonymized and organized into test groups, new shapefiles were created in ArcCatalog (ESRI 2018) for each of the radiograph data layers (Figure 3.2). Shapefiles are a file format for storing location and attribute information about geographic features, which can be represented as a point, a line, or a polygon. In this case, each shapefile was designated as a polygon (Figure 3.3). The new shapefiles and JPEG radiographs were then imported into the table of contents in ArcMap in order to be able to edit the file to create the polygons. (Figures 3.4 and 3.5). For each AM radiograph and the one PM radiograph, the JPEG data layer was selected, its corresponding shapefile was selected, and the polygon tool in the

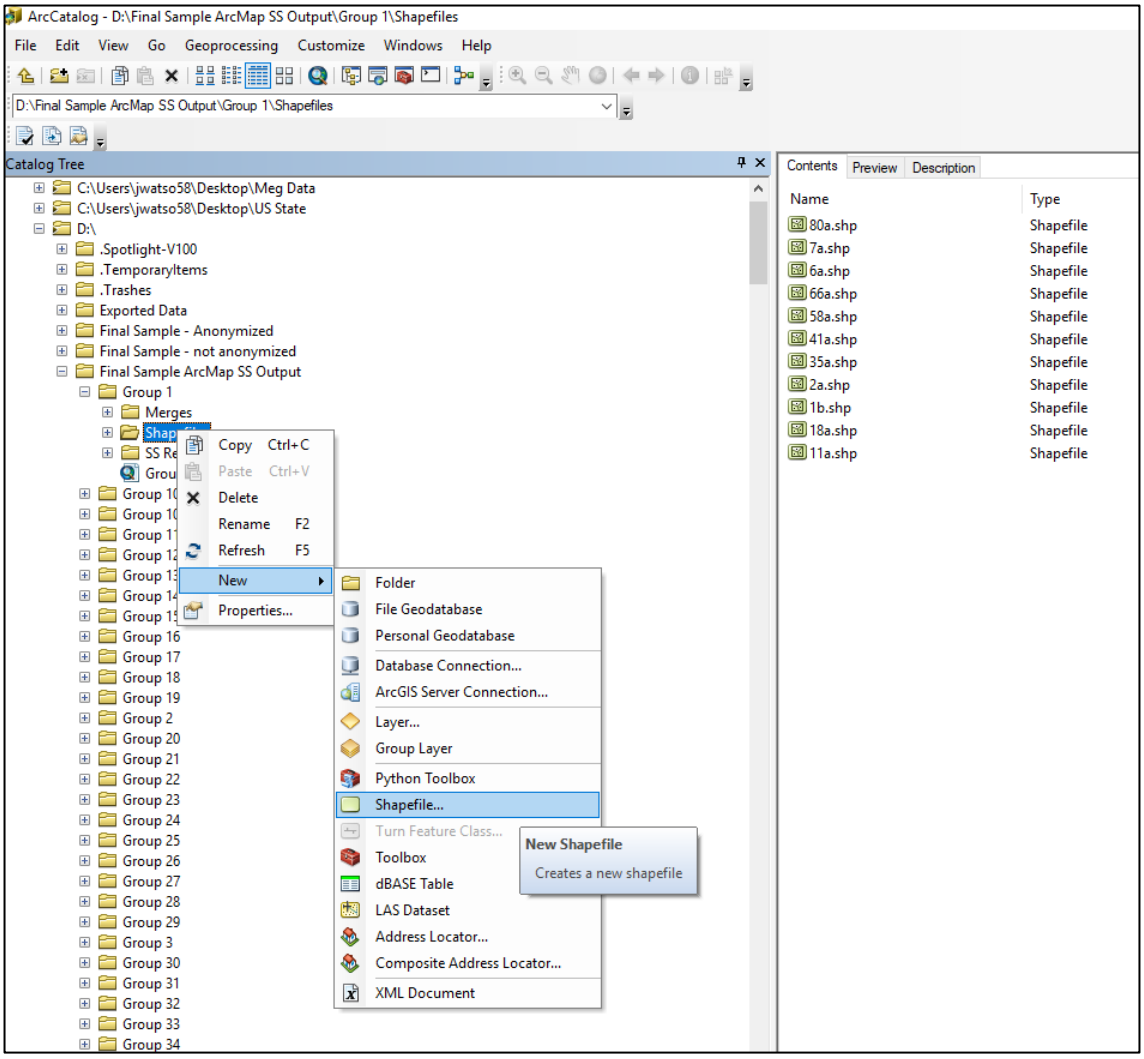

Figure 3.2 *Creation of shapefiles in ArcCatalog*

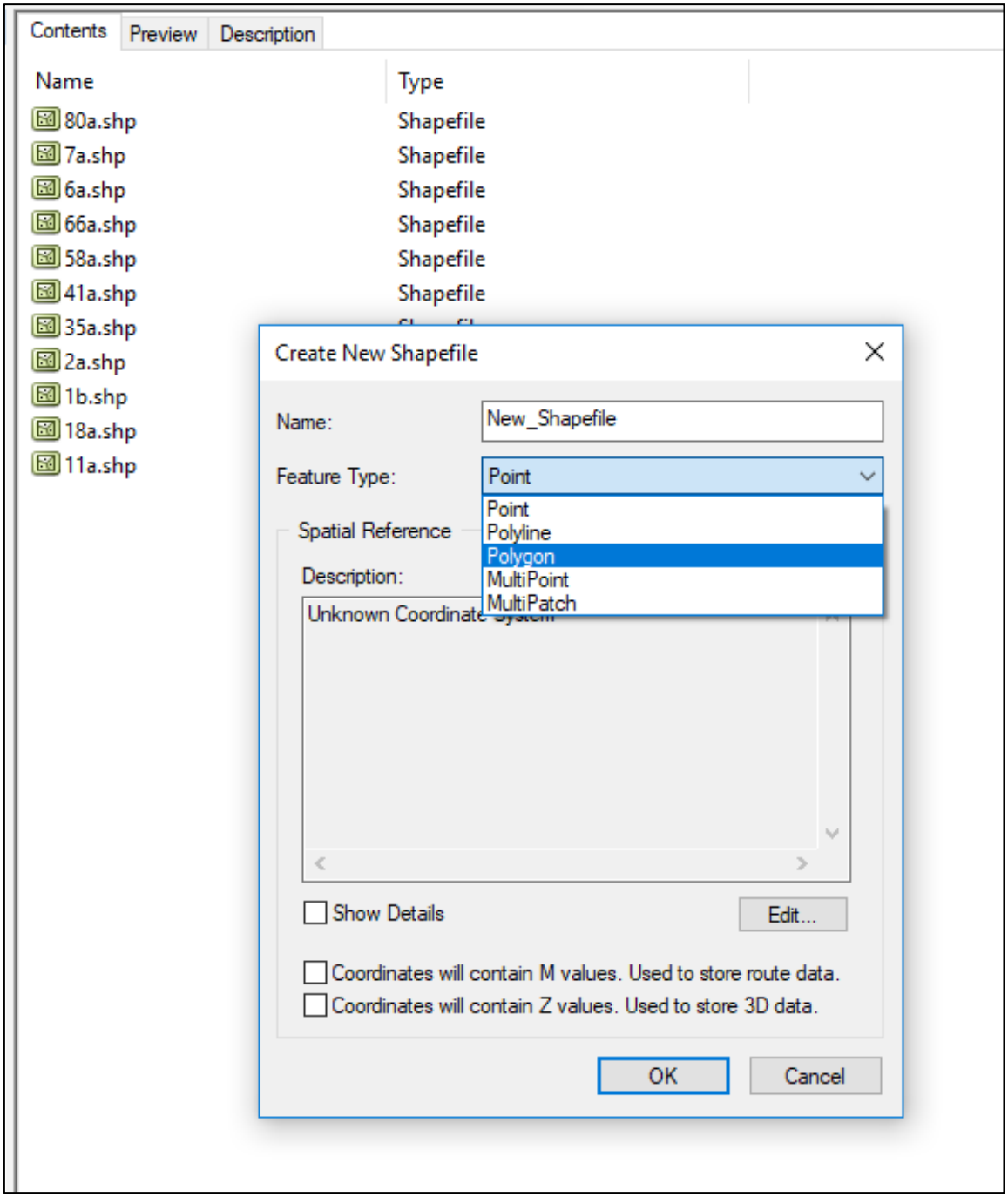

Figure 3.3 *Designating each shapefile as a polygon in ArcCatalog*

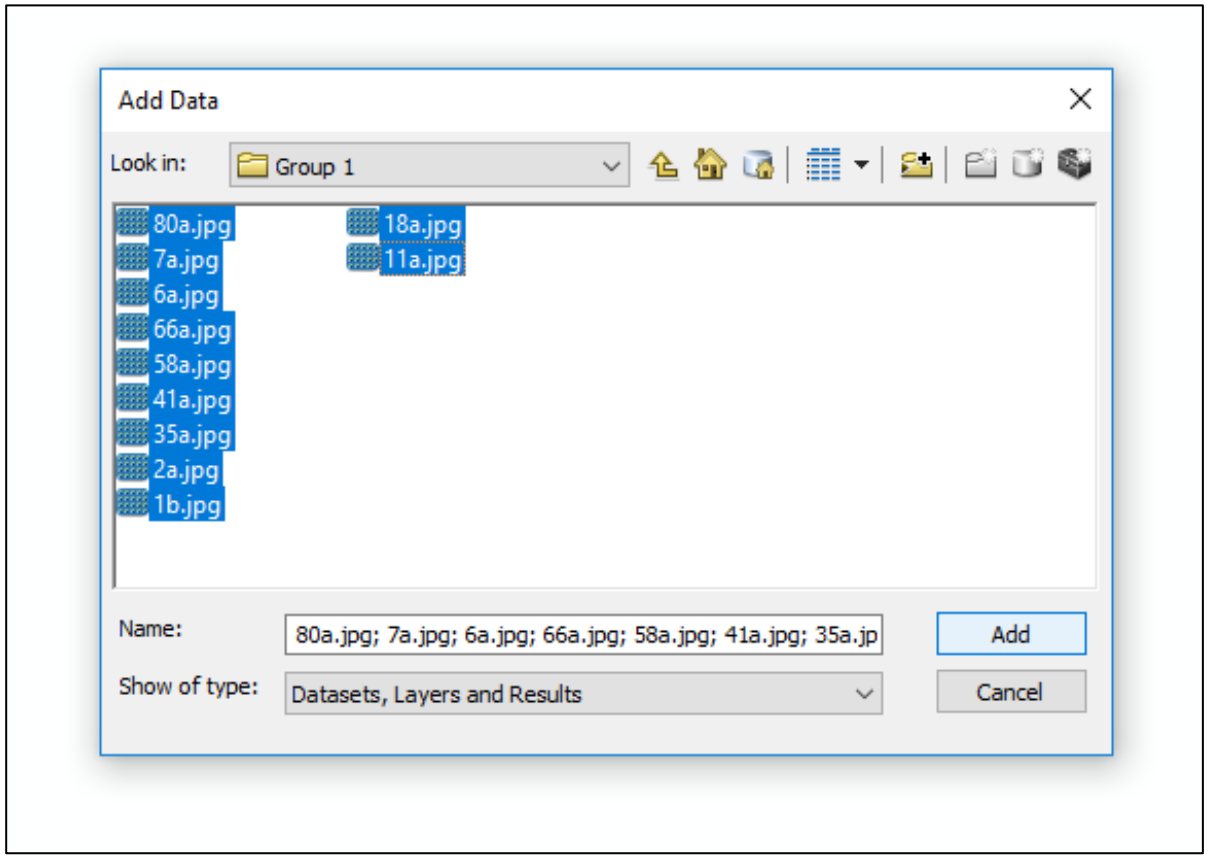

Figure 3.4 *Importing JPEG files into ArcMap*

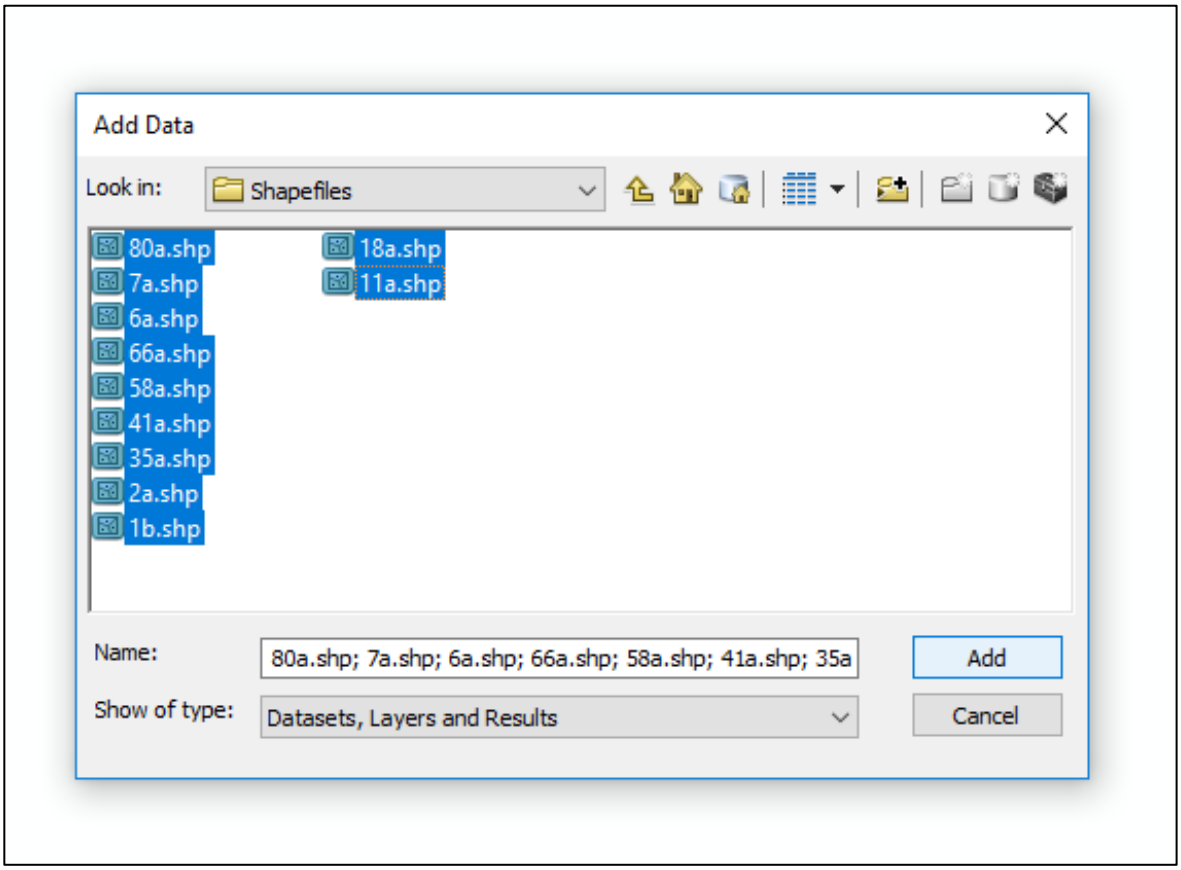

Figure 3.5 *Importing shapefiles into ArcMap*

Create Features toolbar was used to create the outline of the frontal sinus (Figure 3.6). To create the outline, the computer mouse was used to click around the perimeter of the entire sinus (Figure 3.7). The polygon tool places one point per click and the points are linked by lines. Sinuses that have a lot of shape change will require more points to be placed by the user than frontal sinuses that have less shape change and more straight segments. For example, a square can be accurately digitized by only placing a point at each corner, but a lake with very curved borders will require more points to be placed along those borders to accurately capture the curved shape of the lake. Once the user has clicked around the entire sinus with as many points as necessary to sufficiently capture the shape, a polygon is created (Figure 3.8). The polygon is then saved to its corresponding shapefile.

The radiograph JPEG data layers were then unselected in the table of contents so that only the frontal sinus polygons were visible in ArcMap (Figure 3.9). In ArcMap, each polygon shape is considered a feature layer and each polygon or feature has an attribute table automatically produced by ArcMap. An attribute table contains fields (columns) and records (rows), where each field is a specific attribute or characteristic of that feature. For example, a polygon that represents a city may have fields in the attribute table for total population, gross median income, demographics, and more. For each polygon, the attribute table contains three fields: Feature Identifier (FID), Shape (which in this case is polygon), and Identifier (ID). The FID and ID fields are automatically generated by ArcMap. In addition to these fields, other attributes can be manually added as fields by the user. For this study, three new fields were added to each polygon's attribute table: *AM_ID* or *PM_ID* for AM or PM polygons, respectively, *Area*, and *Perimeter* (see Figure 3.10). Using the editor tool, the anonymized donor ID was

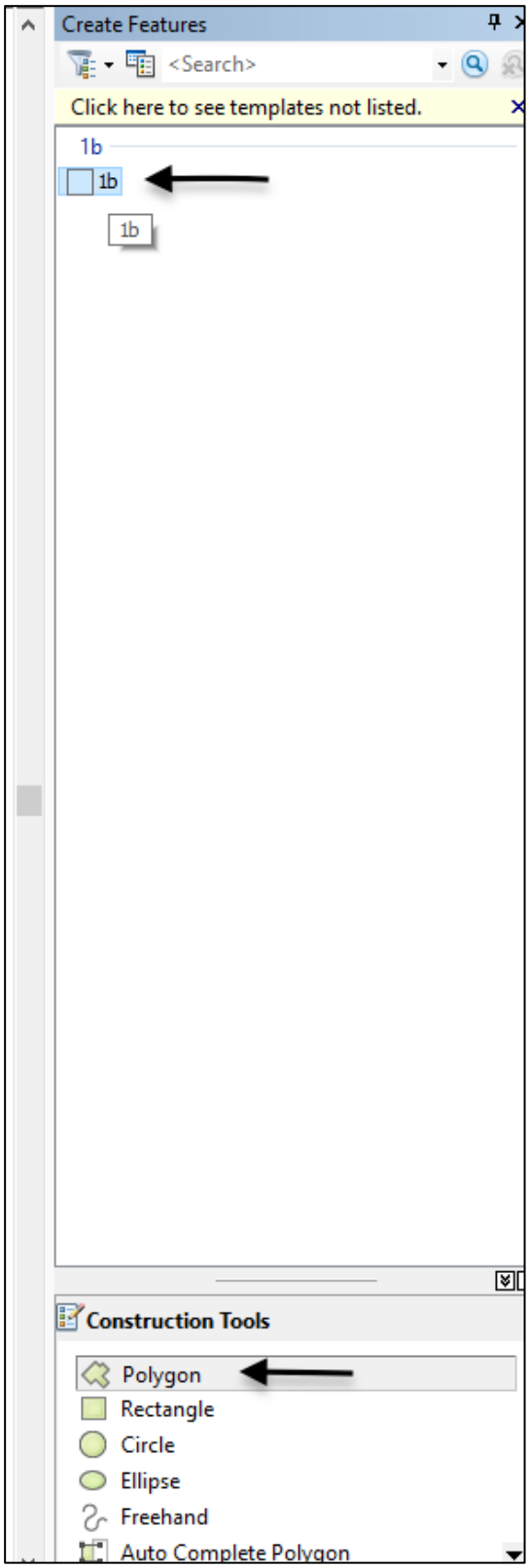

Figure 3.6 *Create Features tool*

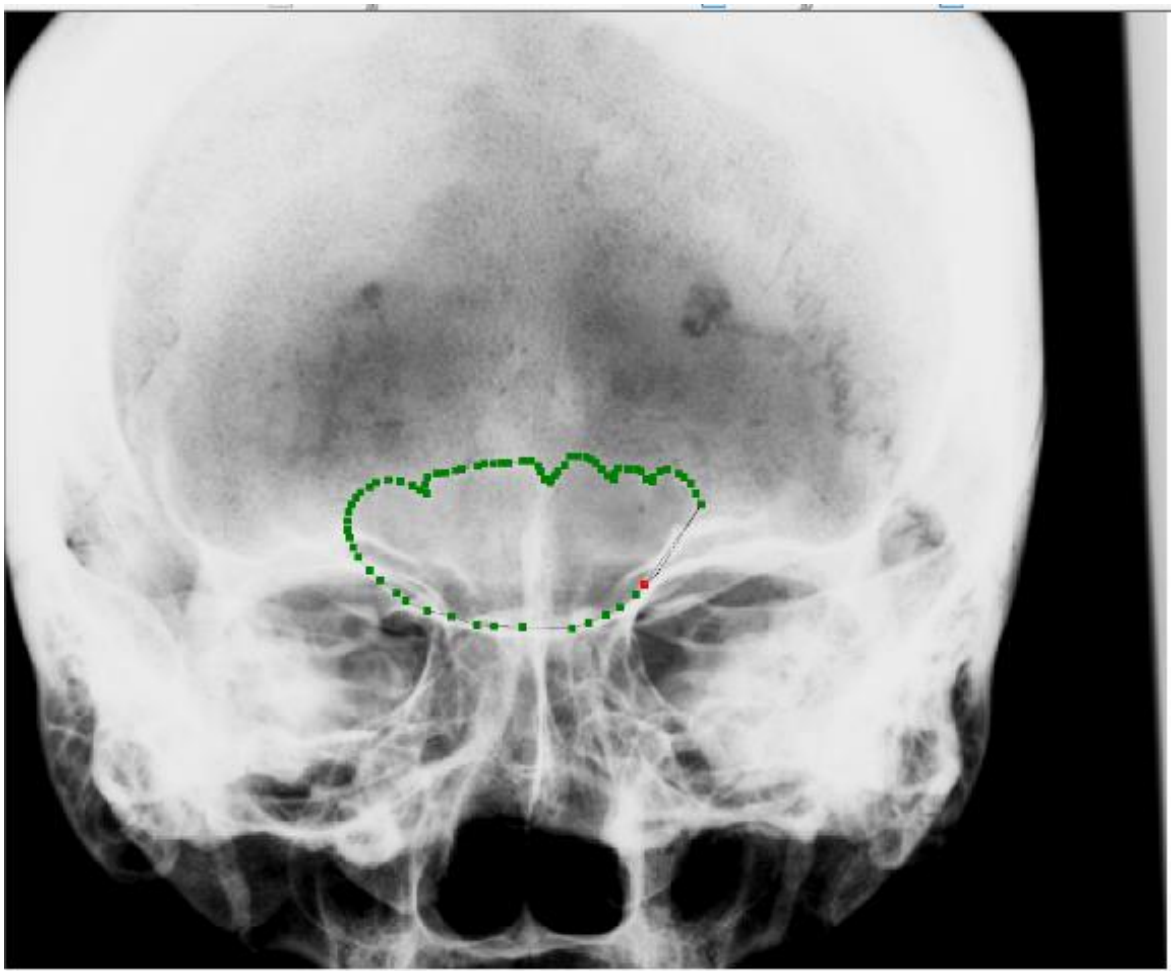

Figure 3.7 *Digitizing the frontal sinus*

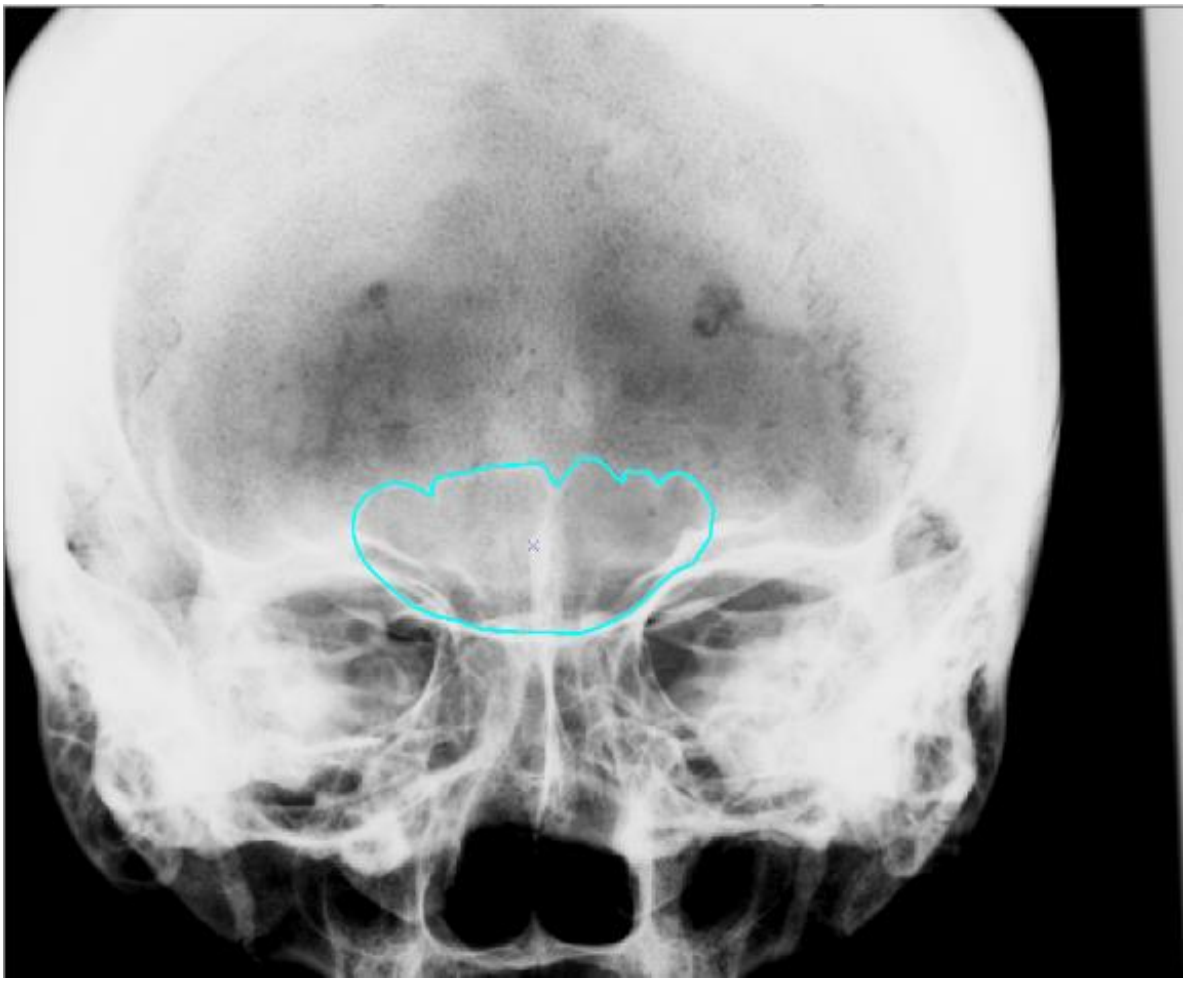

Figure 3.8 *Completed frontal sinus polygon*

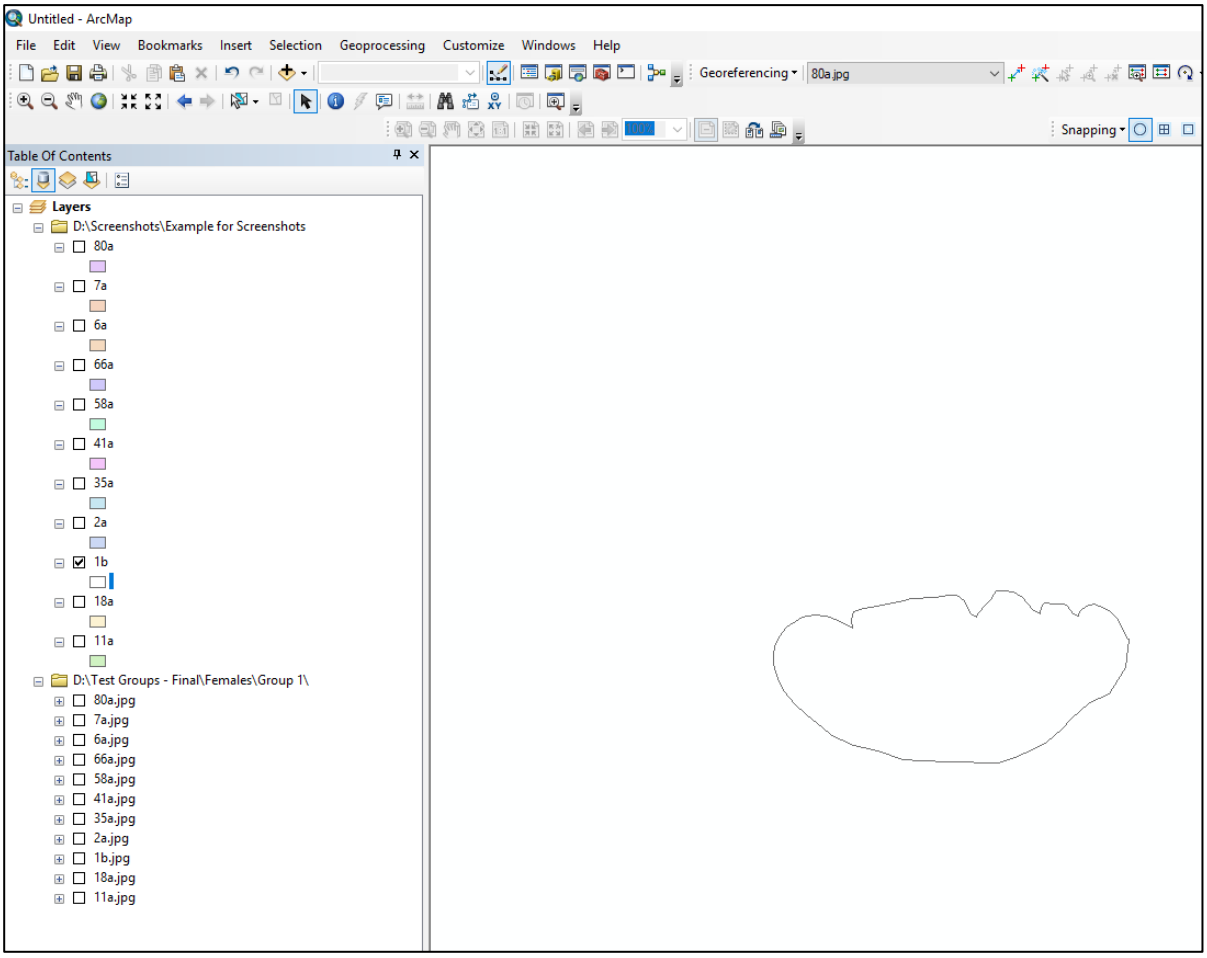

Figure 3.9 *Frontal sinus polygon without the radiograph*

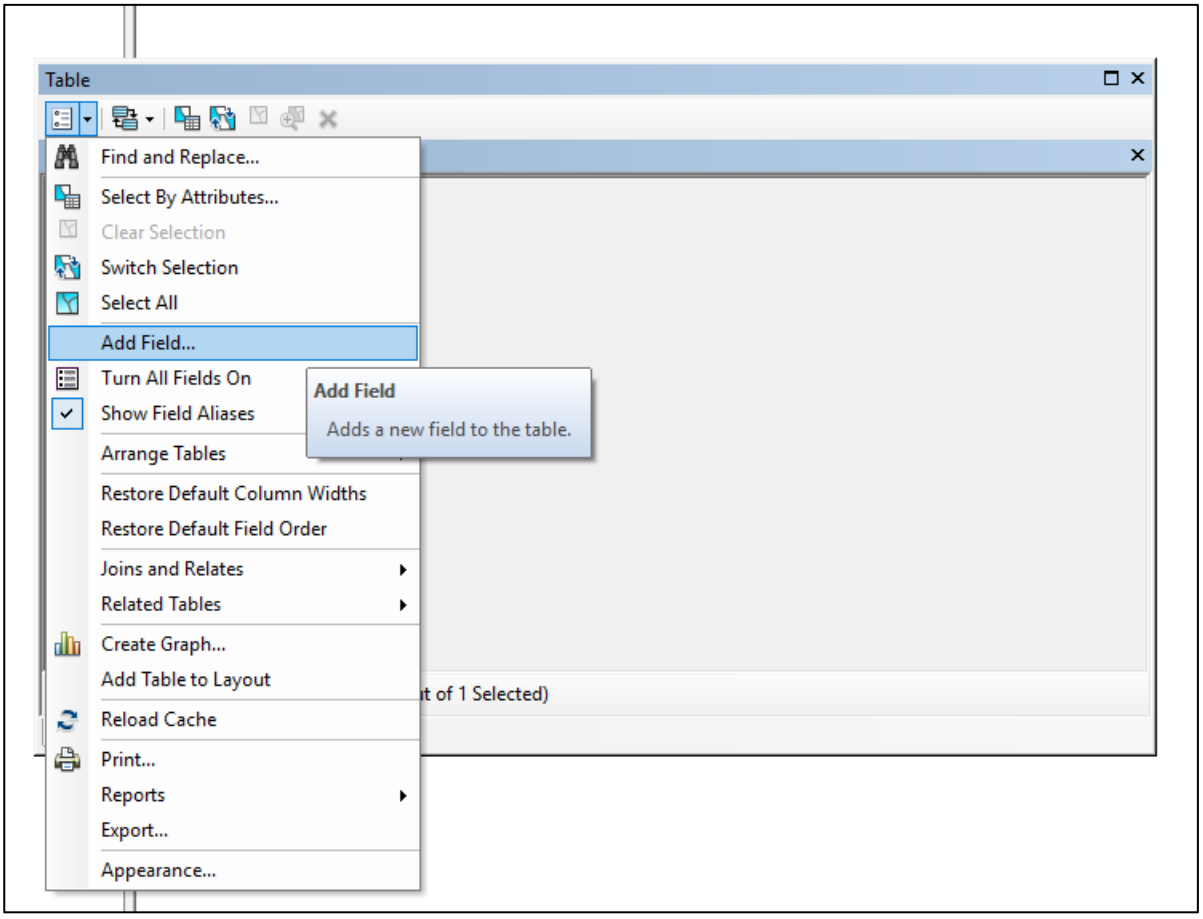

Figure 3.10 *Adding new field to attribute table*

manually entered under the *AM_ID/PM_ID* field for each polygon to ensure that each polygon's attribute table also contained its ID number for easy tracking.

Calculating Area and Perimeter

ArcMap can automatically calculate the geometry of polygons, including the area and perimeter values, by right-clicking on the field in the attribute table. In this case, the user right-clicks on the *Area* and *Perimeter* fields, selects *Calculate Geometry* from the drop-down menu, and then selects either *area* or *perimeter* from the drop-down menu (see Figures 3.11 – 3.13). ArcMap automatically calculates area or perimeter for that polygon and adds the value to the corresponding field in the attribute table (see Figure 3.14).

The resulting values are not labeled with units in the metric or imperial system (meters, centimeters, feet, inches, etc.) because a geographic projection was not applied to the radiographs. For example, an aerial image of a national park will have geographic locational information and units of measurement, like meters, tied to it allowing any measurement to be done in meters. This study is using ArcMap in a way that is outside of its intended purpose by assessing features of the skull *as if* they are geographic features. While skeletal features are not calculated in geographical spatial units and are not geographic features of the Earth, the area and perimeter of the features can still be calculated because the radiographs, once imported, exist in a defined relational space. Each data layer that is added is assumed to be spatially related unless the user tells ArcMap otherwise. So, the area and perimeter values are meaningful in relation to one another and the values can be assessed.

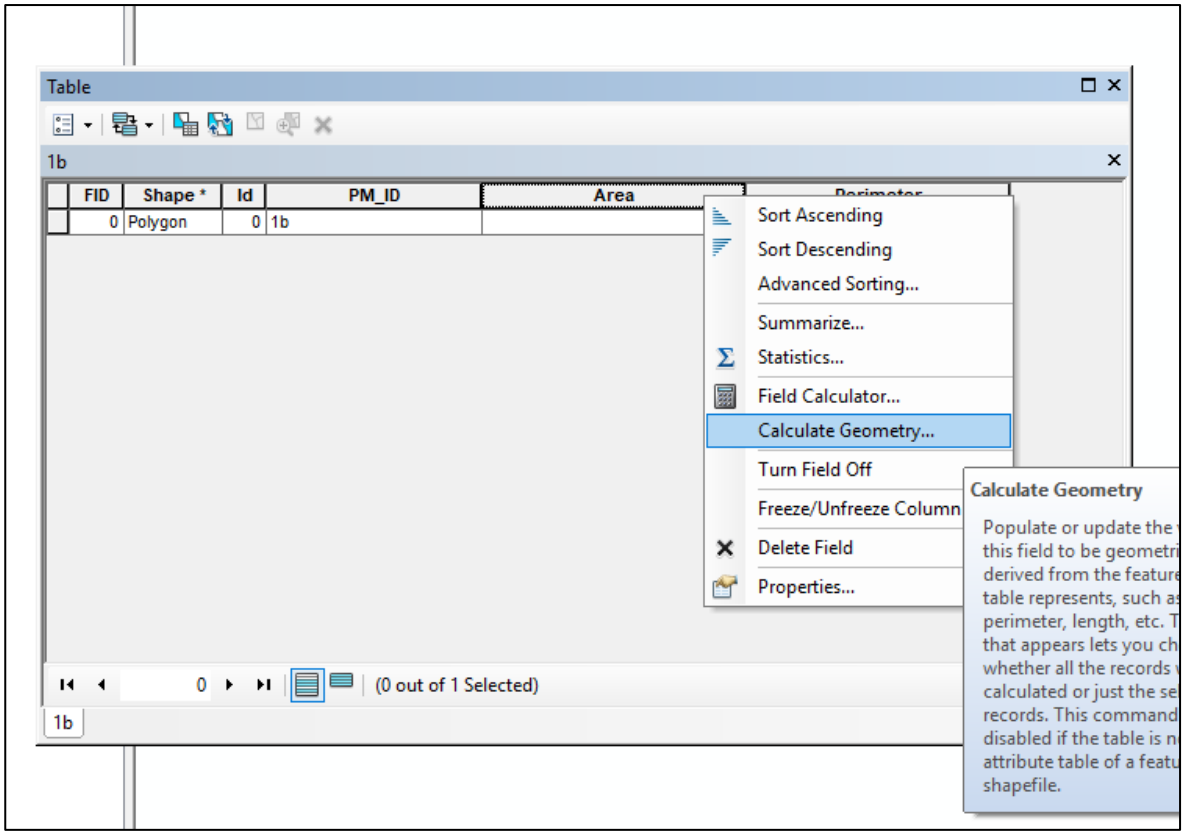

Figure 3.11 *Calculate Geometry tool*

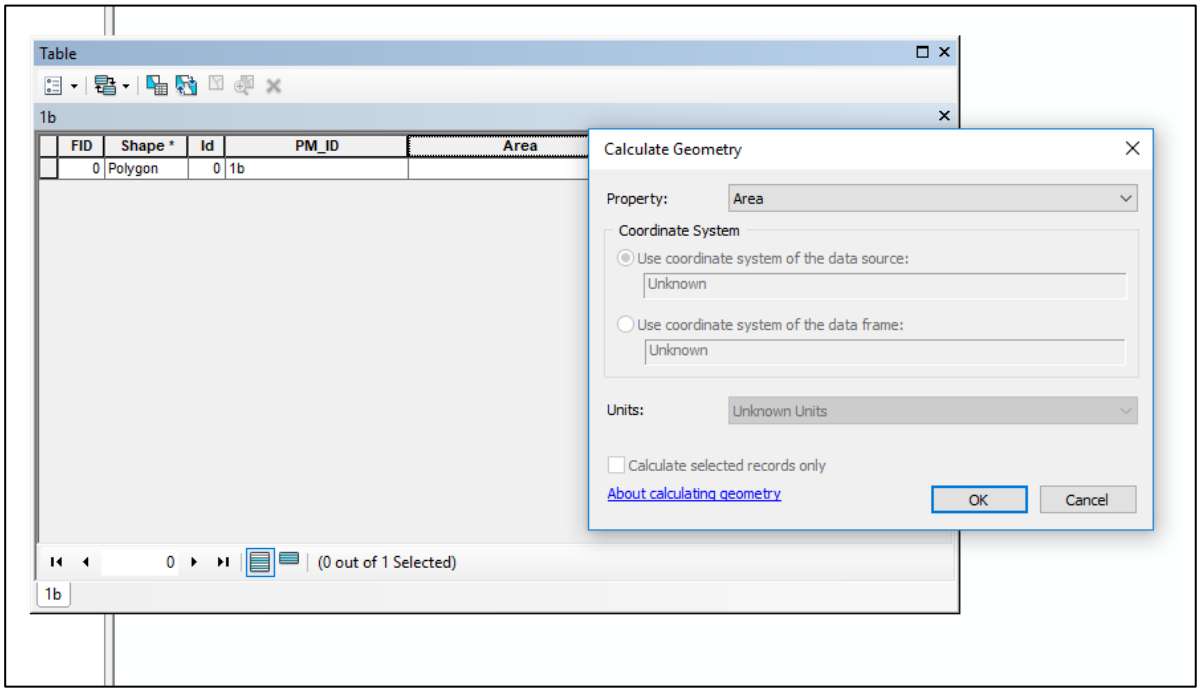

Figure 3.12 *Calculating area*

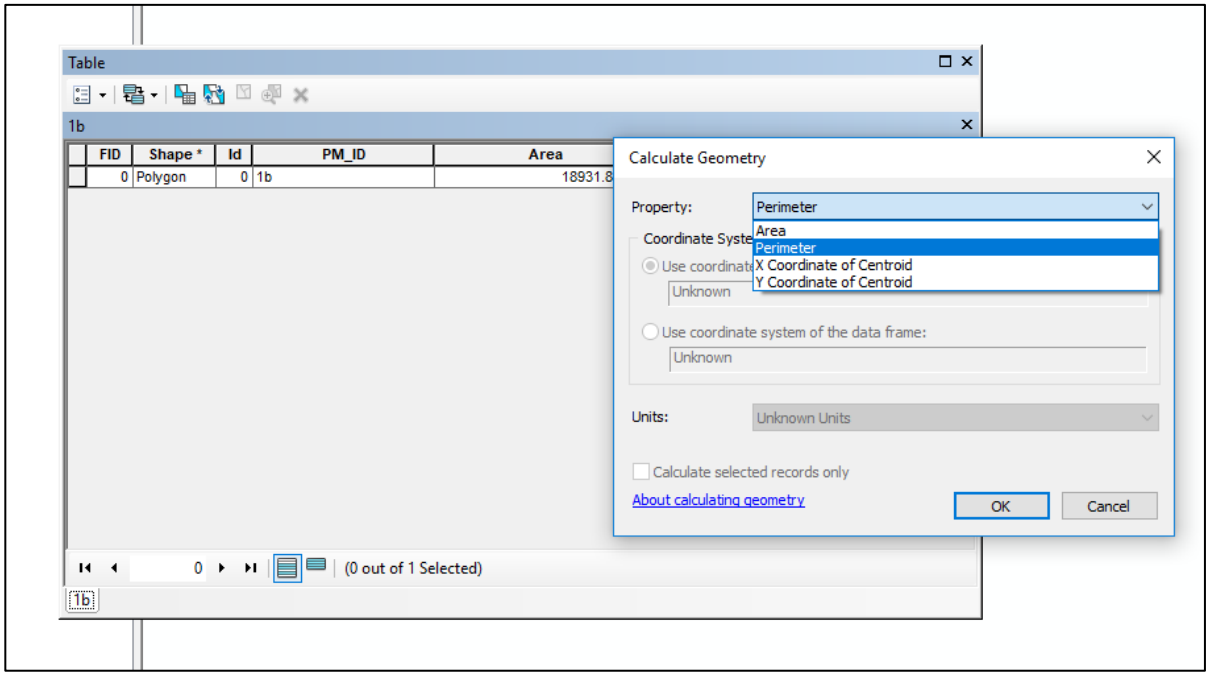

Figure 3.13 *Calculating perimeter*

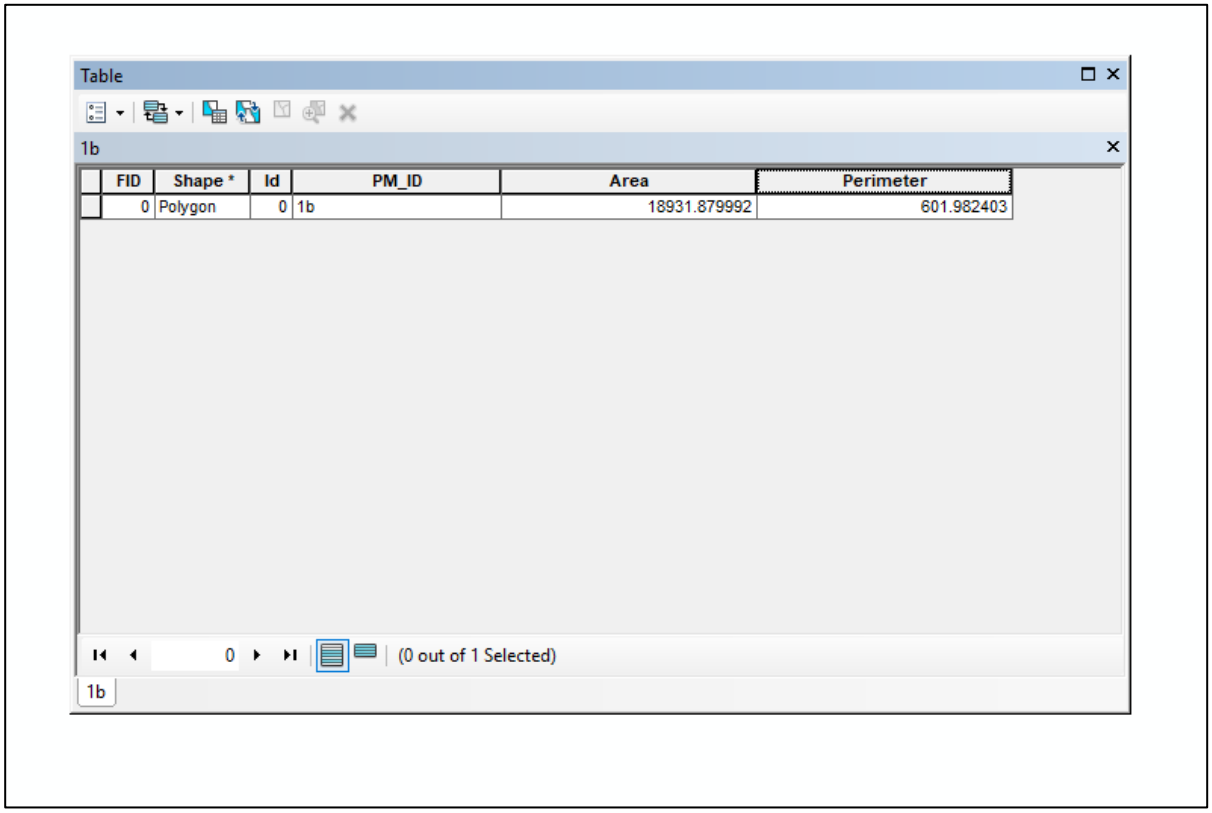

Figure 3.14 *Final geometry calculation in attribute table*

A frontal sinus polygon that has a larger area and perimeter value than another polygon can still be said to be different relative to that polygon. However, if the radiographs are not the same dimensions or were taken at different orientations then the polygons would not be able to be compared directly.

Similarity Search

Once area and perimeter were calculated for each polygon the AM polygon shapefiles were merged into one data layer using the *Merge* tool (see Figure 3.15). This tool combines the polygons into one data layer, which combines their attribute tables into one table where each row represents one polygon (see Figure 3.16). Once the polygons have been merged into a single data layer, the Similarity Search tool can be used. This tool is part of ArcMap's *Mapping Clusters* toolset which is part of the *Spatial Statistics Toolbox* in *Arc Toolbox*. The mapping cluster tools are designed to identify spatial clusters and outliers. Similarity Search can identify *Candidate Features* that are most similar or dissimilar to the *Input Features to Match* based on averages of the *Attributes of Interest*. *Candidate Features* are ranked from most to least similar by a similarity index value that is calculated by Similarity Search. Similarity Search calculates the similarity index from standardized values of the *Attributes of Interest*, which were area and perimeter. This involves a Z – transform of the attribute values. The Z – score is calculated by subtracting the mean of all values from each attribute value and then dividing that by the standard deviation for all values (both the Input Features to Match and Candidate Features). This Z – transform puts all of the data on the same scale. Once this is complete, Similarity Search calculates the similarity index value for each Candidate Feature. This is done by subtracting the standardized values (area and perimeter) of each Candidate Feature from the standardized values of the Input Feature to Match (area and perimeter), squaring the difference, and adding the

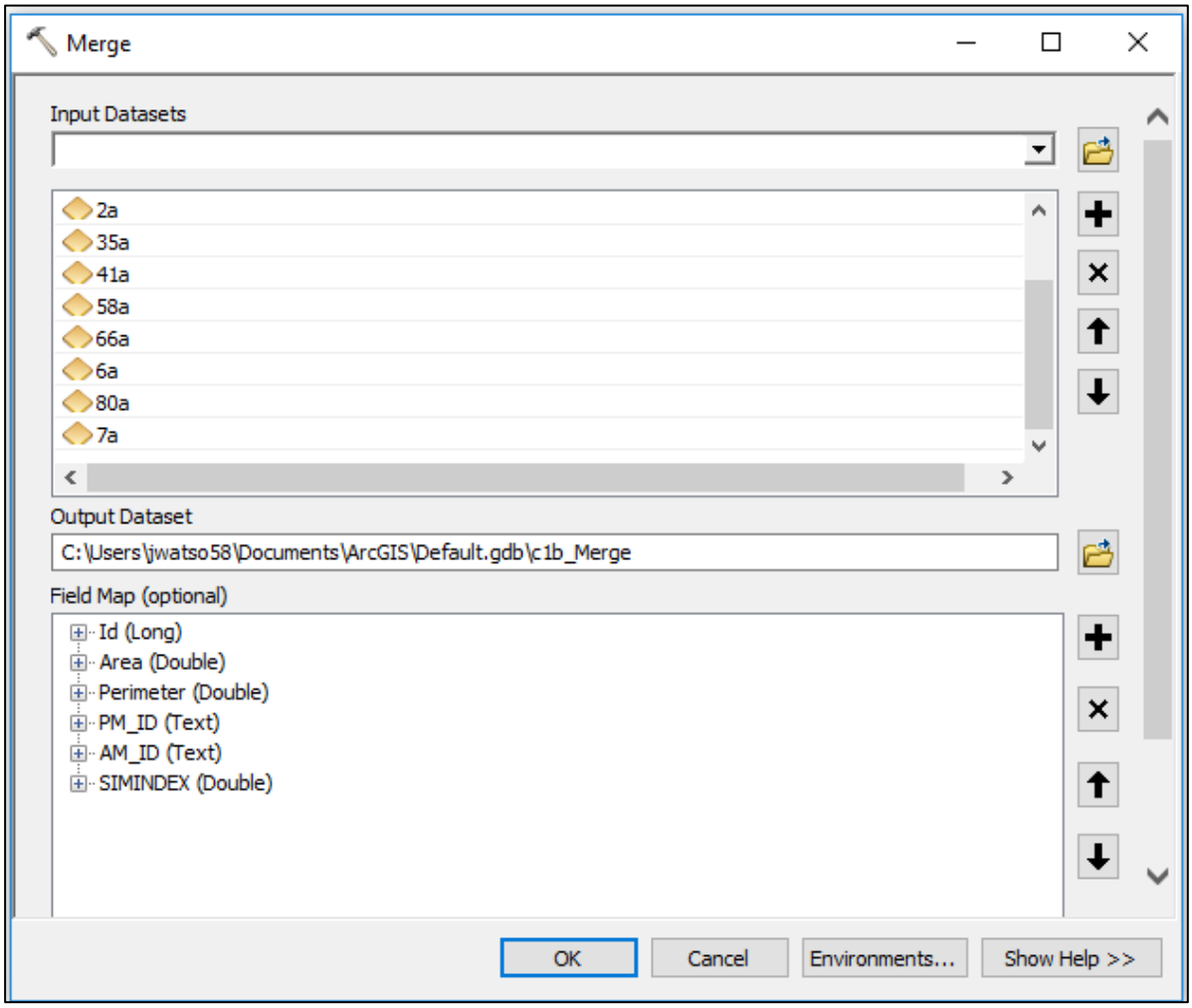

Figure 3.15 *Merge tool*

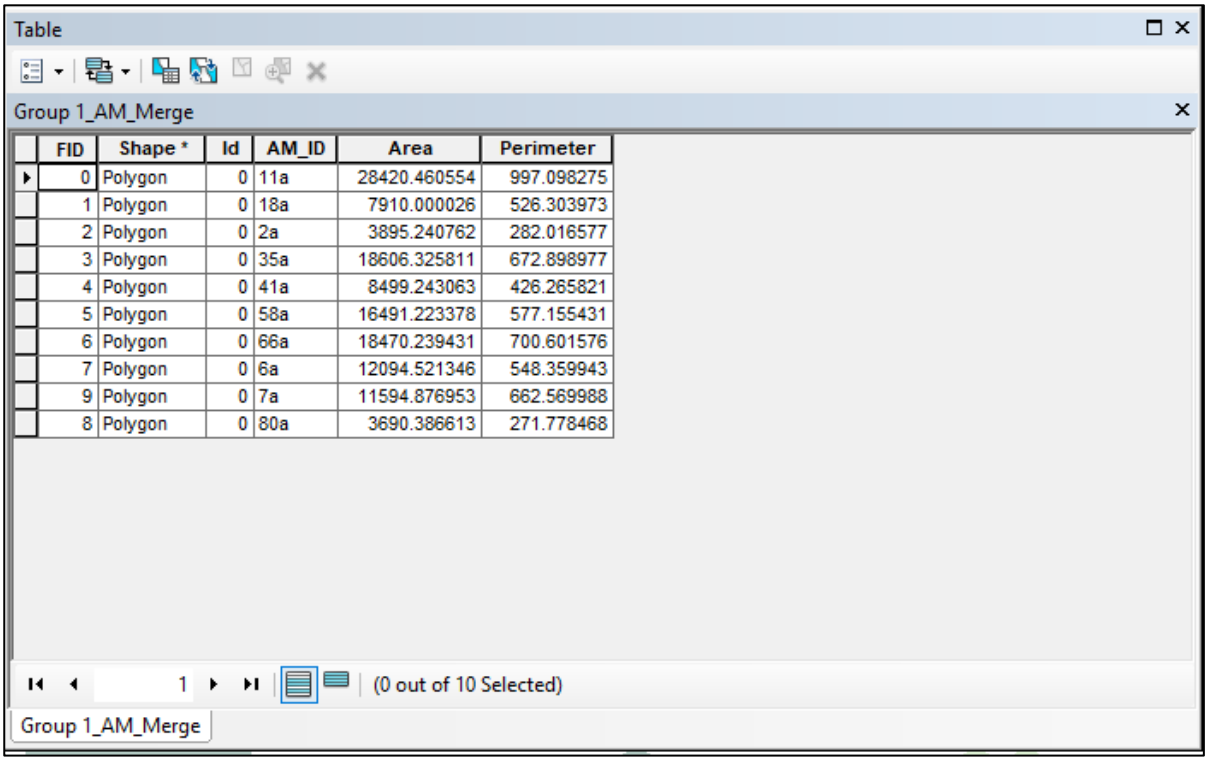

FID	Shape *	Id	AM_ID	Area	Perimeter
0	Polygon	0	11a	28420.460554	997.098275
1	Polygon	0	18a	7910.000026	526.303973
2	Polygon	0	2a	3895.240762	282.016577
3	Polygon	0	35a	18606.325811	672.898977
4	Polygon	0	41a	8499.243063	426.265821
5	Polygon	0	58a	16491.223378	577.155431
6	Polygon	0	66a	18470.239431	700.601576
7	Polygon	0	6a	12094.521346	548.359943
9	Polygon	0	7a	11594.876953	662.569988
8	Polygon	0	80a	3690.386613	271.778468

Figure 3.16 *Attribute table for merged AM polygons*

squared differences together. The sum of the squared differences is the similarity index value that is used to rank each Candidate Feature from lowest index value (most similar) to highest index value (least similar) (pro.arcgis.com 2018a).

This tool is used in many scenarios within geography such as finding cities that have similar population levels and demographics or finding crimes within the past month that share specific attributes such as location and number of victims with one specific type of crime. For this study, Similarity Search identifies which AM frontal sinus polygon (Candidate Features) is most similar to the PM frontal sinus polygon (Input Features to Match) based on area and perimeter values (Attributes of Interest) in order to test the hypothesis that ArcMap and its tools (Similarity Search) can identify a frontal sinus match for the purpose of positive identification (pro.arcgis.com 2018b).

For each of the 120 test groups the *Input Features to Match* was the PM frontal sinus polygon, the *Candidate Features* was the merged data layer of all 10 AM frontal sinus polygons, and the Similarity Search tool was instructed to produce a list of 10 results ranking the polygons from most similar to least similar based on the area and perimeter values of the PM polygon (Figure 3.17). Once this information was entered, Similarity Search began its analysis and produced 10 polygons that were all color-coded in a blue gradient based on their similarity to the PM frontal sinus (Figure 3.18). In the ArcMap table of contents each color is coded with a number one through five. One, most similar, is coded as dark blue and five, least similar, is coded as a light blue/green to visually show the most and least similar polygons as well as the progression of the polygons from most to least similar (Figure 3.19).

The Similarity Search results also have an attribute table that lists the similarity rank of each polygon and its similarity index (SIMINDEX), which is a numerical value that represents

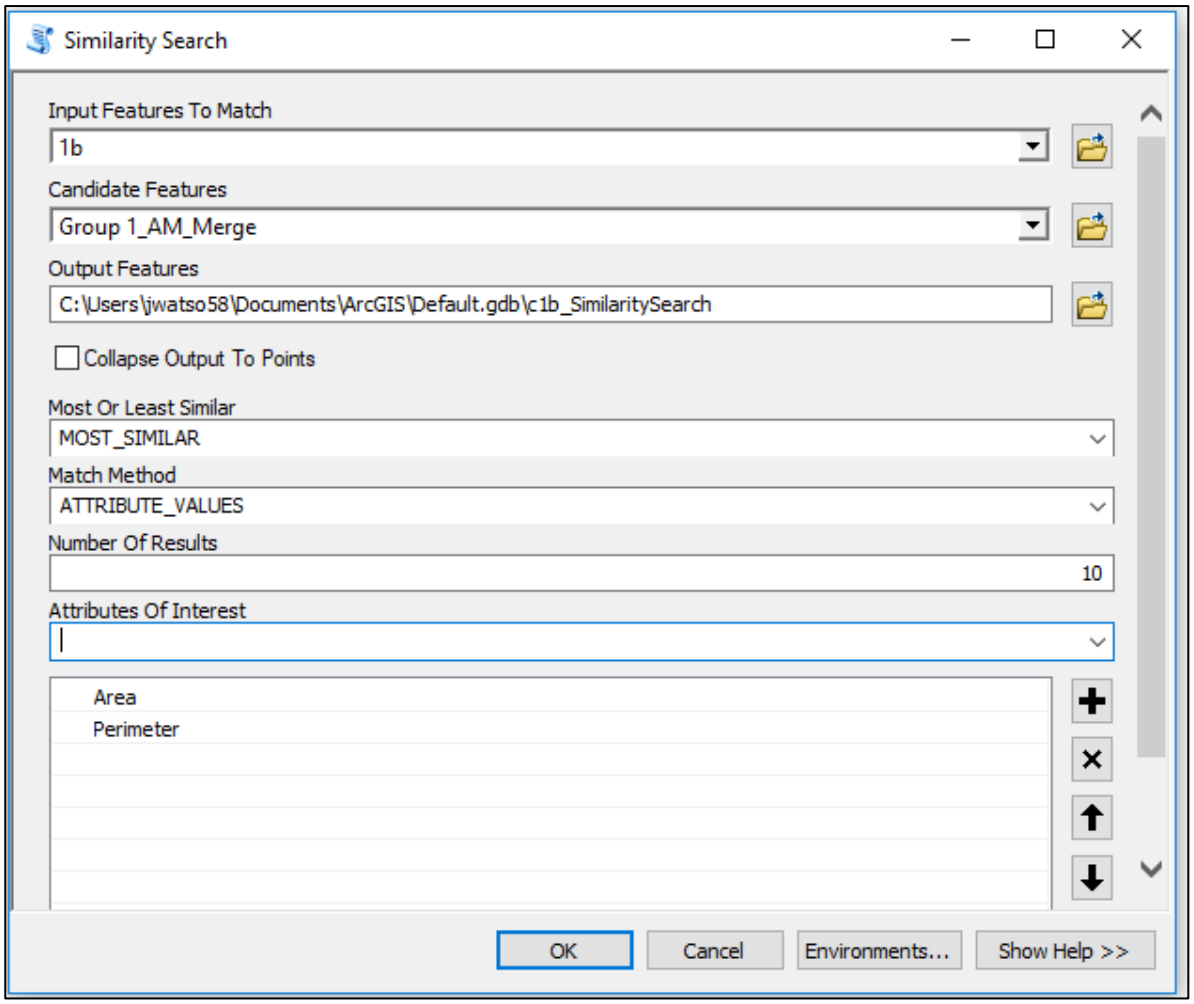

Figure 3.17 *Similarity Search tool*

Figure 3.18 *Polygons color coded from most similar (blue) to least similar (light green)*

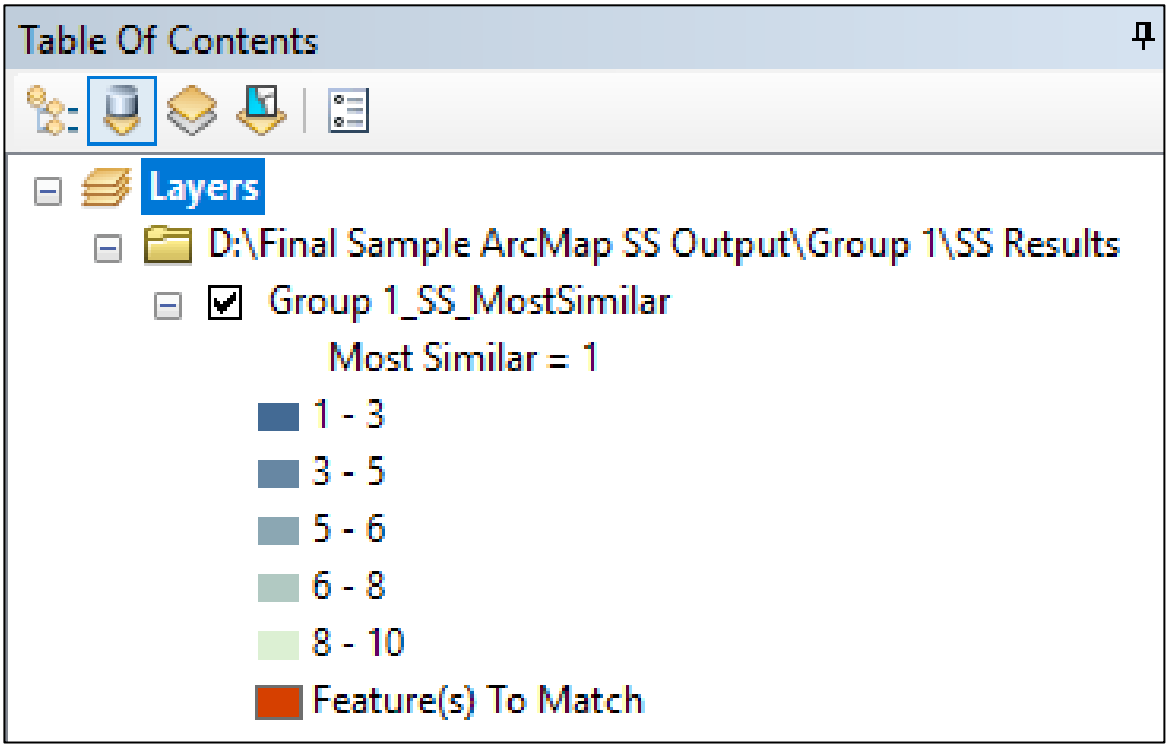

Figure 3.19 *Table of Contents displaying color codes*

how similar that polygon is to the PM polygon. Polygons with a similarity index closer to zero are more similar to the PM polygon than polygons with a similarity index farther from zero. A similarity index of 0 indicates a perfect match (Figure 3.20).

Analysis

Inter-observer Variation

SPSS 25 was used to calculate all of the statistical tests for this study (IBM Corp Released 2017). An inter-observer study was conducted to assess how different practitioners might create differently-shaped polygons based on the same frontal sinus scan. Quality of the JPEG radiograph images, exposure, contrast, the computer screen, and personal experience assessing frontal sinuses can all affect how the observer chooses which areas to include in the frontal sinus outline and how to define the lower boundary of the sinus, which can be very unclear on radiographic images. To assess inter-observer variation, a group of faculty (N = 4), including a post-doctoral researcher, and graduate students (N = 6) from the Department of Anthropology at the University of Tennessee were asked to create polygons for one test group (11 radiographs total) (Appendix 2). Each participant was provided access to the same computer loaded with the ArcGIS 10.5 software, the radiograph images, and shapefiles. Therefore, each participant was only required to digitize the frontal sinuses. Participants were also provided verbal and written instructions on how to create the frontal sinus polygons. Once each participant completed the polygons for the test group, area and perimeter values were calculated for each polygon in the attribute tables using the *Calculate Geometry* tool in ArcMap.

Next, all of the polygons created during the inter-observer study, along with the corresponding polygons created during the original study, were moved into separate folders for

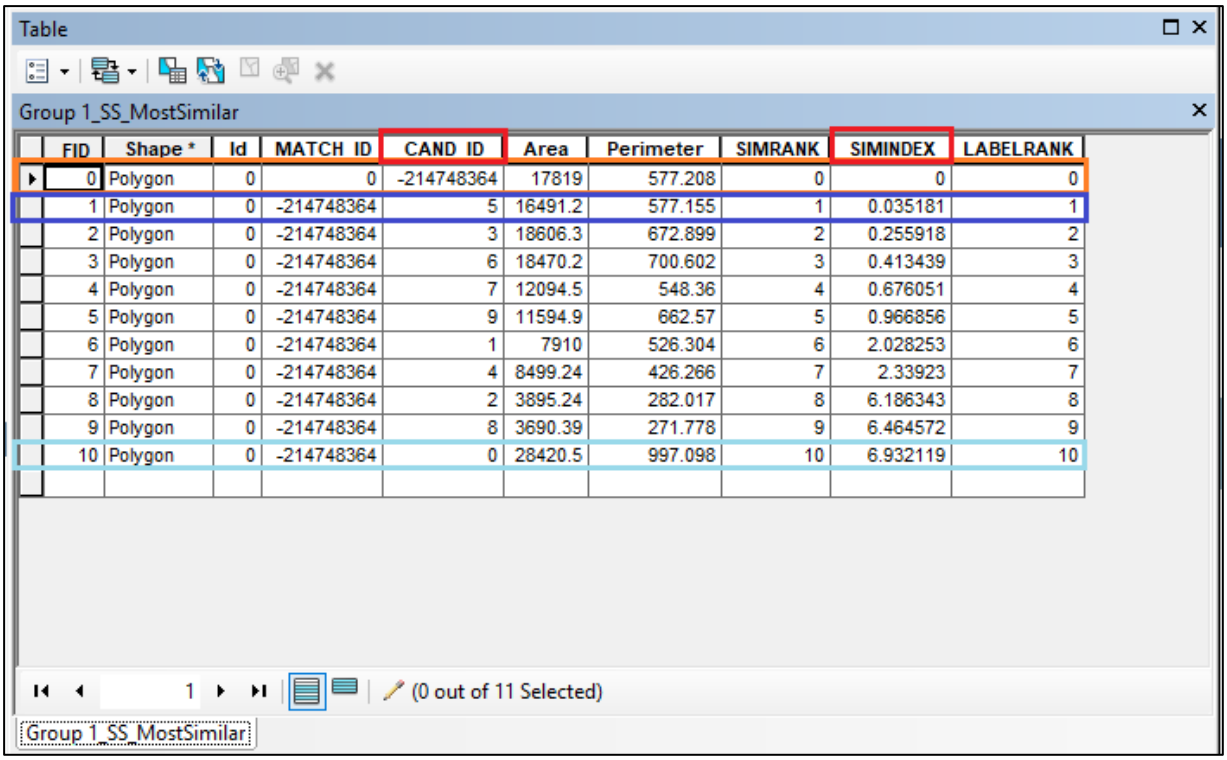

FID	Shape *	Id	MATCH_ID	CAND_ID	Area	Perimeter	SIMRANK	SIMINDEX	LABELRANK
0	Polygon	0	0	-214748364	17819	577.208	0	0	0
1	Polygon	0	-214748364	5	16491.2	577.155	1	0.035181	1
2	Polygon	0	-214748364	3	18606.3	672.899	2	0.255918	2
3	Polygon	0	-214748364	6	18470.2	700.602	3	0.413439	3
4	Polygon	0	-214748364	7	12094.5	548.36	4	0.676051	4
5	Polygon	0	-214748364	9	11594.9	662.57	5	0.966856	5
6	Polygon	0	-214748364	1	7910	526.304	6	2.028253	6
7	Polygon	0	-214748364	4	8499.24	426.266	7	2.33923	7
8	Polygon	0	-214748364	2	3895.24	282.017	8	6.186343	8
9	Polygon	0	-214748364	8	3690.39	271.778	9	6.464572	9
10	Polygon	0	-214748364	0	28420.5	997.098	10	6.932119	10

Figure 3.20 *Similarity Search results attribute table. Red = the similarity index value and the Candidate ID of each polygon. Orange = Input Feature to Match (PM polygon. Dark Blue = polygon ranked as most similar. Light blue = polygon ranked as least similar*

each individual using ArcCatalog. Once all of the individuals were organized into their respective folders in ArcCatalog, each donor's polygons (11 total) were imported into a new ArcMap file. The 10 polygons created by the inter-observer participants were merged into a single data layer using the *Merge* tool. The Similarity Search tool was run for each donor's group of 11 polygons where the polygon I created was the *Input Feature to Match,* and the inter-observer participants' merged polygons (10 total) were the *Candidate Features*. Similarity Search was instructed to produce 10 results and to indicate the most similar polygon based on the area and perimeter values. The Similarity Search output was the same as the 100 test groups described previously with the most similar polygon labeled as "1" and indicated with a dark blue color, and the least similar polygon labeled as "10" and indicated with a pale blue/green color. Once this was complete for all 11 donors in the inter-observer test group, the Similarity Search attribute tables for each donor were exported as an electronic spreadsheet.

Hierarchical cluster analysis using Ward's Method with four defined clusters was used to see how the inter-observer participants clustered based on the area and perimeter values of their polygons. Kolmogorov-Smirnov (KS) and Shapiro-Wilk (SW) tests of normality were also run and Q-Q Plots were produced on the clusters for area, perimeter, and similarity index values to see if the data for each of these values was normally distributed. The Coefficient of Variation ($Cv = \frac{\sigma}{\mu}$), which is the ratio of the standard deviation (σ) to the mean (μ), was calculated from the average area and perimeter values of the polygons created for each donor by the interobserver participants. The C_v value will show the extent of variability in relation to the mean of each donor polygon. It is important to establish the variability in how the frontal sinus polygons were created by different individuals as this variability could affect the area and perimeter values of the polygons, which in turn could affect the Similarity Search results. Using

the means of the area and perimeter values of each observer's polygons, Levene's test and a one – way ANOVA were conducted to analyze the variance among observers. Descriptive statistics were produced for the area, perimeter, and similarity index values for each cluster and each observer. Finally, the inter-observer polygons Similarity Search identified as most and least similar for each donor were reported.

Intra-observer Variation

Intra-observer analysis was conducted to assess my consistency in creating multiple polygons for the same individual. Some of the same factors that may influence the shape of the polygons between observers may also affect the shape of polygons created by a single observer. For example, image quality and familiarity with the frontal sinus will affect the ability of the observer to distinguish the full boundaries of the sinus, as well as overall fatigue from repetitive clicking with a mouse. Using a computer mouse, I created frontal sinus polygons in ArcMap for 120 test groups, each containing 11 individuals for a total of 1,320 polygons. The 60 female groups and 60 male groups were each created from a pool of 49 males and 49 females, respectively. As a result, an individual's AM radiograph is present in multiple test groups – and each time it was part of a test group the sinus was traced to create a new polygon. Therefore, multiple polygons from a single individual can be compared for variability in similarity index, area, and perimeter values. Of the 100 donors in my sample, 98 could be assessed for intra-observer variability. Two individuals that could not be assessed for intra-observer variation because one (192a) was only present in one test group, and the other (162a) was only present in three groups, which is too few replicates to successfully conduct a Similarity Search test. This condition occurred because the test groups were created by randomly selecting donors from the sample pool so not all donors appeared in the same number of test groups.

In order to assess intra-observer variability, all of the polygons created for each donor were moved into their own folders using ArcCatalog in the order in which they were created. For example, individual 11a was digitized 25 times. The polygons for individual 11a were moved into a new folder in the order in which they were digitized, with the first polygon labeled as 11a and all subsequent polygons named 11a (1), 11a (2), etc. so that each polygon could be differentiated. Once each donor was contained in an individual folder, their polygons were imported into a new ArcMap file. All polygons, except for the first one created, were merged into a single data layer using the *Merge* tool. Similarity Search was run for each donor's group of AM polygons. The first polygon, which was left out of the merged set, was the *Input Feature to Match* and the merged polygons were the *Candidate Features*. I instructed Similarity Search to produce the same number of results as there were polygons in the merged data layer so that each one would receive a similarity rank, and I instructed the tool to indicate which was most similar to the Input polygon based on the area and perimeter values. Once this was complete for all 98 donors, each donor's Similarity Search output attribute table was exported into a separate electronic spreadsheet. This attribute table contained the similarity rank of each AM polygon for that donor, the area and perimeter values, and the similarity index value. The mean, standard deviation, minimum and maximum values were calculated for each donor's polygons from the area, perimeter, and similarity index values. The Coefficient of Variation (C_v) was calculated from the average area and perimeter values of the polygons for each donor that appeared in multiple test groups (N = 98). The C_v will show the extent of variability in terms of area and perimeter within each donor.

Similarity Search Accuracy

A spreadsheet was developed to track the Similarity Search results and record whether Similarity Search identified the true match as the most similar or not. Out of the 100 test groups that contained a true match, the number of groups where Similarity Search correctly identified the true match as "most similar" was recorded. The percentage of correct identifications was calculated and recorded in the spreadsheet. Descriptive statistics were also produced for area, perimeter, and similarity index values of the male and female AM polygons that were correctly identified as most similar. Where Similarity Search did not correctly identify the true match as "most similar", the ID of the polygon identified as most similar was recorded along with the similarity rank of the true match.

No True Match vs. True Match

Radiographs from the 20 donors who comprised the 20 no-match groups were also included in the 100 groups that contained a match, as part of the comparative polygons. Therefore, the similarity index value of each donor's true match polygon was able to be compared to the similarity index value of the polygon that Similarity Search identified as most similar, when no true match was present. A new electronic spreadsheet was developed to include Donor ID, True Match, No True Match, and SIMRANK (Similarity Rank). The True Match column contained the similarity index value of each donor's true match, regardless of whether Similarity Search correctly identified it as "most similar". The No True Match column contained the similarity index value of the polygon Similarity Search identified as "most similar" when no true-match was present. The SIMRANK column contained the Similarity Rank of the true match value. This was done to show whether Similarity Search correctly identified the true match as "most similar" (rank = 1) or not. The similarity index values are non-normal data so non-

parametric tests were required. A Wilcoxon Signed Rank test was run to assess the statistical difference between the True Match and No True Match similarity index values.

Similarity Index Range for Correctly Identified Polygons

In addition to assessing inter-observer and intra-observer error, the threshold for what is considered a match by the Similarity Search tool had to be established. First, each test group where Similarity Search correctly identified the match was opened in ArcMap. The attribute tables for the Similarity Search results and the AM polygon that is the true match were opened. A new field called *SIMINDEX* was added to the AM polygon's attribute table. From the Similarity Search attribute table, the similarity index value of that same polygon was copied and pasted into the attribute table of the AM polygon. This was done for each test group where Similarity Search correctly identified the match. Each female AM polygon that was correctly identified by Similarity Search was imported into a new ArcMap file, and the same was done for each male AM polygon that was correctly identified by Similarity Search. The attribute tables for these polygons then contained their similarity index value. All of the female AM polygons were merged into one data layer using the *Merge* tool, and the same was done for all of the male AM polygons. Once this was complete all of the polygons and their attributes were combined into one attribute table and the similarity index values of the female sample and the male sample were able to be viewed. This allows the observer to see the entire range of similarity index values for polygons that were correctly identified by Similarity Search, which will inform the threshold for a similarity index value to be considered a potential match.

Each Donor to Entire Sample

Similarity Search was re-run again on each individual in the sample. The *Input Feature to Match* was the PM polygon of each donor, but instead of only searching for *Candidate Features* in a test group of 10 individuals it searched for matches from the entire sample of 100 male or female AM and PM frontal sinus polygons. So, each PM polygon for the female donors was compared to one AM and one PM polygon from every female in the sample (100 polygons total). The same process was completed for the male donors. Each process produced 100 Similarity Search output attribute tables (one for each donor in the sample), which were exported into electronic spreadsheets. Hierarchical cluster analysis using Ward's Method with four defined clusters was conducted based on the area and perimeter similarity index values of the polygons. For each donor's PM polygon, descriptive statistics were produced from the area, perimeter, and similarity index values of the donor polygons that appeared in each of the four clusters. So, the mean, standard deviation, minimum, and maximum values were produced for clusters 1 – 4. Using the minimum and maximum similarity index values of cluster 1 for every donor, a similarity index range can be determined.

Summary

The inter-observer and intra-observer analyses will help to determine if there was significant variation within and between observers. This is important because statistically significant intra and inter-observer variation would mean that the area and perimeter values of each donor's polygons and the polygons created by different observers are significantly different, potentially limiting the universal applicability of this method. Since Similarity Search is identifying which polygon is the most similar based on the area and perimeter values of other

polygons in the test group, significant variation in these values within and between observers will affect the ability of Similarity Search to correctly identify a match.

In addition to understanding the accuracy of Similarity Search and the intra and inter-observer variation, a threshold of similarity index values needs to be established. Using the results of the cluster analyses, and the range of similarity index values of correctly identified polygons, an overall range of similarity index values can be established. If successful, this range is designed to be used by an examiner to determine if the similarity index value of the frontal sinus polygon Similarity Search identified as the "most similar" indicates a potential match or not.

CHAPTER 4: RESULTS

This chapter presents results from the statistical analyses discussed in chapter 3. First, the results of the inter-observer cluster analyses and the coefficient of variation and descriptive statistics for each observer are presented. Next, the coefficient of variation results for the intra-observer analysis are presented. The overall accuracy of the Similarity Search tool and descriptive statistics for the donors it correctly identified as most similar are presented. The two similarity index values for the donors present in test groups where the true match was present, and where the true match was not present, assessed using Wilcoxon Signed Rank test, are presented. Finally, the similarity index range for correctly identified polygons, and Hierarchical Cluster Analyses of the Similarity Search results for each male and female donor compared to every other male and female donor, respectively, are presented. The overall similarity index range for males and females is determined from these cluster analyses. The following chapter, chapter 5, is a discussion of these results.

Inter-observer Variation

Hierarchical Cluster Analysis

Hierarchical Cluster Analysis using Ward's Method with four defined clusters was conducted to show which donors and which polygons appeared in clusters one through four. Clusters represent groups of polygons that are different from each other, with Clusters 1 and 4 being the most different. All observers (0-9) except for observer 10 had their 11a polygon present in Cluster 1 (Table 4.1).

Table 4.1 *Donors present in Cluster 1 for each observer*

Observer ID	**Donor ID**
0	11a
1	11a
2	11a
3	11a
4	11a
5	11a
6	11a
7	11a
8	11a
9	11a

Cluster 2 consisted of polygons from all 11 observers (0-10). Seven of the observers all had polygons for donors 18a, 41a, 6a and 7a present in Cluster 2, while four observations (4, 5, 8 and 10) deviated from this pattern (Table 4.2). Cluster 3 consisted of polygons for all 11 observers (0-10). Seven of the observers had polygons from donors 1b, 35a, 58a, and 66a present. Again, observers 4, 5, 8 and 10 deviated from this pattern (Table 4.3).

Finally, Cluster 4 consisted of polygons for all 11 observers (0-10) with all observers except observer 5 having polygons 2a and 80a present. The main inter-observer outliers of the observer group were observers 4, 5, 8 and 10. Observers 4 and 5 differed from the majority for donors 41a, 7a, 6a and 80a. Observer 8 differed from the majority for donors 7a and 58a. Observer 10 differed from the majority for donors 1b, 35a, 41a, and particularly 11a which appeared in Cluster 3 as opposed to all other observers whose 11a polygons all appeared in Cluster 1 (Table 4.4).

The Kolmogorov-Smirnov (KS) and Shapiro-Wilk tests show that the area values for all four clusters are not significantly different from a normal distribution (Table 4.5). The KS test showed that the perimeter values in Clusters 1 and 4 are not significantly different from a normal distribution whereas the KS test showed that Clusters 2 and 3 are significantly different from a normal distribution (see Table 4.5). The Q-Q plots for the perimeter values of Clusters 2 and 3 show points deviating from the trend line, but Cluster 4's values fit the trend line (see Figures 4.1 – 4.3). The Shapiro-Wilk test showed that only the perimeter values of Cluster 4 are not significantly different from a normal distribution, which is consistent with the Q-Q plot which shows the Cluster 4 values following the trend line (see Figure 4.3).

Table 4.2 *Donors present in Cluster 2 for each observer*

Observer ID	Donor ID
0	18a, 41a, 6a, 7a
1	18a, 41a, 6a, 7a
2	18a, 41a, 6a, 7a
3	18a, 41a, 6a, 7a
4	18a, 6a
5	18a, 41a, 80a
6	18a, 41a, 6a, 7a
7	18a, 41a, 6a, 7a
8	18a, 41a, 58a, 6a
9	18a, 41a, 6a, 7a
10	18a, 1b, 35a, 6a, 7a

Table 4.3 *Donors present in Cluster 3 for each observer*

Observer ID	**Donor ID**
0	1b, 35a, 58a, 66a
1	1b, 35a, 58a, 66a
2	1b, 35a, 58a, 66a
3	1b, 35a, 58a, 66a
4	1b, 35a, 41a, 58a, 66a, 7a
5	1b, 35a, 58a, 66a, 6a, 7a
6	1b, 35a, 58a, 66a
7	1b, 35a, 58a, 66a
8	1b, 35a, 66a, 7a
9	1b, 35a, 58a, 66a
10	11a, 58a, 66a

Table 4.4 *Donors present in Cluster 4 for each observer*

Observer ID	**Donor ID**
0	2a, 80a
1	2a, 80a
2	2a, 80a
3	2a, 80a
4	2a, 80a
5	2a
6	2a, 80a
7	2a, 80a
8	2a, 80a
9	2a, 80a
10	2a, 41a, 80a

Table 4.5 *Tests of Normality for area, perimeter and SIMINDEX by cluster*

Ward Method		**Kolmogorov-Smirnov[a]**			**Shapiro-Wilk**		
		Statistic	**df**	**Sig.**	**Statistic**	**df**	**Sig.**
Area	1	0.199	10	.200*	0.915	10	0.315
	2	0.096	42	.200*	0.963	42	0.193
	3	0.063	47	.200*	0.986	47	0.822
	4	0.171	22	0.092	0.938	22	0.176
Perimeter	1	0.222	10	0.179	0.828	10	**0.031**
	2	0.161	42	**0.008**	0.844	42	**0.000**
	3	0.152	47	**0.008**	0.778	47	**0.000**
	4	0.149	22	.200*	0.941	22	0.210
SIMINDEX	1	0.226	10	0.161	0.808	10	**0.018**
	2	0.247	42	**0.000**	0.720	42	**0.000**
	3	0.239	47	**0.000**	0.792	47	**0.000**
	4	0.202	22	**0.020**	0.839	22	**0.002**
*. This is a lower bound of the true significance.							
a. Lilliefors Significance Correction							

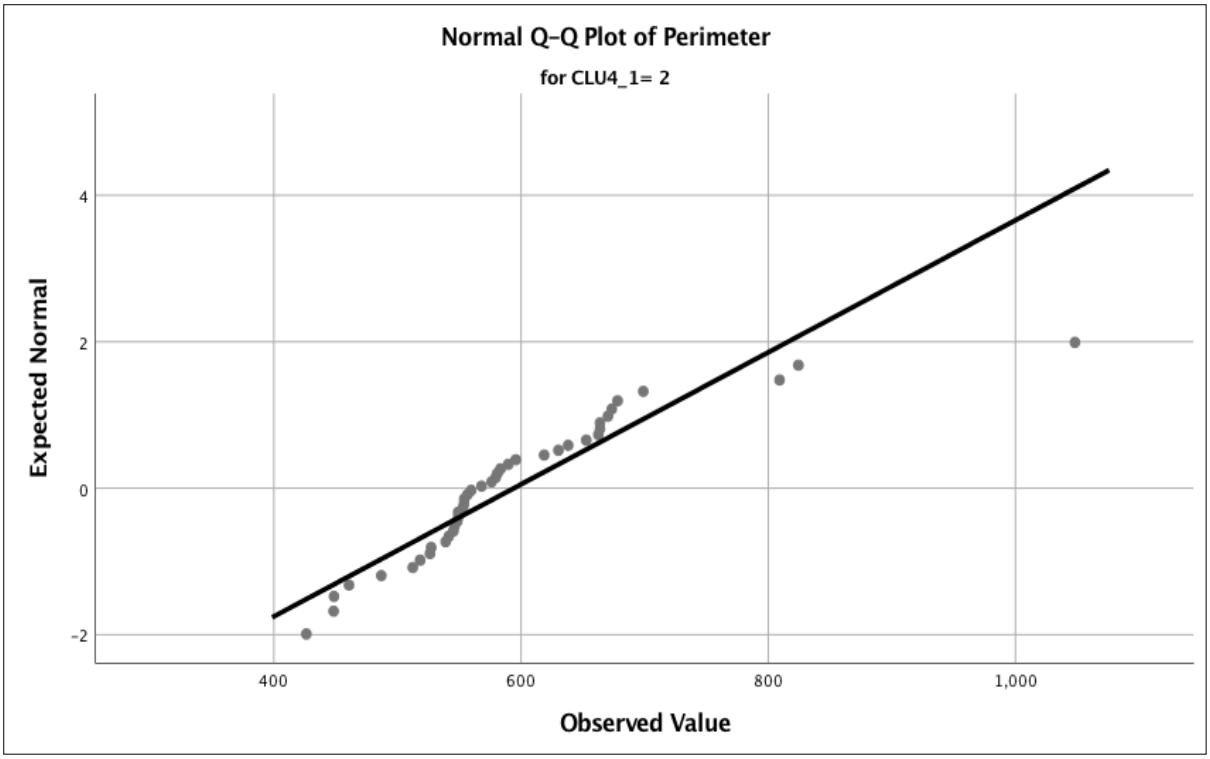

Figure 4.1 *Normality plot of perimeter values for Cluster 2*

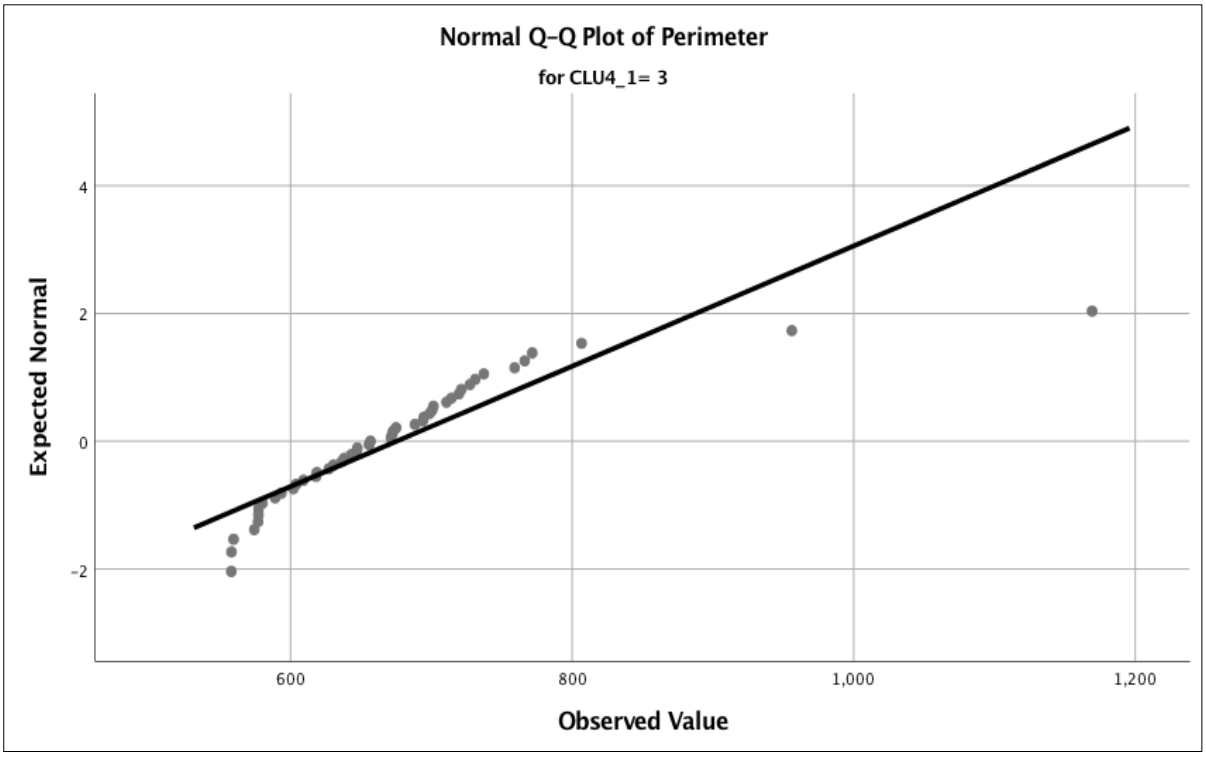

Figure 4.2 *Normality plot of perimeter values for Cluster 3*

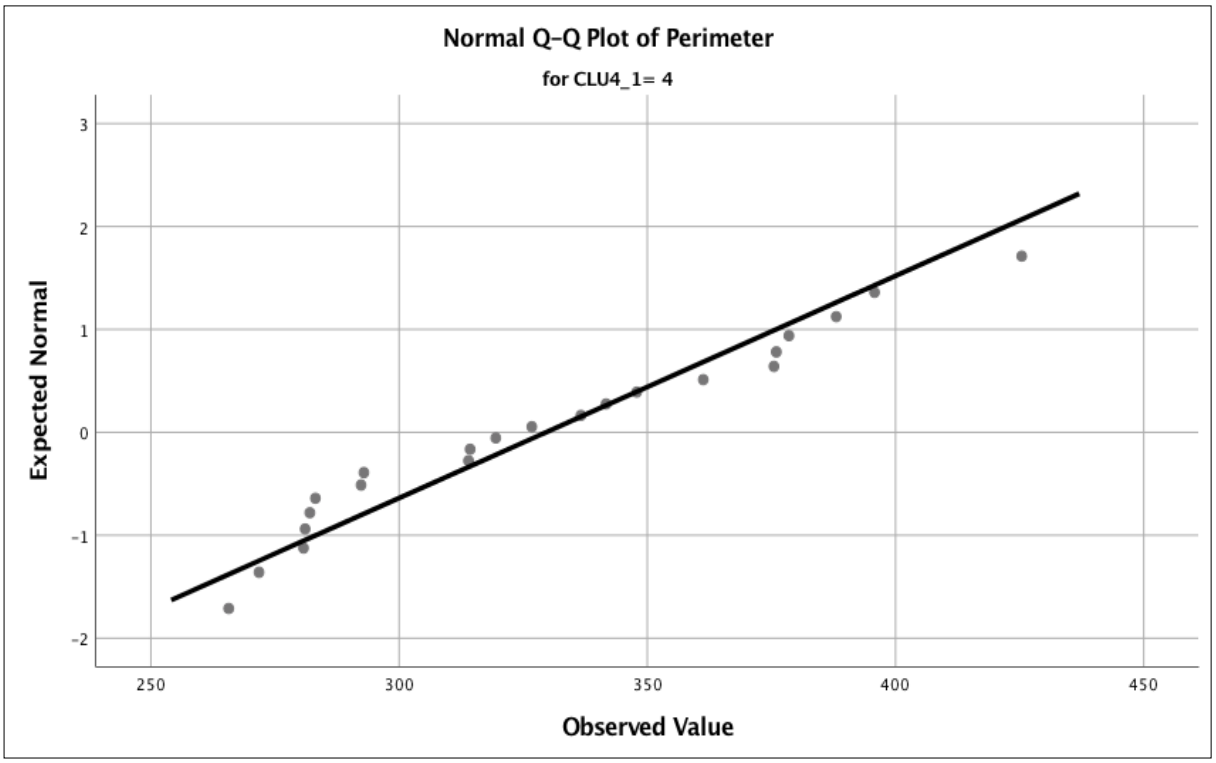

Figure 4.3 *Normality plot of perimeter values for Cluster 4*

The KS test showed that only the Cluster 1 similarity index values are not significantly different from a normal distribution, and the Shapiro-Wilk test showed that the similarity index values for all four clusters are significantly different from a normal distribution (see Table 4.5). The Q-Q Plots for all four clusters show similarity index values that do not follow the trend line, which supports the conclusion of the Shapiro-Wilk test that the similarity index values are not normally distributed (see Figures 4.4 – 4. 7). The mean area, perimeter, and similarity index values for Clusters 1, 2, 3 and 4 are presented in Tables 4.6 – 4.9.

Coefficient of Variation (C_v) and Analysis of Variance (ANOVA)

The Coefficient of Variation was calculated from the average area and perimeter values of the polygons from the donors in the inter-observer test group. For area, donor 66a had the lowest variance (7%) and donor 41a had the highest variance (38%) (Table 4.10). For perimeter, donor 1b had the lowest variance (4%) and donor 41a had the highest variance (26%) (Table 4.11). The Test of Homogeneity of Variances shows that Levene's test is not significant for area ($F(10, 110) = 0.135$, $p = 0.999$) or perimeter ($F(10, 110) = 0.377$, $p = 0.954$) so the variance in area and perimeter values between observers is not significant. The One-Way ANOVA results showed that there was not a statistically significant difference between observers for the area ($F(10, 110) = 2.661$, $p = 0.935$) and perimeter values ($F(10, 110) = 0.470$, $p = 0.906$). This supports the C_v results which show the low variance for area (38%) and perimeter (26%).

Descriptive Statistics and Similarity Search Results

The mean area, perimeter, and similarity index values for all polygons created by inter-observer participants (N = 121) are presented in Table 4.12. The mean area, perimeter, and

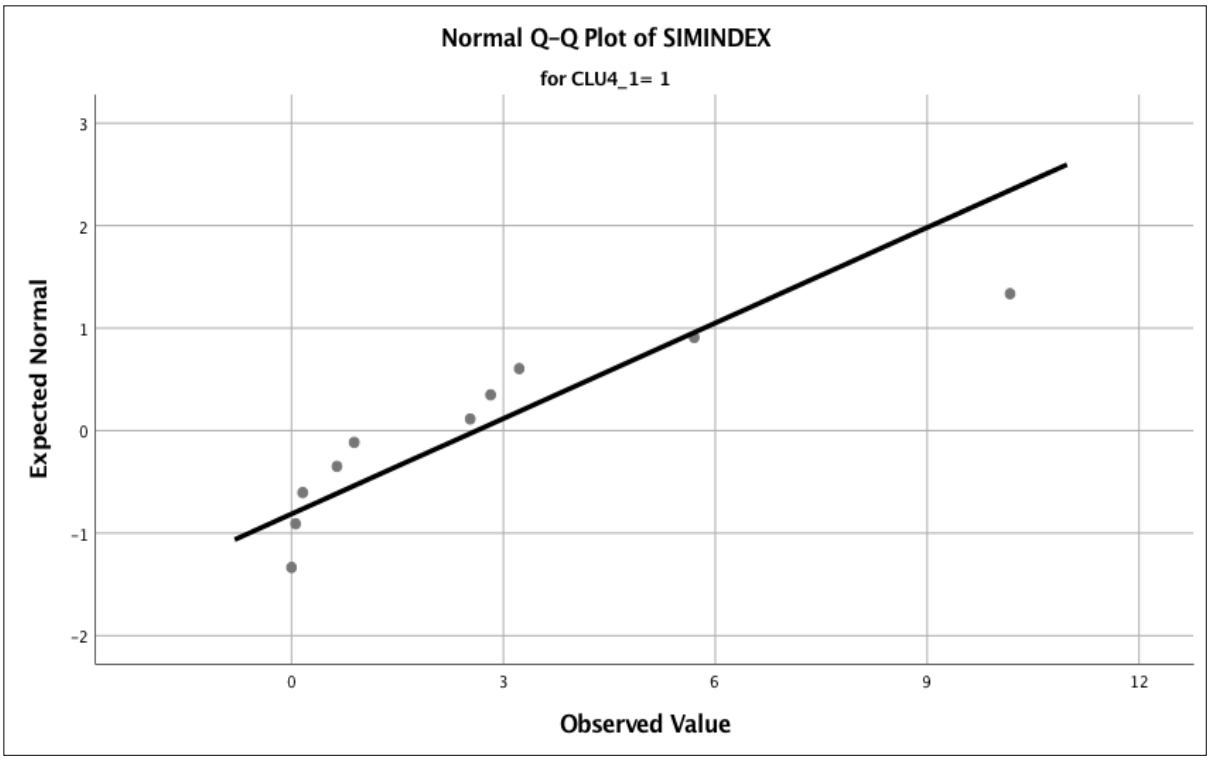

Figure 4.4 *Normality plot of similarity index values for Cluster 1*

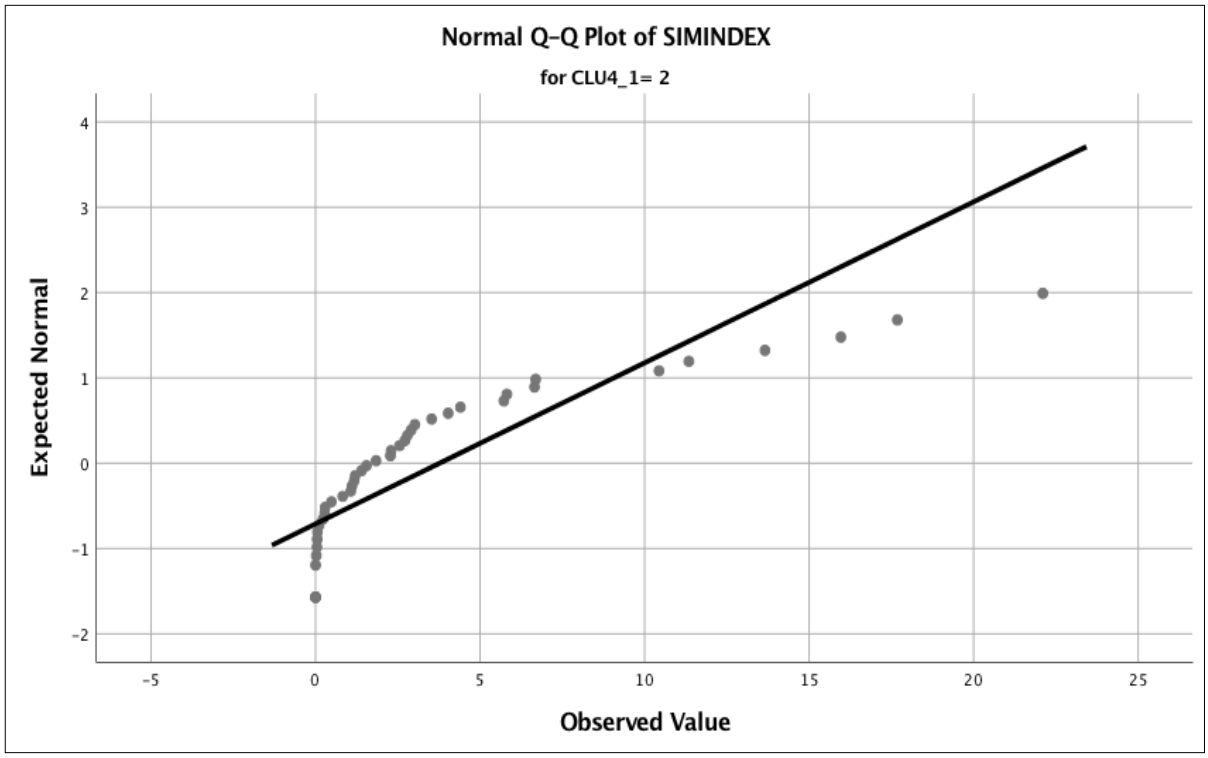

Figure 4.5 *Normality plot of similarity index values for Cluster 2*

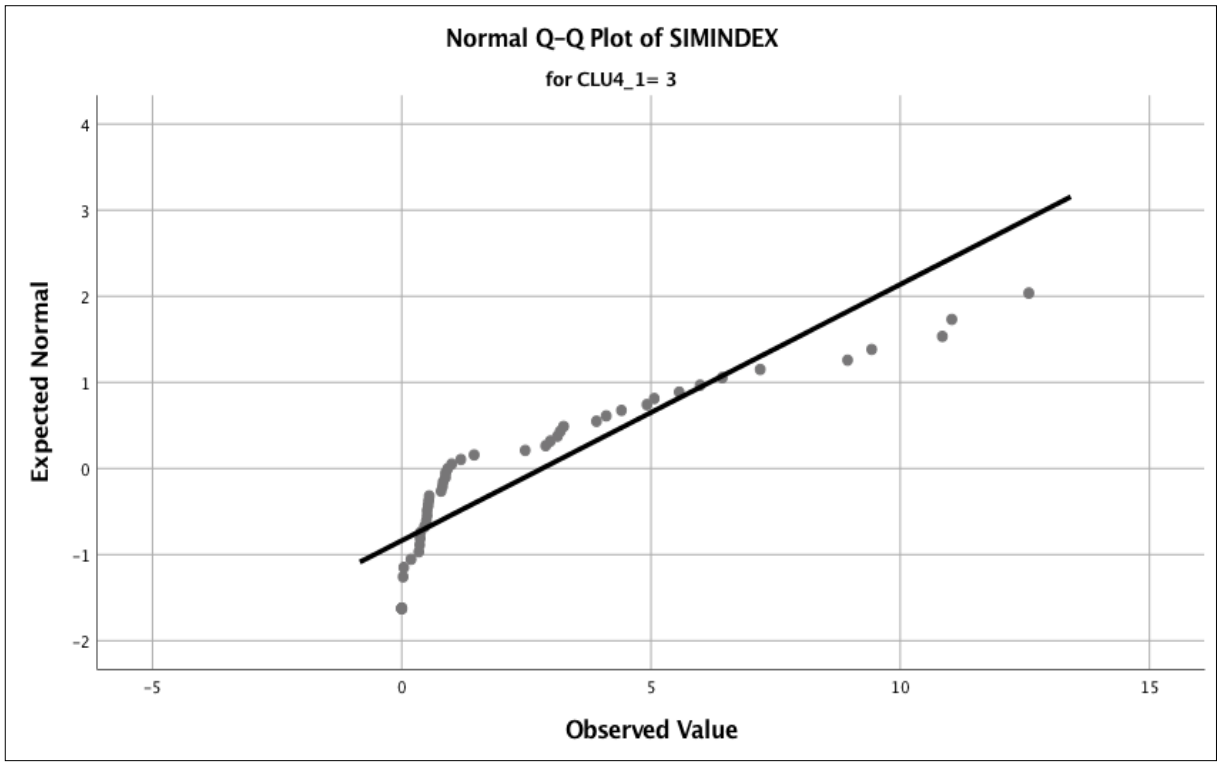

Figure 4.6 *Normality plot of similarity index values for Cluster 3*

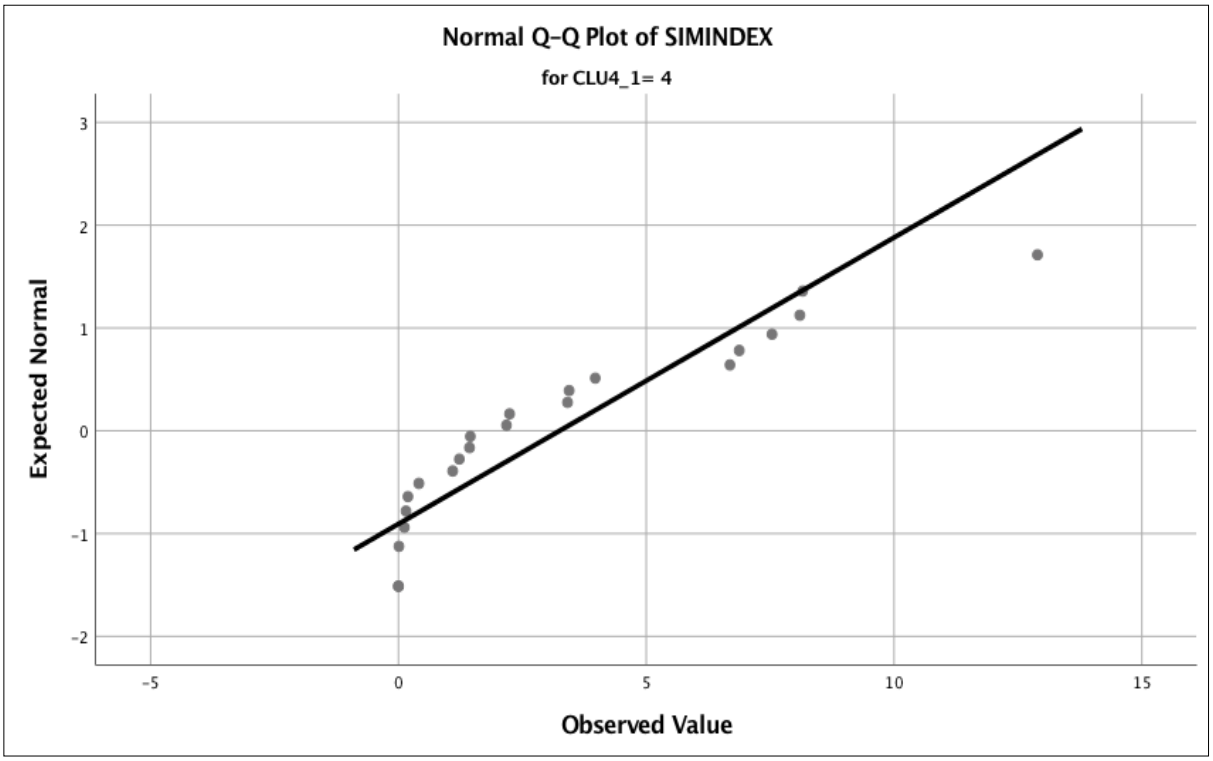

Figure 4.7 *Normality plot of similarity index values for Cluster 4*

Table 4.6 *Descriptive statistics for Cluster 1*

Cluster 1	**Minimum**	**Maximum**	**Mean**	**Std. Deviation**
Area	28420.50	32946.40	30644.00	1624.90
Perimeter	995.46	1245.74	1064.86	80.67
SIMINDEX	0.00	10.17	2.62	3.22

Table 4.7 *Descriptive statistics for Cluster 2*

Cluster 2	**Minimum**	**Maximum**	**Mean**	**Std. Deviation**
Area	7414.26	14405.90	10970.17	304.39
Perimeter	426.27	1048.12	594.19	17.11
SIMINDEX	0.00	22.10	3.77	0.82

Table 4.8 *Descriptive statistics for Cluster 3*

Cluster 3	Minimum	Maximum	Mean	Std. Deviation
Area	15039.70	22398.70	18058.97	230.63
Perimeter	557.87	1169.33	675.24	15.50
SIMINDEX	0.00	12.58	2.82	0.49

Table 4.9 *Descriptive statistics for Cluster 4*

Cluster 4	Minimum	Maximum	Mean	Std. Deviation
Area	2819.54	6741.99	4540.56	1092.91
Perimeter	265.68	425.42	329.58	46.33
SIMINDEX	0.00	12.89	3.25	3.59

Table 4.10 *Mean, standard deviation, and C_v of area values for each donor*

Donor ID	**Mean**	**Stand Deviation**	**Coefficient of Variation**
1b	18057.12	2705.91	0.15
2a	4461.00	1088.52	0.24
6a	12835.64	2143.35	0.17
7a	13815.63	3672.16	0.27
11a	29894.43	2925.19	0.10
18a	9135.20	1308.82	0.14
35a	17693.73	1720.88	0.10
41a	10550.30	3960.87	0.38
58a	16159.70	1582.44	0.10
66a	18100.61	1310.79	0.07
80a	5283.11	1875.75	0.36
		Min	**0.07**
		Max	**0.38**

Table 4.11 *Mean, standard deviation, and C_v of perimeter values for each donor*

Donor ID	**Mean**	**Stand Deviation**	**Coefficient of Variation**
1b	610.07	26.28	0.04
2a	332.57	39.32	0.12
6a	599.91	66.91	0.11
7a	689.81	76.94	0.11
11a	1074.36	82.76	0.08
18a	555.41	21.55	0.04
35a	736.35	135.36	0.18
41a	531.43	139.99	0.26
58a	596.47	59.82	0.10
66a	711.96	33.84	0.05
80a	342.74	65.31	0.19
		Min	**0.04**
		Max	**0.26**

Table 4.12 *Descriptive statistics for all observations*

	N	Minimum	Maximum	Mean	Std. Deviation
Area	121	2819.54	32946.40	14180.59	7198.47
Perimeter	121	265.68	1245.74	616.46	206.79
SIMINDEX	121	0.00	22.10	3.21	4.14

Table 4.13 *Descriptive statistics of area, perimeter, and similarity index values for each observer*

Obs ID		N	Minimum	Maximum	Mean	Std. Deviation
0	Area	11	3690.39	28420.50	13408.32	7424.60
	Perimeter	11	271.78	997.10	567.48	203.36
	SIMINDEX	11	0.00	0.00	0.00	0.00
1	Area	11	4067.06	32460.60	14314.40	7923.42
	Perimeter	11	326.73	1080.80	638.72	194.40
	SIMINDEX	11	0.02	7.54	2.80	2.37
2	Area	11	3443.17	32198.60	13889.84	8219.57
	Perimeter	11	265.68	1062.85	563.10	213.37
	SIMINDEX	11	0.01	2.91	1.05	1.14
3	Area	11	3641.13	31951.00	13614.67	7938.18
	Perimeter	11	292.34	1156.85	613.76	225.99
	SIMINDEX	11	0.12	13.66	3.14	4.11
4	Area	11	4392.60	28933.40	15967.12	7363.93
	Perimeter	11	314.31	1009.26	625.64	198.08
	SIMINDEX	11	0.06	10.84	2.64	3.67
5	Area	11	6219.10	29588.50	16640.39	6459.98
	Perimeter	11	347.87	1063.65	629.63	179.70
	SIMINDEX	11	0.03	22.10	5.44	6.52
6	Area	11	6577.13	30655.30	14117.36	6792.06
	Perimeter	11	375.50	995.46	605.26	168.22
	SIMINDEX	11	0.04	12.89	3.11	4.02
7	Area	11	5124.37	29488.60	14079.98	7075.06
	Perimeter	11	341.69	1005.79	582.59	176.40
	SIMINDEX	11	0.06	3.97	1.89	1.31
8	Area	11	4155.96	32946.40	14494.46	7875.48
	Perimeter	11	313.98	1031.13	602.64	194.64
	SIMINDEX	11	0.04	15.97	4.13	4.79
9	Area	11	4033.50	29797.10	14484.13	7616.65
	Perimeter	11	292.90	1245.74	723.60	260.20
	SIMINDEX	11	0.15	12.58	6.66	3.64
10	Area	11	2819.54	22398.70	10975.79	6191.88
	Perimeter	11	280.75	1169.33	628.67	282.61
	SIMINDEX	11	0.00	17.68	4.46	5.65

similarity index values for all observations are presented in Table 4.13. Observer 3's mean area was the closest to observer 0's mean area. Observer 2's mean perimeter was the closest to observer 0's mean perimeter. Observer 2's mean similarity index was closest to observer 0's mean similarity index (see Table 4.13).

All of the polygons the inter-observer participants created for each donor from the test group were run in Similarity Search. The *Input Features to Match* was observer 0's polygon (me), and the *Candidate Features* were the polygons created by observers 1 – 10. Table 4.14 presents the Similarity Search rank order of the first (most similar) and last (least similar) observers for each donor.

Intra-observer Variation

Coefficient of Variation

Intra-observer variation was assessed for donors with polygons present in multiple test groups (98/100). The Coefficient of Variation (C_v) was calculated from the average area and perimeter values of the polygons created for 98 of the 100 donors in the sample. For the female donors, donor 48a had the lowest variance (0.6%) for area and donor 80a has the highest variance (35%) (Table 4.15). For perimeter, donor 82a had the lowest variance (0.7%) and donor 80a had the highest variance (20%) (Table 4.16). For the male donors, donor 105a had the lowest variance (7%) for area and donor 176a had the highest variance (22%) (Table 4.17). For perimeter, donor 163a had the lowest variance (0.4%) and donor 132a had the highest variance (5%) (Table 4.18). Graphs of donors 48a, 80a, 82a, 105a, 176a, 163a, 132a illustrate the

Table 4.14 *Observers ranked first and last by Similarity Search for each donor*

Donor ID	First Ranked Observer	Last Ranked Observer
1b	7	10
2a	2	6
6a	6	5
7a	10	4
11a	4	9
18a	4	8
35a	6	10
41a	8	9
58a	5	9
66a	2	9
80a	2	5

Table 4.15 *Coefficient of Variation of average area for female donors*

Donor ID	Mean	Std. Deviation	Coefficient of Variation (CV)
48a	9627.31	60.36	0.006
45a	10383.88	194.62	0.019
23a	14593.18	279.82	0.019
50a	10886.07	222.15	0.020
83a	6918.56	221.78	0.032
82a	23666.58	786.68	0.033
66a	19468.12	678.74	0.035
34a	12476.05	438.49	0.035
99a	819.86	34.36	0.042
58a	16568.77	723.94	0.044
52a	22390.84	1032.12	0.046
11a	33595.17	1619.40	0.048
86a	8682.11	441.37	0.051
54a	7558.67	384.66	0.051
95a	10998.84	737.95	0.067
35a	19678.16	1367.90	0.070
27a	30551.83	2236.24	0.073
15a	15939.53	1235.99	0.078
53a	27927.55	2276.43	0.082
47a	12660.00	1120.26	0.088
94a	8681.51	786.03	0.091
38a	7172.14	654.79	0.091
72a	10146.61	960.54	0.095
73a	20667.21	1967.30	0.095
37a	9697.60	935.68	0.096
57a	10449.27	1026.65	0.098
100a	6755.70	696.47	0.103
36a	6865.87	726.23	0.106
71a	13130.51	1398.57	0.107
97a	11388.58	1221.53	0.107
29a	11293.63	1261.37	0.112
79a	4982.63	604.49	0.121
68a	46067.11	5710.58	0.124
87a	7733.82	984.15	0.127
18a	9401.80	1262.93	0.134
44a	9105.88	1236.60	0.136
67a	12495.08	1834.96	0.147
6a	14439.53	2160.28	0.150

Table 4.15 Continued

Donor ID	Mean	Std. Deviation	Coefficient of Variation (CV)
76a	7033.23	1057.76	0.150
40a	12765.60	1969.98	0.154
7a	12210.16	1949.26	0.160
2a	3638.01	604.88	0.166
62a	7128.06	1303.78	0.183
25a	16895.80	3215.19	0.190
55a	11604.26	2325.50	0.200
28a	10011.44	2412.04	0.241
41a	9902.45	2657.22	0.268
46a	10313.82	3321.41	0.322
92a	4759.71	1539.37	0.323
80a	4522.63	1569.22	0.347

Table 4.16 *Coefficient of Variation of average perimeter for female donors*

Donor ID	Mean	Std. Deviation	Coefficient of Variation (CV)
48a	462.61	3.03	0.007
82a	683.52	4.75	0.007
58a	575.25	4.75	0.008
23a	565.83	4.92	0.009
50a	689.10	7.31	0.011
11a	984.67	12.40	0.013
45a	546.74	7.40	0.014
27a	994.83	16.18	0.016
18a	529.87	10.04	0.019
57a	493.90	9.38	0.019
86a	458.09	9.43	0.021
100a	448.49	9.40	0.021
66a	699.24	15.42	0.022
73a	737.52	16.36	0.022
99a	129.43	2.92	0.023
37a	486.97	11.11	0.023
34a	542.29	13.25	0.024
44a	509.49	12.82	0.025
53a	963.63	25.65	0.027
28a	541.22	15.30	0.028
72a	441.74	14.06	0.032
54a	394.31	12.96	0.033
95a	535.74	18.37	0.034
15a	560.23	19.96	0.036
25a	608.25	23.51	0.039
94a	516.46	20.97	0.041
67a	608.05	25.81	0.042
52a	712.12	30.85	0.043
35a	677.17	29.59	0.044
71a	602.39	30.34	0.050
55a	495.70	24.97	0.050
97a	519.36	27.28	0.053
47a	608.23	33.12	0.054
6a	628.75	34.61	0.055
29a	482.83	28.59	0.059

Table 4.16 Continued

Donor ID	Mean	Std. Deviation	Coefficient of Variation (CV)
40a	532.40	32.65	0.061
68a	1131.48	69.40	0.061
87a	420.16	26.35	0.063
7a	665.45	43.94	0.066
79a	325.76	22.17	0.068
92a	370.48	25.51	0.069
2a	299.15	21.38	0.071
36a	411.66	32.83	0.080
38a	441.11	37.65	0.085
76a	380.70	32.57	0.086
62a	459.08	45.18	0.098
83a	480.12	52.44	0.109
46a	524.50	60.38	0.115
41a	482.73	92.23	0.191
80a	304.36	61.31	0.201

Table 4.17 *Coefficient of Variation of average area for male donors*

Donor ID	Mean	Std. Deviation	Coefficient of Variation (CV)
105a	21460.04	153.60	0.007
163a	35325.92	274.15	0.008
139a	31589.55	248.19	0.008
131a	18582.47	159.66	0.009
140a	19937.83	205.51	0.010
135a	33790.08	488.86	0.014
160a	29245.97	514.98	0.018
186a	19512.60	364.05	0.019
193a	20261.80	388.15	0.019
164a	23851.82	463.83	0.019
156a	17891.74	385.15	0.022
130a	19499.26	424.43	0.022
115a	38690.32	854.15	0.022
161a	37348.40	835.95	0.022
112a	24068.36	544.67	0.023
101a	13535.49	333.82	0.025
178a	36450.64	902.43	0.025
184a	18554.81	478.17	0.026
138a	20783.19	539.31	0.026
123a	6881.05	201.10	0.029
106a	18474.63	642.10	0.035
124a	17436.13	623.11	0.036
116a	36606.15	1322.42	0.036
141a	16940.42	649.24	0.038
119a	25188.78	1024.07	0.041
190a	24386.17	1000.78	0.041
148a	20931.65	875.01	0.042
177a	11119.53	472.65	0.043
117a	18277.80	777.39	0.043
126a	22907.91	1098.90	0.048
167a	16014.41	776.57	0.048
109a	13568.60	663.94	0.049
195a	15965.52	781.35	0.049
189a	41344.76	2108.01	0.051
129a	24906.21	1310.00	0.053

Table 4.17 Continued

Donor ID	Mean	Std. Deviation	Coefficient of Variation (CV)
152a	16753.28	888.87	0.053
191a	15324.04	829.31	0.054
165a	20170.60	1201.39	0.060
168a	17850.10	1145.96	0.064
200a	17395.73	1170.52	0.067
174a	17785.35	1255.80	0.071
145a	17553.67	1464.65	0.083
118a	9989.05	841.40	0.084
103a	20157.30	1768.69	0.088
111a	10427.48	1107.25	0.106
132a	17926.34	1964.81	0.110
182a	9344.55	1254.08	0.134
176a	19933.62	4351.06	0.218

Table 4.18 *Coefficient of Variation of average perimeter for male donors*

Donor ID	Mean	Std. Deviation	Coefficient of Variation (CV)
163a	959.08	3.74	0.004
190a	775.87	4.15	0.005
140a	617.43	4.63	0.008
106a	691.65	6.03	0.009
103a	775.73	7.21	0.009
186a	678.64	6.37	0.009
130a	622.58	6.62	0.011
105a	735.39	7.86	0.011
131a	630.56	6.77	0.011
139a	902.84	10.09	0.011
101a	595.01	6.71	0.011
138a	655.20	7.92	0.012
161a	895.49	10.95	0.012
109a	550.71	6.91	0.013
167a	615.24	7.79	0.013
177a	525.39	7.32	0.014
119a	759.27	10.81	0.014
115a	925.96	13.23	0.014
184a	636.75	9.64	0.015
200a	682.45	10.34	0.015
145a	695.91	10.59	0.015
118a	479.20	7.99	0.017
148a	656.28	11.89	0.018
124a	732.91	13.30	0.018
135a	977.50	18.02	0.018
195a	577.05	10.67	0.018
123a	433.36	8.76	0.020
164a	810.66	16.70	0.021
141a	601.57	12.46	0.021
116a	1013.18	21.14	0.021
168a	748.77	15.75	0.021
156a	764.17	17.64	0.023
160a	912.65	21.43	0.023
193a	676.04	16.51	0.024
165a	777.08	19.98	0.026

Table 4.18 Continued

Donor ID	Mean	Std. Deviation	Coefficient of Variation (CV)
126a	733.60	19.63	0.027
174a	705.69	18.97	0.027
129a	774.38	22.26	0.029
191a	555.73	16.02	0.029
111a	612.34	18.89	0.031
182a	569.93	18.60	0.033
112a	704.33	24.70	0.035
117a	642.81	23.90	0.037
176a	787.59	29.75	0.038
189a	1095.39	46.42	0.042
152a	654.22	30.84	0.047
178a	952.62	45.06	0.047
132a	643.20	34.27	0.053

previously discussed variance for are and perimeter values. The distribution of each donors' polygons based on area and perimeter values and are coded by their similarity rank (see Figures 4.8 – 4.14).

Similarity Search Accuracy and Correct Identifications

Similarity Search correctly identified the true match AM polygon for 31 of the 50 male test groups (62%). Similarity Search correctly identified the true match AM polygon for 36 of the 50 female test groups (72%). Table 4.19 presents the rank of each true match polygon for males and females that Similarity Search did not identify as most similar (N = 33). All of these polygons were ranked in the top 5 most similar by Similarity Search. The majority (N = 15 out of 33) were ranked second, 10 were ranked third, six were ranked fourth, and two were ranked fifth.

No True Match vs. True Match

Each of the twenty donors used in the test groups that contained a true match, and the test groups that did not contain the true match had their similarity index values recorded. Each donor had two values, the similarity index of their true match and the similarity index of the polygon identified as most similar when no true match was present (Table 4.20). The similarity index data are non-normally distributed so a non-parametric test, Wilcoxon Signed Rank, was performed to compare these two sets of values. The result was not significant (0.433), indicating no statistically significant difference between each donor's true match similarity index value and the similarity index value of the polygon Similarity Search identified as most similar in absence of the true match.

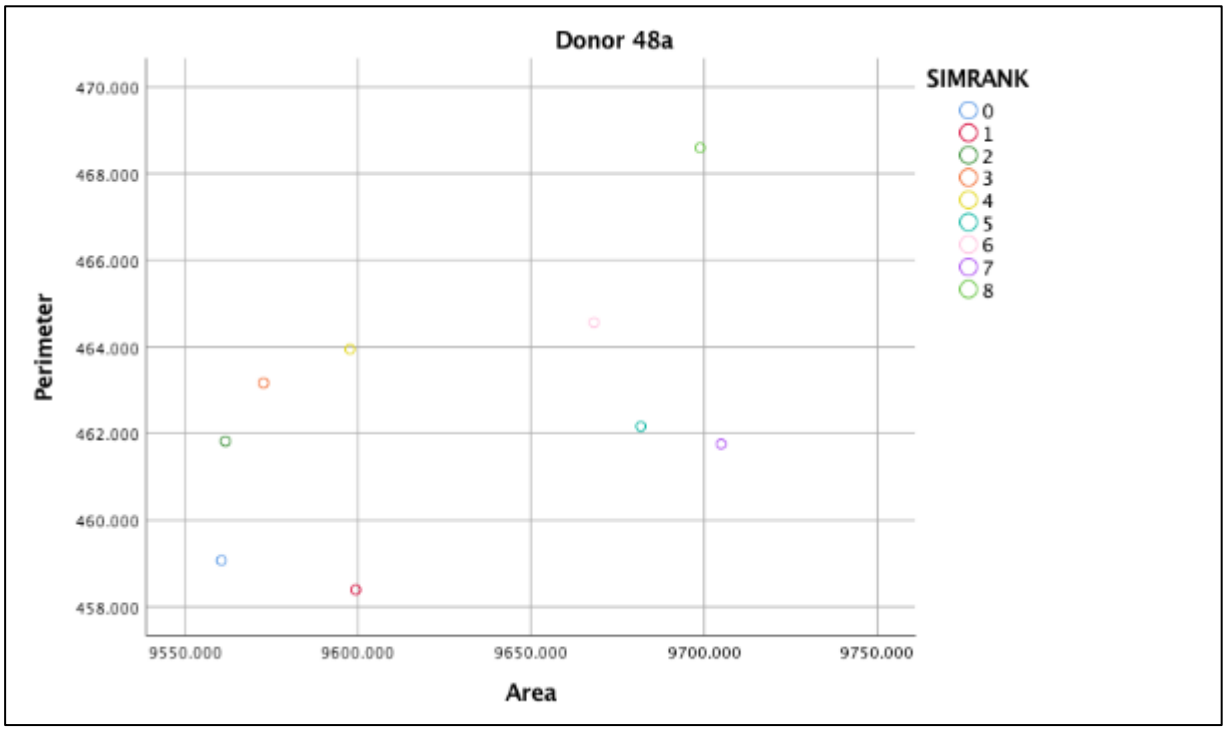

Figure 4.8 *Distribution of area and perimeter values for donor 48a coded by similarity rank. Donor 48a had the lowest variance for area values out of all female donors.*

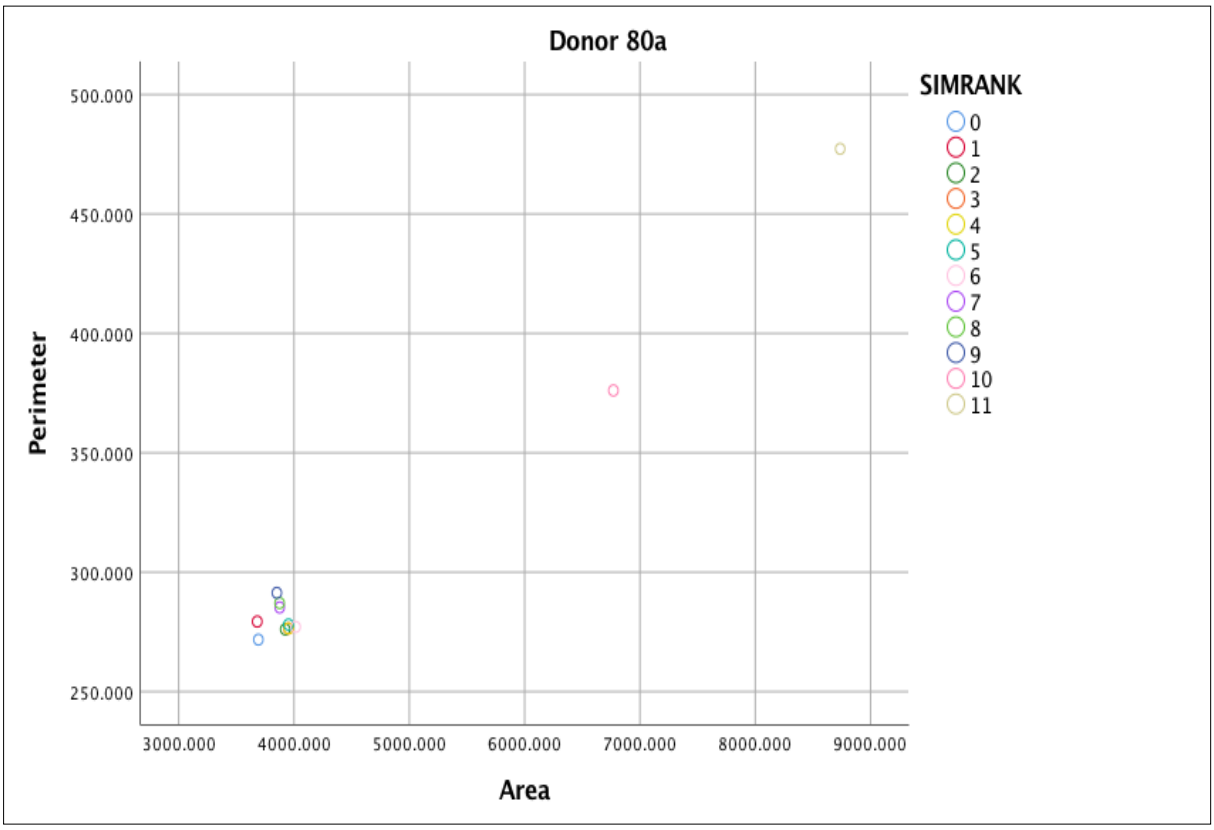

Figure 4.9 *Distribution of area and perimeter values for donor 80a coded by similarity rank. Donor 80a had the highest variance for area and perimeter value out of all female donors.*

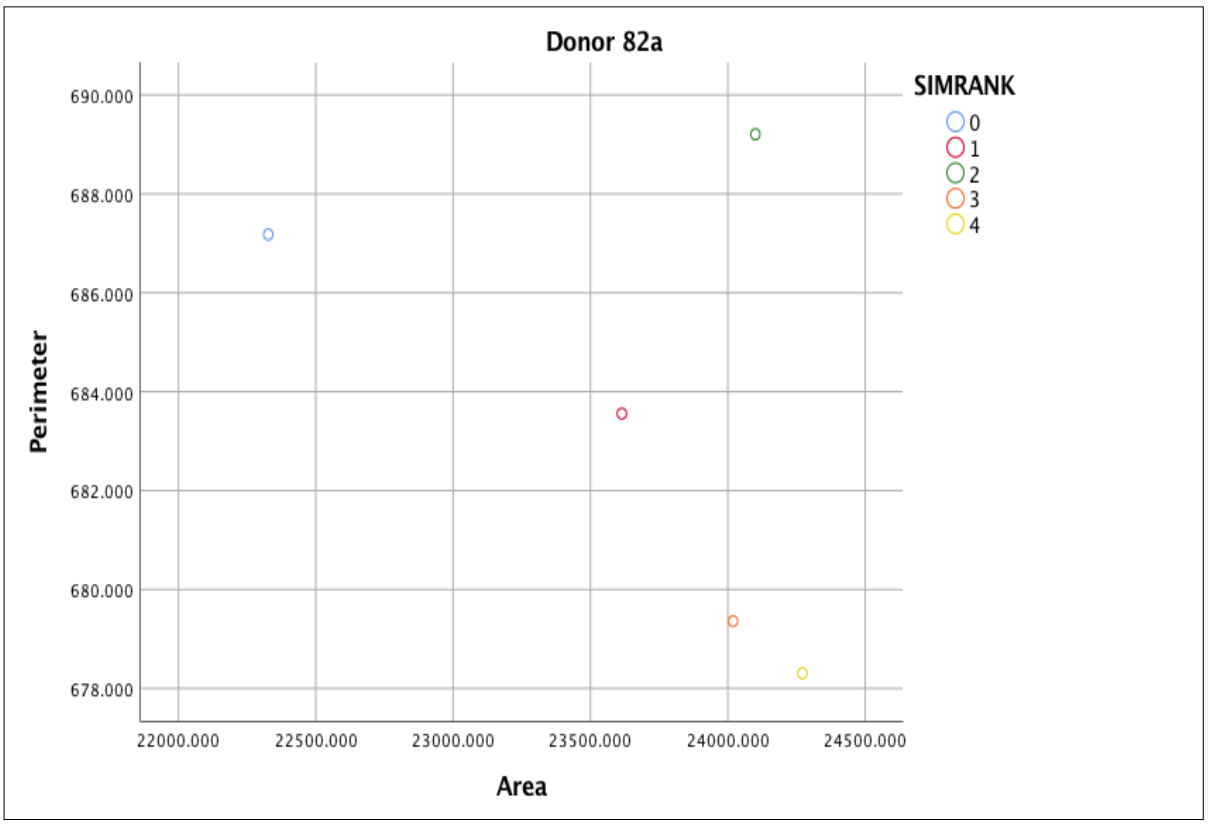

Figure 4.10 *Distribution of area and perimeter values for donor 82a coded by similarity rank. Donor 82a had the lowest variance for perimeter values out of all female donors.*

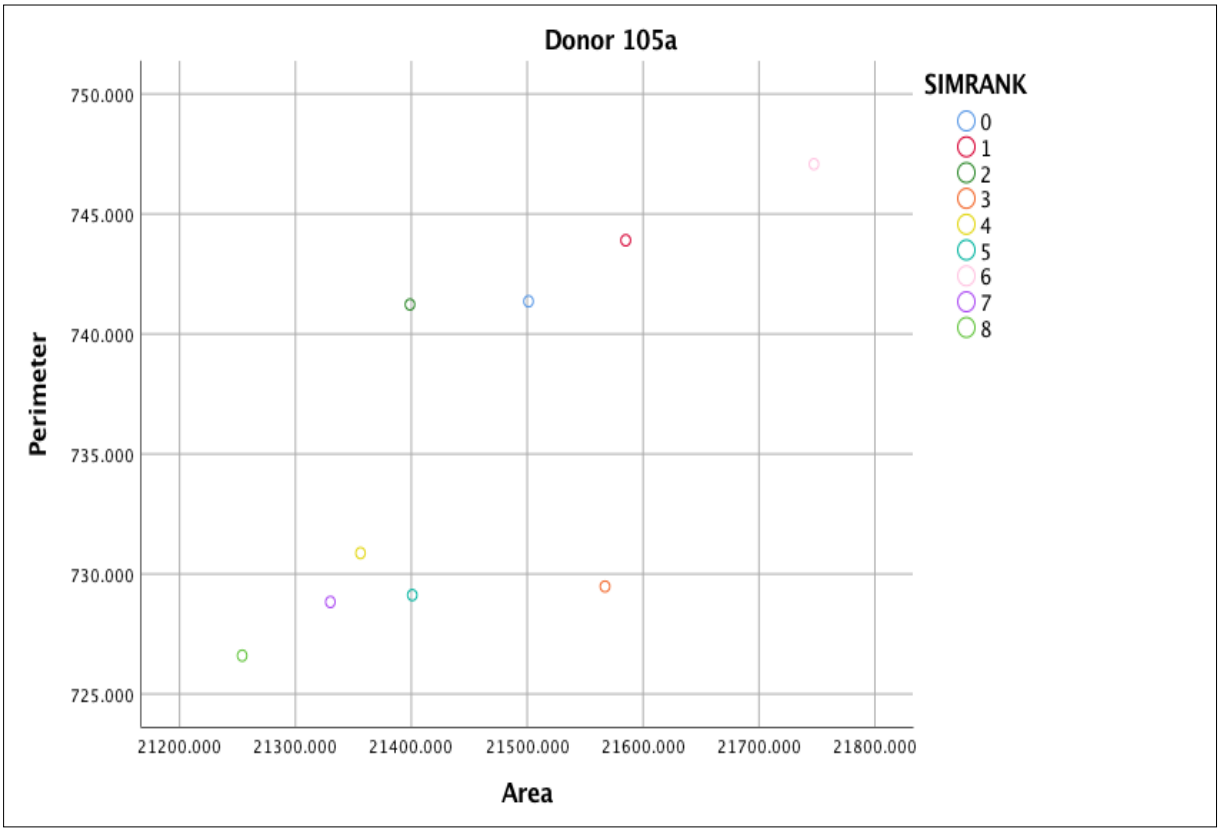

Figure 4.11 *Distribution of area and perimeter values for donor 105a coded by similarity rank. Donor 105a had the lowest variance for area values out of all male donors.*

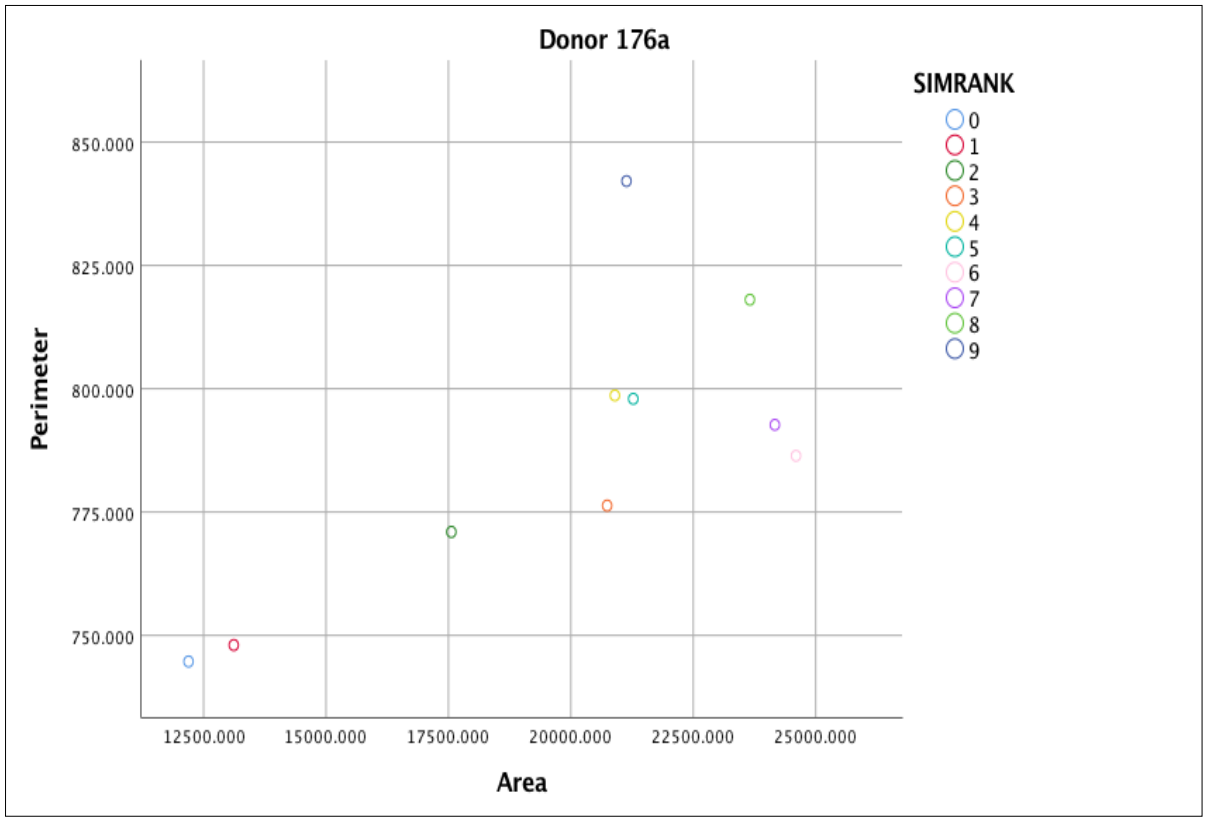

Figure 4.12 *Distribution of area and perimeter values for donor 176a coded by similarity rank. Donor 176a had the highest variance for area values out of all male donors.*

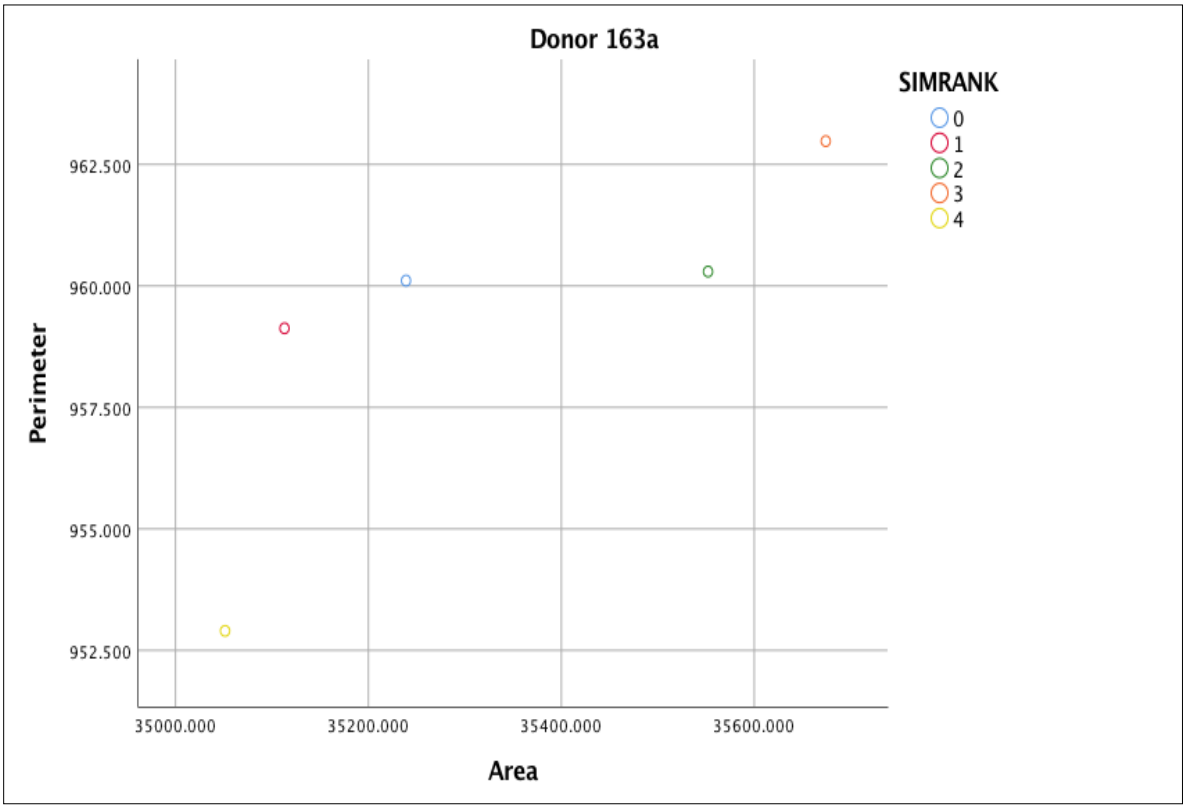

Figure 4.13 *Distribution of area and perimeter values for donor 163a coded by similarity rank. Donor 163a had the lowest variance for perimeter values out of all male donors.*

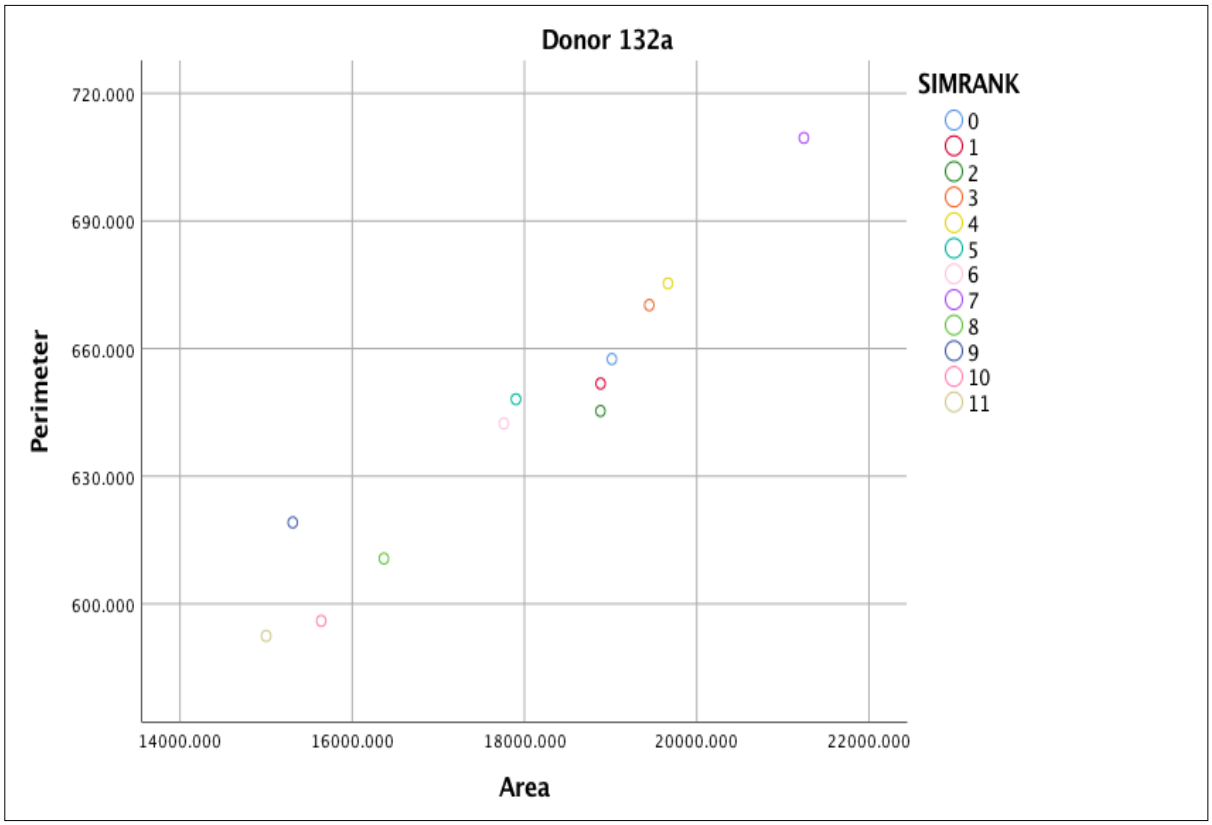

Figure 4.14 *Distribution of area and perimeter values for donor 132a coded by similarity rank. Donor 132a had the highest variance for perimeter values out of all male donors.*

Table 4.19 *Similarity ranks for true match polygons not identified as most similar by Similarity Search*

Group No.	True Match Donor ID	Similarity Rank
7	7a	2
11	25a	2
25	57a	2
33	11a	2
46	66a	2
57	190a	2
61	191a	2
76	138a	2
78	116a	2
86	135a	2
87	167a	2
88	119a	2
93	132a	2
94	124a	2
100	186a	2
12	82a	3
20	29a	3
21	95a	3
48	83a	3
51	162a	3
56	145a	3
62	174a	3
65	164a	3
69	109a	3
82	141a	3
2	40a	4
9	18a	4
13	6a	4
15	45a	4
58	131a	4
90	105a	4
19	76a	5
97	176a	5

Table 4.20 *Similarity index values of each donor's true match and match selected by Similarity Search in absence of the true match*

Donor ID	**True Match SIMINDEX**	**No True Match SIMINDEX**
21b	0.179	0.017
49b	0.001	0.196
13b	0.064	0.127
19b	0.242	0.023
77b	0.001	0.140
4b	0.030	0.010
26b	0.001	0.151
33b	0.002	0.030
61b	0.005	10.765
5b	0.086	0.007
170b	0.011	0.080
125b	0.176	0.236
134b	0.241	0.096
181b	0.112	0.026
121b	0.073	0.930
147b	0.019	0.037
122b	0.016	0.046
196b	0.991	0.262
143b	0.134	0.184
107b	0.093	0.198

Similarity Search Threshold

It is important to establish a range of similarity index values to assess the value of the frontal sinus polygon identified by Similarity Search as the most similar as a potential match based on the range determined from this study. This range of similarity index values is determined from the similarity index values of all correctly identified polygons. It also includes the range of values produced when each male and female donor are compared to every other male and female donor in the sample, respectively.

Similarity Index Range for Correctly Identified Polygons

The area, perimeter, and similarity index values for male and female donors correctly identified by Similarity Search were compiled into two tables (Tables 4.21 and 4.22), with the similarity index values sorted from smallest (most similar) to largest (least similar). The range of similarity index values for all correctly identified females (N = 36) was 0.001 to 1.557. The range of similarity index values for all correctly identified males (N = 31) was 0.000 to 0.305. Descriptive statistics for area, perimeter, and similarity index values were calculated for all correctly identified polygons (Table 4.23).

Each Donor to Entire Sample

Hierarchical Cluster Analysis using Ward's method was conducted for all 100 donors. Each donor's PM polygon was compared to a PM and an AM polygon from every other donor of the same sex (males compared to males and females compared to females). Cluster Analysis was run on each of these groups (N = 100). Ward's Method with four clusters was defined for each cluster analysis. Descriptive statistics (minimum, maximum, mean, and std. deviation) were produced for each of the four clusters for each female test group (N = 50) and each male test

Table 4.21 *Area, perimeter, and similarity index values for all correctly identified females*

Donor ID	Area	Perimeter	SIMINDEX
23a	14654.665	563.068	0.001
28a	6624.851	512.266	0.001
41a	9601.786	456.078	0.001
67a	10756.826	584.891	0.001
79a	4724.464	304.064	0.001
54a	7437.990	398.646	0.002
48a	9572.741	463.168	0.002
62a	6621.158	487.538	0.002
97a	11716.072	514.863	0.003
36a	5984.591	365.536	0.004
2a	3425.884	292.753	0.004
68a	39580.780	1033.962	0.005
27a	29438.390	989.180	0.006
34a	12459.938	552.351	0.006
86a	8633.342	469.550	0.007
92a	3500.091	351.254	0.008
50a	10942.115	695.706	0.008
100a	6210.229	437.708	0.010
37a	10476.380	479.274	0.011
55a	14797.439	522.708	0.012
72a	9873.548	437.330	0.022
44a	10335.346	511.112	0.024
35a	20790.474	663.865	0.030
58a	16491.223	577.155	0.035
46a	8214.470	481.186	0.044
38a	6483.273	383.017	0.045
94a	10255.966	532.550	0.049
47a	12033.400	622.190	0.050
52a	23226.366	718.805	0.062
71a	14007.083	618.780	0.064
87a	7907.719	411.467	0.064
15a	15571.494	554.523	0.068
80a	8735.952	477.266	0.086
53a	25860.804	1009.171	0.164
73a	18020.812	711.980	0.291
99a	810.224	129.265	1.557

Table 4.22 *Area, perimeter, and similarity index values for all correctly identified males*

Donor ID	Area	Perimeter	SIMINDEX
123a	6673.735	421.449	0.000
177a	11382.234	525.187	0.002
148a	20256.931	655.028	0.004
106a	18243.477	681.738	0.005
118a	10010.060	469.651	0.007
101a	13516.691	605.087	0.008
152a	17759.529	699.361	0.009
115a	37609.063	911.272	0.011
139a	31833.606	905.172	0.012
111a	9315.485	590.967	0.016
184a	18163.117	637.306	0.019
193a	20156.008	658.368	0.020
140a	19909.752	616.876	0.027
178a	37057.042	880.209	0.027
192a	30622.071	881.565	0.031
156a	17864.025	753.231	0.032
168a	18429.229	759.301	0.033
200a	16950.149	683.994	0.034
130a	19405.122	617.737	0.037
129a	24647.683	781.936	0.042
189a	44099.493	1186.337	0.061
161a	36738.408	902.120	0.065
112a	25350.419	759.142	0.066
160a	28234.509	915.010	0.073
182a	12207.737	611.247	0.093
117a	17964.366	611.368	0.112
163a	35051.381	952.901	0.137
103a	19276.934	772.096	0.150
195a	16254.932	575.706	0.282
165a	17991.186	790.466	0.285
126a	23988.200	741.210	0.305

Table 4.23 *Descriptive statistics for correctly identified male and female polygons*

Sex		N	Minimum	Maximum	Mean	Std. Deviation
Male	**Area**	31	6673.74	44099.49	21837.50	9291.96
	Perimeter	31	421.45	1186.34	727.52	161.57
	SIMINDEX	31	0.00	0.30	0.06	0.08
Female	**Area**	36	810.22	39580.78	12104.94	7802.77
	Perimeter	36	129.27	1033.96	536.51	189.12
	SIMINDEX	36	0.00	1.56	0.08	0.26

group (N = 50). Cluster 1 descriptive statistics for each male and female donor are reported in Tables 4.24 and 4.25. Only Cluster 1 was reported and used in the establishment of the similarity index range because Cluster 1 represents the values that were closest to the input donor values and thus most similar. These values will be of most use in determining the similarity index range that a practitioner could use to determine if Similarity Search identified a potential frontal sinus match. In Tables 4.29 and 4.30 each donor has a minimum and maximum similarity index value for Cluster 1. The minimum similarity index value out of all of the minimum similarity index values and the maximum similarity index value of all of the maximum similarity index values, along with the averages of all minimum values, maximum values, means, and standard deviations are reported in Tables 4.24 and 4.25. Based on these results the similarity index value range for females is 0 to 11.56, and for males it is 0 to 5.51.

Table 4.24 *Cluster 1 descriptive statistics of similarity index values for each female donor*

Donor ID	**Minimum**	**Maximum**	**Mean**	**Std. Deviation**
1b	0.00	1.22	0.37	0.39
3b	0.00	5.82	0.56	0.95
4b	0.00	1.76	0.58	0.46
5b	0.00	5.22	0.50	0.82
8b	0.00	7.57	0.88	1.28
9b	0.00	6.37	0.64	1.05
10b	0.00	1.89	0.95	0.43
12b	0.00	2.62	1.02	0.75
13b	0.00	5.46	0.50	0.87
14b	0.00	5.10	0.54	0.79
16b	0.00	0.85	0.24	0.21
17b	0.00	1.45	0.49	0.37
19b	0.00	1.11	0.27	0.26
20b	0.00	2.43	0.77	0.64
21b	0.00	1.23	0.32	0.30
22b	0.00	3.24	0.53	0.72
24b	0.00	2.54	0.56	0.76
26b	0.00	5.46	1.42	1.29
30b	0.00	5.80	0.56	0.95
31b	0.00	2.61	0.58	0.78
32b	0.00	1.37	0.40	0.35
33b	0.00	4.71	0.46	0.78
39b	0.00	3.77	0.78	0.89
42b	0.00	5.12	0.56	0.84
43b	0.00	7.62	0.89	1.30
49b	0.00	1.49	0.48	0.39
51b	0.00	10.44	1.72	1.85
56b	0.00	3.93	0.48	0.68
59b	0.00	5.71	0.53	0.92
60b	0.00	2.92	1.12	0.82
61b	0.00	1.85	0.68	0.79
63b	0.00	1.37	0.42	0.36
64b	0.00	3.60	0.77	1.24
65b	0.00	4.53	0.45	0.75
69b	0.00	11.56	2.17	2.05
70b	0.00	8.16	1.02	1.40

Table 4.24 Continued

Donor ID	Minimum	Maximum	Mean	Std. Deviation
74b	0.00	3.84	0.80	0.90
75b	0.00	4.08	0.89	0.96
77b	0.00	4.80	0.48	0.86
78b	0.00	5.04	1.37	1.19
81b	0.00	3.38	0.71	1.17
84b	0.00	2.28	0.55	0.64
85b	0.00	5.97	0.59	0.98
88b	0.00	7.10	0.80	1.20
89b	0.00	1.95	0.38	0.65
90b	0.00	1.10	0.33	0.27
91b	0.00	5.18	0.58	0.79
93b	0.00	3.16	0.54	0.71
96b	0.00	6.01	1.69	1.43
98b	0.00	6.07	1.76	1.45
Range	0.00	11.56		
Average	0.00	4.16	0.73	0.85

Table 4.25 *Cluster 1 descriptive statistics of similarity index values for each male donor*

Donor ID	Minimum	Maximum	Mean	Std. Deviation
102b	0.00	0.96	0.41	0.31
104b	0.00	2.05	0.65	0.76
107b	0.00	3.31	0.71	0.89
108b	0.00	3.59	0.98	0.81
110b	0.00	3.70	0.48	0.96
113b	0.00	1.88	0.34	0.39
114b	0.00	2.66	0.79	0.99
120b	0.00	2.11	0.47	0.63
121b	0.00	2.25	0.73	0.60
122b	0.00	1.50	0.52	0.59
125b	0.00	2.51	0.67	0.65
127b	0.00	4.26	1.17	0.99
128b	0.00	1.39	0.39	0.36
133b	0.00	3.94	0.68	1.10
134b	0.00	4.08	1.11	0.94
136b	0.00	3.84	1.23	1.33
137b	0.00	4.37	2.39	1.38
142b	0.00	4.67	0.73	1.22
143b	0.00	2.88	0.82	0.76
144b	0.00	2.64	0.75	0.92
146b	0.00	2.42	0.47	0.69
147b	0.00	1.36	0.36	0.37
149b	0.00	2.37	0.49	0.51
150b	0.00	2.58	0.46	0.72
151b	0.00	1.58	0.30	0.32
153b	0.00	1.85	0.51	0.43
154b	0.00	1.33	0.28	0.29
155b	0.00	2.21	0.33	0.54
157b	0.00	5.51	1.18	1.55
158b	0.00	1.35	0.32	0.32
159b	0.00	2.47	0.53	0.53
166b	0.00	2.59	0.70	0.68
169b	0.00	2.95	1.18	0.97
170b	0.00	2.80	0.39	0.71
171b	0.00	1.25	0.40	0.37
172b	0.00	2.84	0.48	0.70
173b	0.00	2.26	0.48	0.64
175b	0.00	2.87	0.84	1.06
179b	0.00	1.24	0.32	0.30
180b	0.00	1.43	0.33	0.29
181b	0.00	1.16	0.35	0.34
183b	0.00	2.25	0.48	0.64

Table 4.25 Continued

Donor ID	Minimum	Maximum	Mean	Std. Deviation
185b	0.00	1.29	0.31	0.31
187b	0.00	1.68	0.32	0.34
188b	0.00	2.36	0.51	0.50
194b	0.00	1.83	0.51	0.53
196b	0.00	2.79	0.64	0.62
197b	0.00	3.79	0.49	0.98
198b	0.00	1.97	0.74	0.60
199b	0.00	1.26	0.28	0.28
Range	0.00	5.51		
Average	0.00	2.48	0.62	0.67

CHAPTER 5: DISCUSSION

The purpose of this study was to investigate the use of ArcMap's spatial analyst tool Similarity Search to identify an AM/PM radiograph match using polygons representative of the frontal sinus. This project sought to answer three main research questions:

1) Are the area and perimeter values of a frontal sinus polygon sufficient variables for Similarity Search to be able to identify a match?

2) Can ArcMap Similarity Search identify a PM to AM radiographic match using the frontal sinus polygon?

3) If ArcMap Similarity Search can match a PM to AM radiograph is this a quantifiable and reproducible method for positive identification using radiographs?

This chapter will discuss the results presented in chapter 4 as they relate to each of these research questions. The chapter concludes with a discussion of the limitations of the study, the significance of these findings, future directions of this research, and a discussion of recent research reassessing the uniqueness of certain features used for human identification.

Are area and perimeter sufficient for Similarity Search identification?

Area and perimeter were the selected parameters investigated for this proposed method for human identification. Given that these were the sole parameters used in Similarity Search, the first research question focused on whether area and perimeter values of each frontal sinus polygon were sufficient attributes for the Similarity Search tool to be able to correctly identify a match. Based on the results presented in chapter 4, area and perimeter fail to capture and quantify all of the characteristics of the frontal sinus that makes it unique to each individual. Similarity Search, like statistical models in general, is a tool that is only as good as the information it is given to compare. Inaccurate or minimal information is going to limit its ability

to identify the most similar cases. In this case, Similarity Search was provided with the area and perimeter values of the polygons in each test group and was instructed to rank the polygons from most similar to least similar using the similarity index, which is automatically calculated by the Similarity Search tool.

Similarity Search performed well with just those two values for both females (72%) and males (62%), but area and perimeter do not adequately capture the shape of the frontal sinus, particularly to discern those with similar area and perimeter values. The method of visually comparing and matching frontal sinus radiographs to identify an unknown individual is based on the tested and well-accepted notion that the shape of the frontal sinus is unique to each individual. Visually assessing those shape differences from radiographic images allows a practitioner to identify a match and establish a positive identification. The method tested in this study only provided Similarity Search with the area and perimeter values of each polygon, which does not tell the program anything about the shape of the polygons. Area and perimeter provide basic metric data about each polygon and can certainly tell Similarity Search which polygons are bigger or smaller than other polygons, but it does not capture the billowing shape of the sinus and the prevalence of scalloped edges, all features that contribute to the distinctive and unique shape of the frontal sinus. Two polygons can have very similar area and perimeter values yet have completely different shapes.

Despite the lack of shape information, Similarity Search was able to identify the correct match in over 60% of the cases for males and females. However, an informal visual assessment of the groups where Similarity Search was able to correctly identify a match, and the groups where it was not able to correctly identify a match, indicates that the size of the other polygons in the test group may influence Similarity Search's ability to distinguish between polygons and

select the correct match, based on area and perimeter alone. For example, in test group 33 the PM polygon and its corresponding AM polygon were very similar in overall shape and had area and perimeter values that were very similar (Figure 5.1). However, Similarity Search identified another AM polygon that was not the true match as the most similar because its area and perimeter values were closer to the PM polygon's area and perimeter values, even though visually two polygons had different shapes (Figure 5.2). Similarity Search relied exclusively on the area and perimeter, regardless of the obvious shape differences. If area and perimeter values could be combined with a shape assessment, a more robust model for identification is possible. Similarly, in test group 48 the polygon that was determined to be the most similar to the PM polygon, based on its area and perimeter values, had a very different shape (see Figure 5.3). The opposite phenomenon is also true. In test group 45, the PM polygon was very large with many scalloped edges while the other polygons in the group were relatively small (Figure 5.4). Therefore, based on area and perimeter values, Similarity Search was able to correctly identify the match due to the distinctive size (Figure 5.5). These groups are examples of Similarity Search's inability to correctly identify a match based on area and perimeter values when more than one comparative polygon has a similar overall size, regardless of its shape. Unless the size difference between polygons is distinct, area and perimeter will need additional comparative values (i.e. shape, max height/length, or number of billows) before this method is ready for implementation.

Sex may also be influencing these results. Recent research has explored the use of the frontal sinus for sex determination based on the assumption that male sinuses are larger with more billows than females (Akhlaghi, et al. 2016; Choi, et al. 2018; Cossellu, et al. 2015; Tatlisumak, et al. 2007).

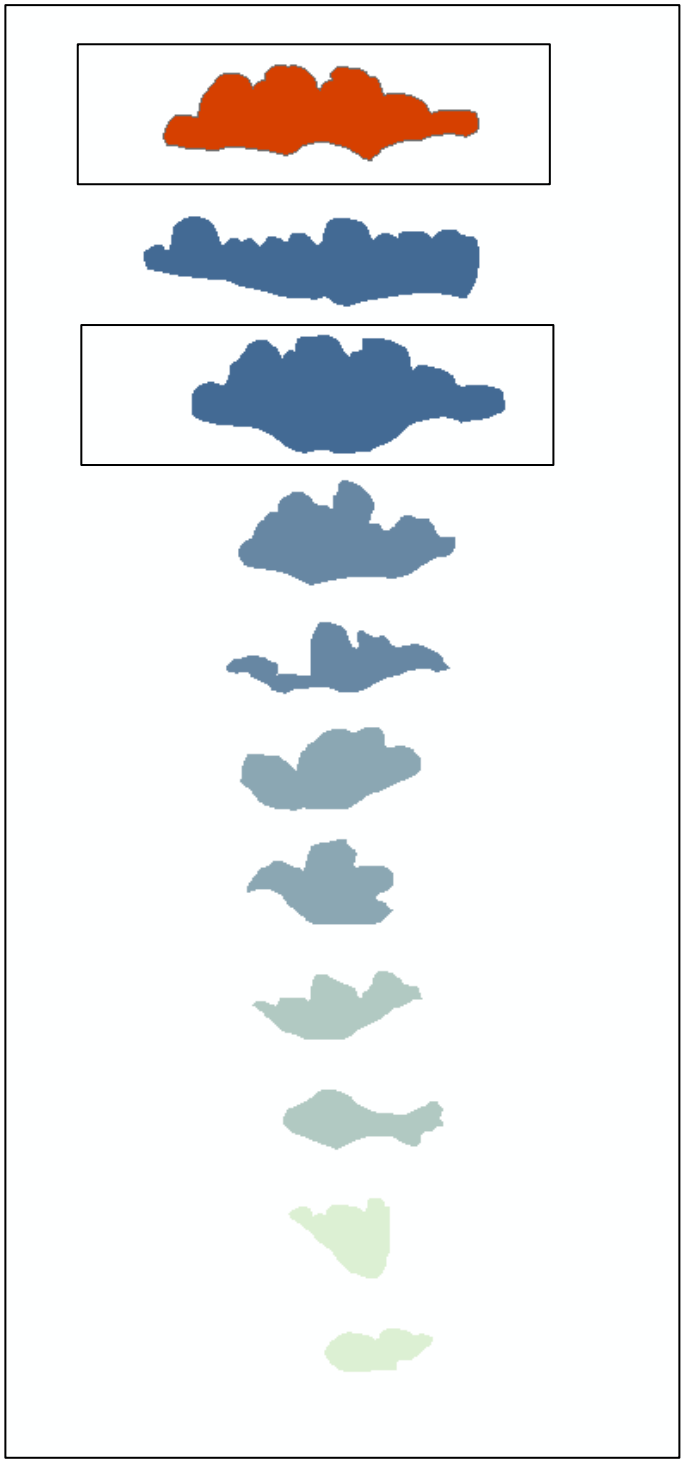

Figure 5.1 *Group 33 frontal sinus polygons (most to least similar). Boxes denote the PM polygon (orange) and its AM match (dark blue).*

Table

Group 33_SS_MostSimilar

FID	Shape *	Id	MATCH_ID	CAND_ID	Area	Perimeter	SIMRANK	SIMINDEX	LABELRANK
0	Polygon	0	0	-214748364	25995	940.073	0	0	0
1	Polygon	0	-214748364	3	29106.3	1022.16	1	0.24132	1
2	Polygon	0	-214748364	0	34520.3	959.017	2	0.834422	2
3	Polygon	0	-214748364	6	19854.9	706.495	3	1.49094	3
4	Polygon	0	-214748364	5	11293.9	703.426	4	3.550294	4
5	Polygon	0	-214748364	2	14727	561.681	5	4.231808	5
6	Polygon	0	-214748364	9	11512.3	523.67	6	5.762144	6
7	Polygon	0	-214748364	1	9543.68	522.905	7	6.467841	7
8	Polygon	0	-214748364	4	8474.73	476.684	8	7.673299	8
9	Polygon	0	-214748364	7	7343.83	394.395	9	9.754882	9
10	Polygon	0	-214748364	8	5058.52	324.714	10	12.359213	10

1 (0 out of 11 Selected)

Group 33_SS_MostSimilar

Figure 5.2 *Group 33 Similarity Search attribute table. Orange = the Input Feature to Match (PM polygon). Blue= the AM polygon that is the true match but was ranked second most similar.*

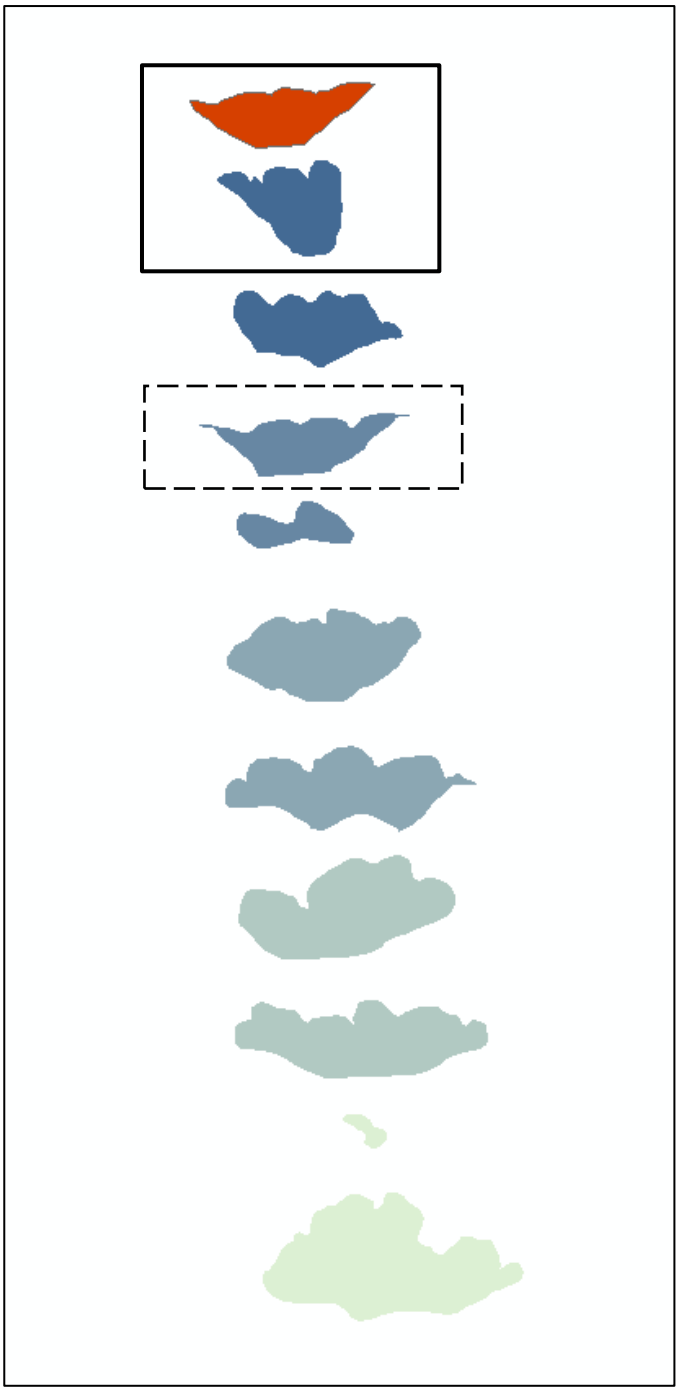

Figure 5.3 *Group 48 frontal sinus polygons. Solid line box denotes the PM polygon (orange) and AM polygon ranked as most similar (dark blue). The dash line box denotes the true AM match.*

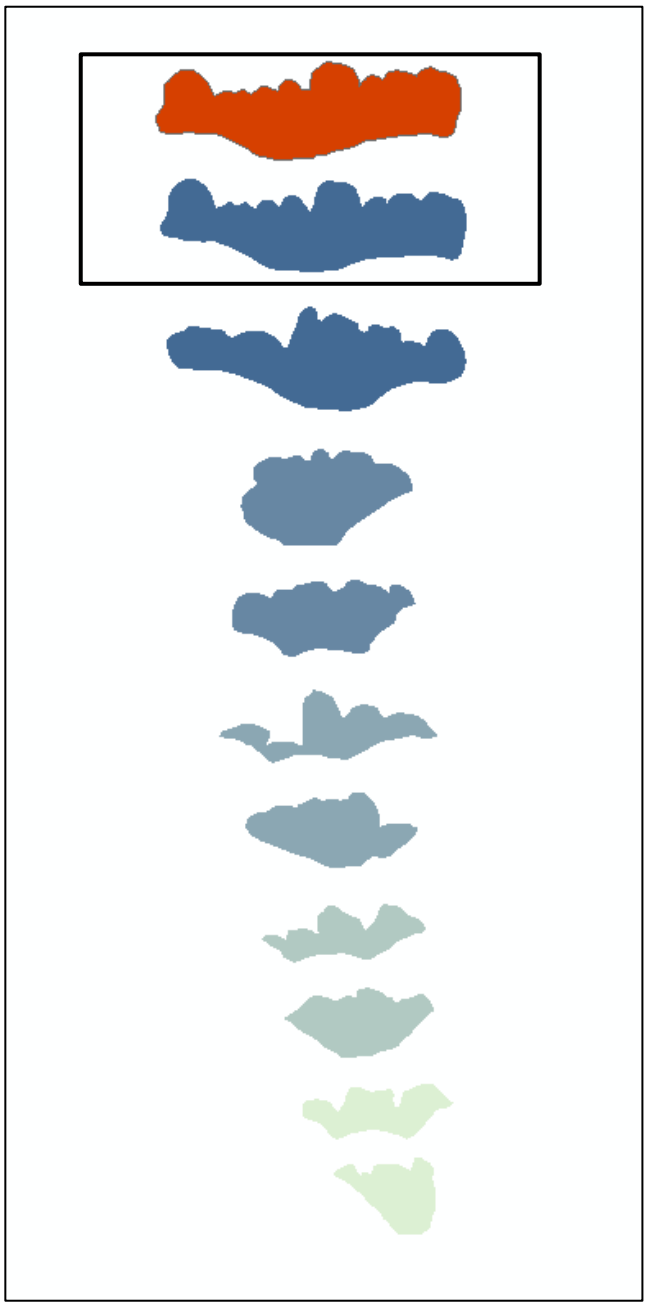

Figure 5.4 *Group 45 frontal sinus polygons. Box denotes the PM polygon (orange) and the AM true match polygon (dark blue) that was ranked as most similar.*

Table

Group 45_SS_MostSimilar

FID	Shape *	Id	MATCH_ID	CAND_ID	Area	Perimeter	SIMRANK	SIMINDEX	LABELRANK
0	Polygon	0	0	-214748364	29581.3	973.776	0	0	0
2	Polygon	0	-214748364	7	27249.9	934.796	2	0.112389	2
1	Polygon	0	-214748364	2	29438.4	989.18	1	0.00572	1
8	Polygon	0	-214748364	3	10310.2	451.193	8	11.551637	8
3	Polygon	0	-214748364	0	17866.3	567.419	3	5.737716	3
4	Polygon	0	-214748364	8	15001.2	573.769	4	6.69657	4
5	Polygon	0	-214748364	6	10647.1	694.057	5	6.910147	5
7	Polygon	0	-214748364	1	8066.75	517.173	7	11.380394	7
10	Polygon	0	-214748364	9	7319.07	394.19	10	14.763222	10
9	Polygon	0	-214748364	5	8088.84	491.833	9	11.910925	9
6	Polygon	0	-214748364	4	12505.8	516.432	6	8.949331	6

1 (0 out of 11 Selected)

Group 45_SS_MostSimilar

Figure 5.5 *Group 45 Similarity Search attribute table*

Visually, the frontal sinuses of the male donors in the sample were larger than the female sinuses. It is difficult to say what exactly contributed to the lower percentage of correct identifications for the male test groups (62% versus 72%) but given the large size of the male sinuses on average, and the fact that area and perimeter do not capture shape, a sample of relatively large sinuses may have made it more difficult for Similarity Search to identify matches on area and perimeter alone.

The inability of Similarity Search to correctly identify the true match using only area and perimeter values also became apparent when the similarity index values of polygons identified as the most similar for the same PM polygon were compared: one value was for the true match polygon, and the other value was for the polygon identified as the most similar by Similarity Search in the absence of the true match. A Wilcoxon Signed Rank test was used to compare these two values. The results of this test showed that there was no significant difference between these two values. This means that the similarity index value of the true match was not statistically significantly different from the similarity index value of a polygon that was not the true match – it only had the closest perimeter and area values.

These results are indicative of Similarity Search's inability to truly distinguish between polygons in order to identify the correct match. Similarity Search uses the data it is given to rank features from most to least similar, and area and perimeter are not sufficient data for it to be able to distinguish the true match polygon as most similar with a high level of accuracy. Radiograph quality, and even slight distortions could be affecting the area and perimeter values as well, which will affect how Similarity Search ranks the AM polygons.

Alternatively, this result could have something to do with the way the similarity index value is calculated for each Candidate Feature. Each attribute value undergoes a Z – transform

prior to the index calculation. For the groups where no true match was present, Similarity Search was forced to select the polygon that was most similar to the Input Feature based on a standard index that was calculated from standardized area and perimeter values. This standardization may be affecting the amount of variance between the true match similarity index and no true match similarity index to the point where statistical tests do not find any significant difference.

Overall, these results, combined with the accuracy rates and examples of visually similar polygons not being identified as a match, suggest that another variable is needed that can be used by Similarity Search to identify matches. This other variable is some aspect of shape. In order for this method to be rigorous, viable, and accurate it needs to include a shape analysis component in addition to basic measurements of size like area and perimeter. Many studies have proposed methods that quantify and capture frontal sinus shape using single metric measurements and pattern coding (max height, max breadth, etc.) (Cameriere, et al. 2005; Kirk, et al. 2002; Yoshino, et al. 1987). However, the purpose of testing and developing this method was to make the tools of ArcMap and other already existing spatial analyst tools (e.g., computer graphics software) work for the observer to create a user-friendly and potentially automated process.

One possibility is to incorporate Zonal Geometry. Zonal Geometry is located within the Spatial Analyst toolbox in ArcMap and is a way to calculate the geometry of a raster dataset. Four types of geometry can be calculated for zones of the raster data: area, perimeter length, thickness (distance from the farthest cell to all other cells), and centroid (an ellipse fixed at the geometric center of the zone) (desktop.arcgis.com 2018a). This tool would not tell the user about the actual shape of the data, but it would provide a standardized way to calculate additional metrics of a frontal sinus polygon that would provide more characteristics than just overall area and perimeter to assess. Zonal Geometry may provide sufficient data for Similarity Search to be

able to more accurately and reliably distinguish between different frontal sinus polygons, particularly those with similar area and perimeter values.

Another possibility is the implementation of shape analysis algorithms that can be coded into ArcMap using Python coding software. Python is already used to code basic functions in ArcMap that would otherwise be tedious and take up time and resources to manually complete. One type of shape analysis algorithm that could be utilized is facial recognition software. Facial recognition algorithms work to mimic the ability humans already possess for recognizing different faces in order to allow computers to have this same ability. It uses landmarks on the face like the nose, eye sockets, and jaw line to establish nodes or points and then measures the distances between the nodes. The software can then compare the measurements to a database to find a match. The addition of a facial recognition algorithm would allow Similarity Search to assess more than just the size of the polygon, but also the shape by automatically identifying landmarks and features of the sinus, such as the number of scalloped edges, and measure the distances between those features. This would allow Similarity Search to assess not only the size of the polygon, but the shape as well, which would increase the accuracy of the tool and make this a more complete and usable method for frontal sinus identification.

Similarity Search: An accurate tool for identifying a frontal sinus match?

Overall Accuracy

The second question in this study addressed the ability of using ArcMap's Similarity Search tool to identify a PM to AM radiographic match from a frontal sinus polygon. The percentage of cases where Similarity Search correctly identified a match using the frontal sinus polygons was 72% for females and 62% for males. For the true match polygons that were not

identified by Similarity Search as the most similar, all were ranked in the top 5 (N = 33) with the 45% ranked second (N = 15). So even when Similarity Search did not correctly identify the match, the true match was still ranked in the top half.

While Similarity Search was able to identify the correct match in the majority of male and female groups, accuracy rates are not much better than chance. Therefore, the ability of using ArcMap's Similarity Search tool to identify a PM to AM radiographic match from a frontal sinus polygon is not supported. However, the 72% and 62% correctly identified males and females, respectively, bolstered by the majority of the incorrect matches ranked second, indicates that additional parameters beyond area and perimeter may strengthen the accuracy, reliability, and forensic utility of this method.

Similarity Search: A new method for frontal sinus positive identification?

The third research question was whether ArcGIS and its spatial analyst tools could be used to create a reproducible method for quantifying and spatially assessing frontal sinus morphology for the purpose of positive identification. Given the results discussed above, the answer is no in its current state. However, this method has the potential to be a quantifiable, viable, and accurate method for quantifying and spatially assessing the frontal sinus, but shape analysis must be incorporated so that Similarity Search can assess each polygon on more than just size. Further, a standardized method for determining the lower boundary of the sinus is needed in order to improve repeatability and reliability because the lower boundary presented the most difficulty for the observers during the digitization process due to overlapping cranial structures that obscure the lower boundary.

Inter-observer and Intra-observer Variation

The Coefficient of Variation (C_v) for each of the donor polygons created by the inter-observer participants demonstrated low variance overall. For the area values, seven out of the 11 donors used for the inter-observer study had a C_v value of 17% or lower and the remaining values were between 24% and 38%. For the perimeter values, 10 out of the 11 donors had a C_v value of 19% or lower. This means that for all of the polygons created for each donor by the observers, the area and perimeter values were clustered together and had low variability between observers. The ANOVA also showed no statistically significant difference between observers for both area and perimeter values, and cluster analysis showed most observers and their polygons clustering together, with only a few observers deviating from the majority. These results support the statistical reliability of the area and perimeter values between observers and the reliability of the method of digitizing the frontal sinus.

Intra-observer analysis showed that the polygons created for each donor clustered together and had low variation between them indicating high reliability and low intra-observer variation. The C_v values of the area and perimeter values for the female donors were all 34% or lower. The average area values for the male donors had lower variation ranging from 0.7% to 22%, but the perimeter values for the male donors had a C_v of 5% or lower. These results indicate that intra-observer variation was low and the area and perimeter values for both males and females clustered together and were not widely dispersed.

Even with low overall variation, there was no C_v value of 0, indicating that in some instances donor polygons did deviate from one another. For example, donor 80a has a C_v of 0.347 for area values. Figure 5.6 shows the polygons I created for 80a and the shape differences that contributed to the variable area and perimeter values. Figure 5.7 shows the polygons I

created for donor 176a, which had a C_v value of 0.218 for area, and Figure 5.8 shows the polygons I created for donor 132a which had a C_v value of 0.053 for perimeter. This variation is to be expected due to human error, but two factors may be contributing, in part, to the overall variation in area and perimeter values: the quality of the radiographs and difficulty visualizing the lower boundary of the frontal sinus. The hard-copy radiograph images were scanned into JPEG image files. The higher the resolution of an image, the clearer and higher quality the image is. The process of scanning hard-copy radiographs files to JPEG could have affected the image quality resulting in a sinus outline more difficult to visualize.

No standardized method for determining the lower boundary of the frontal sinus was employed in this study. Locating and determining the lower boundary of the frontal sinus was a problem that arose during the digitization process and during the inter-observer study. Each participant was instructed to digitize the polygon and use their own judgement to determine the lower boundary of the frontal sinus. Even though inter-observer variation was low, each participant, myself included, had a different idea of what was considered the outline of the lower boundary of the sinus. Figures 5.9 - 5.11 show the polygons created for three of the 10 donors used in the inter-observer study and highlight the variation in the polygons' shape. This is a common problem when assessing the frontal sinus from radiographs due to the 2D nature of radiographs. Christensen (2003) addressed this issue in her dissertation. Christensen acknowledged that while the upper and lateral borders of the frontal sinus are clearly discernable, the lower boundary is often obscured by overlapping structures making it difficult to visualize. The author discussed several different methods that have been proposed by other researchers for delineating the lower boundary, including drawing a line at the planum sphenoidale, drawing a horizontal line at nasion, and drawing a line tangent to the upper margins of the orbits

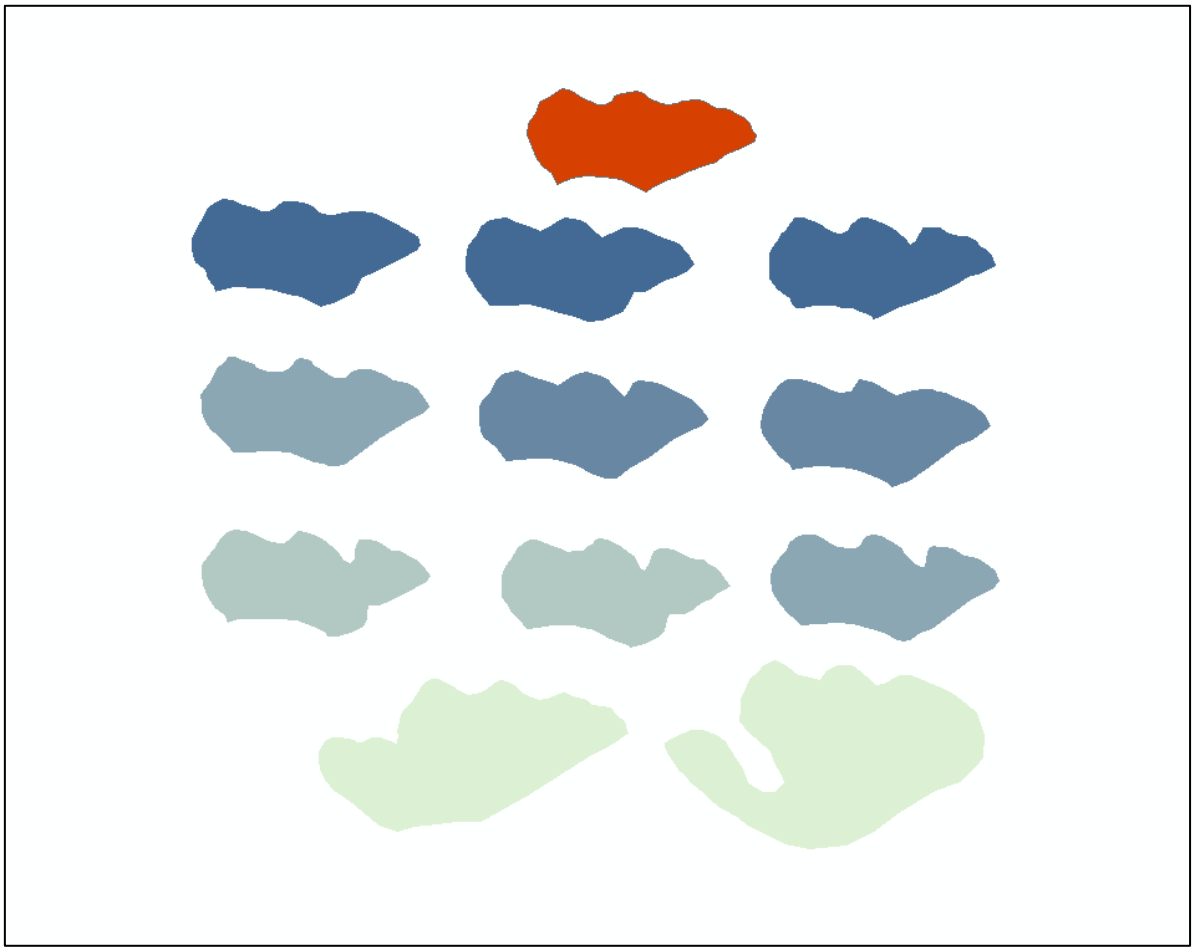

Figure 5.6 *80a frontal sinus polygons*

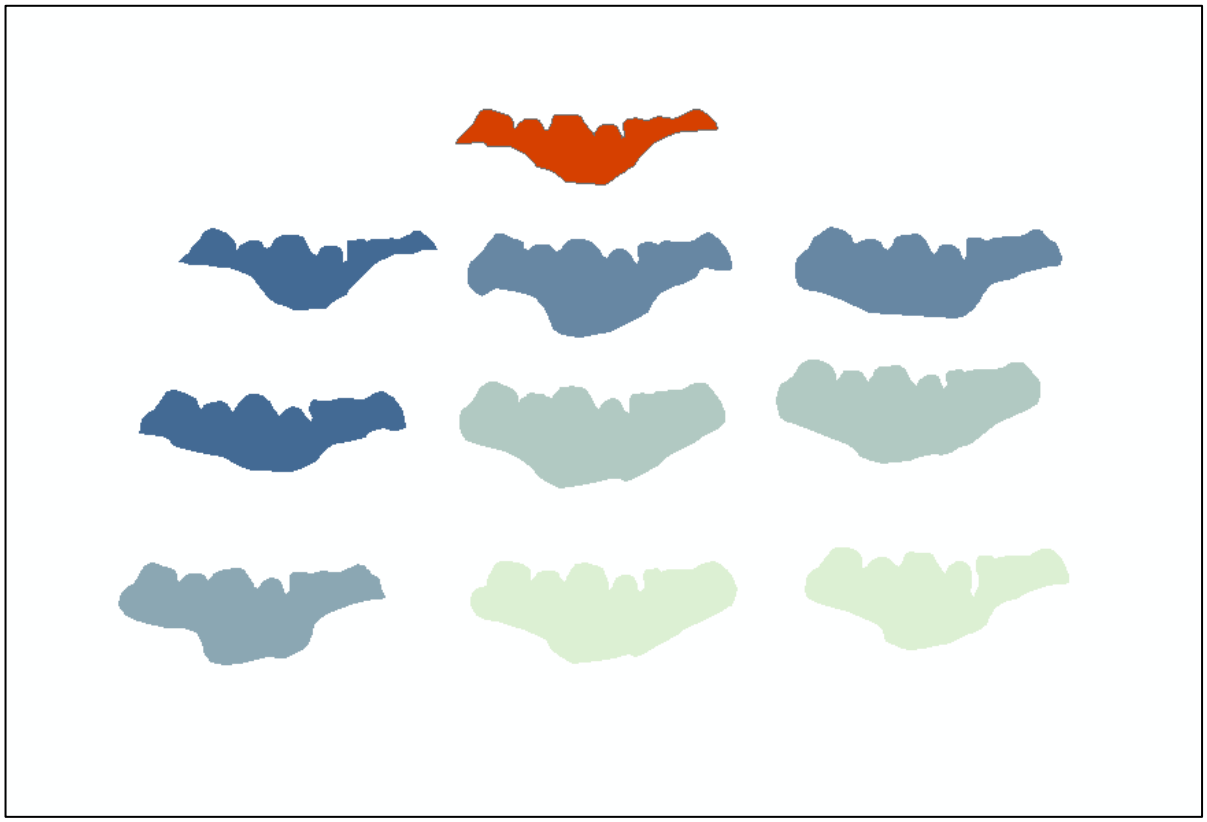

Figure 5.7 *176a frontal sinus polygons*

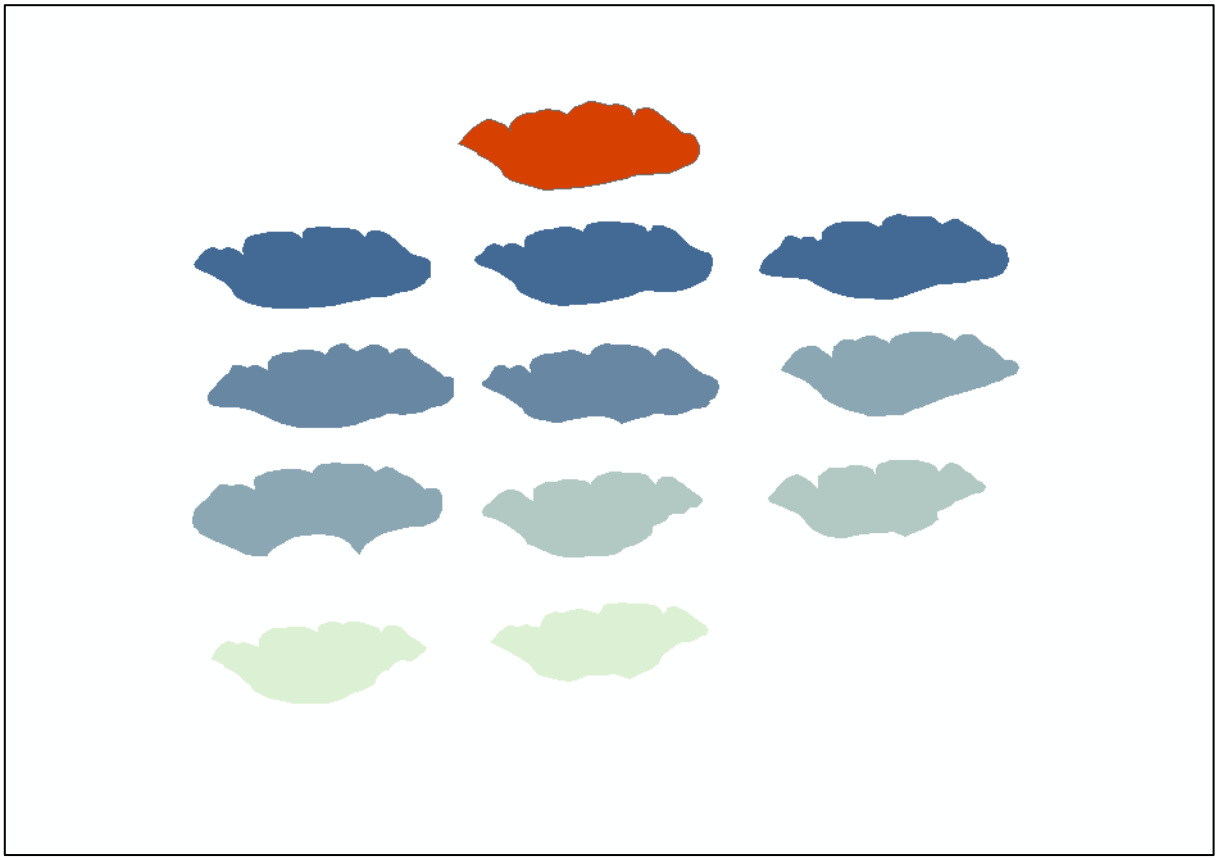

Figure 5.8 *132a frontal sinus polygons*

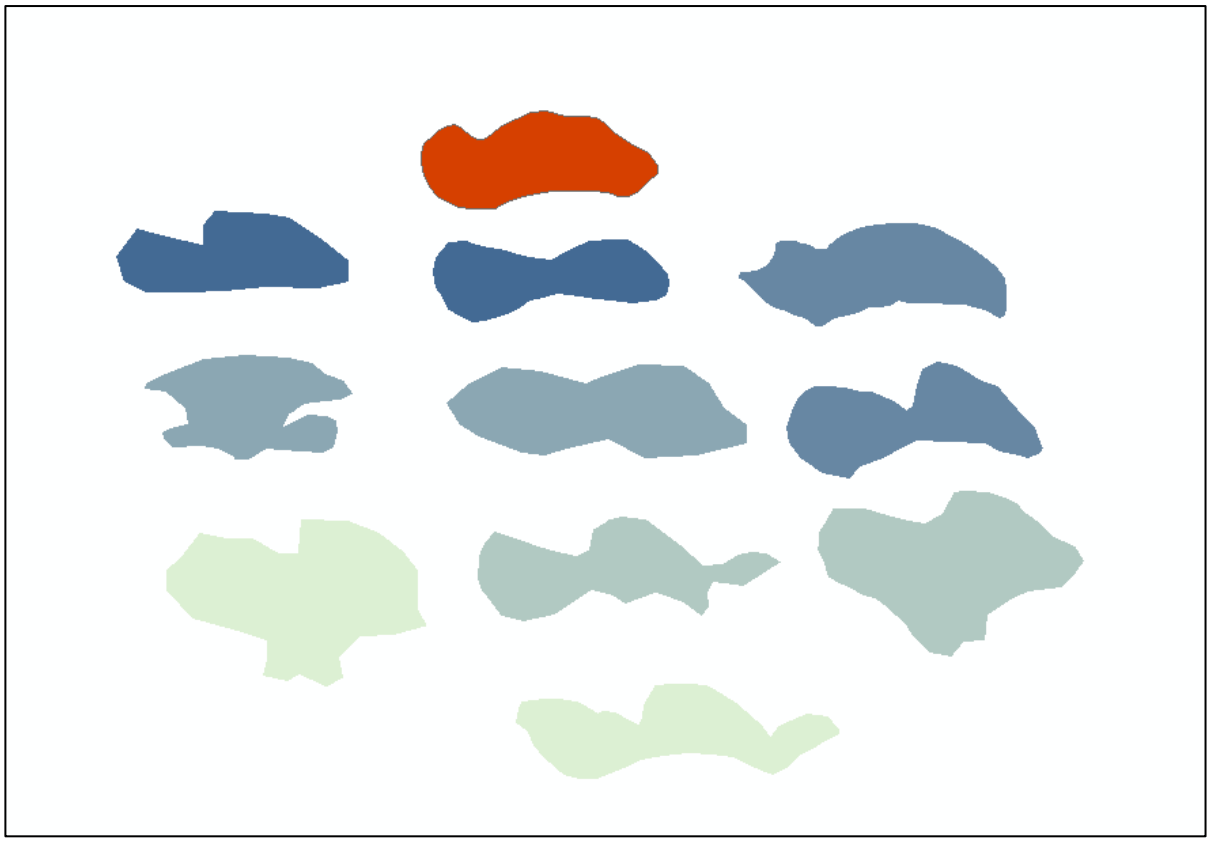

Figure 5.9 *Inter-observer polygons for donor 2a*

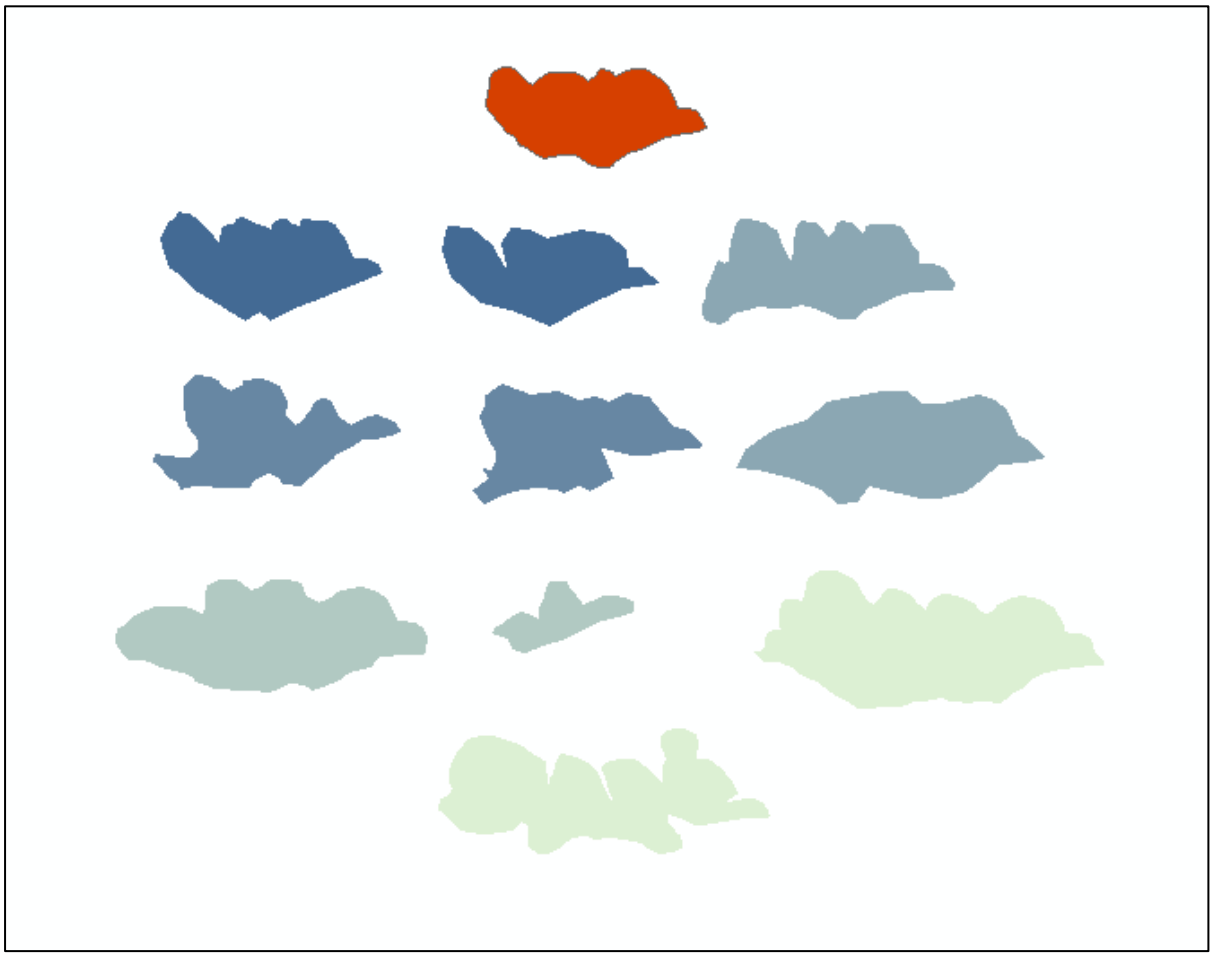

Figure 5.10 *Inter-observer polygons for donor 41a*

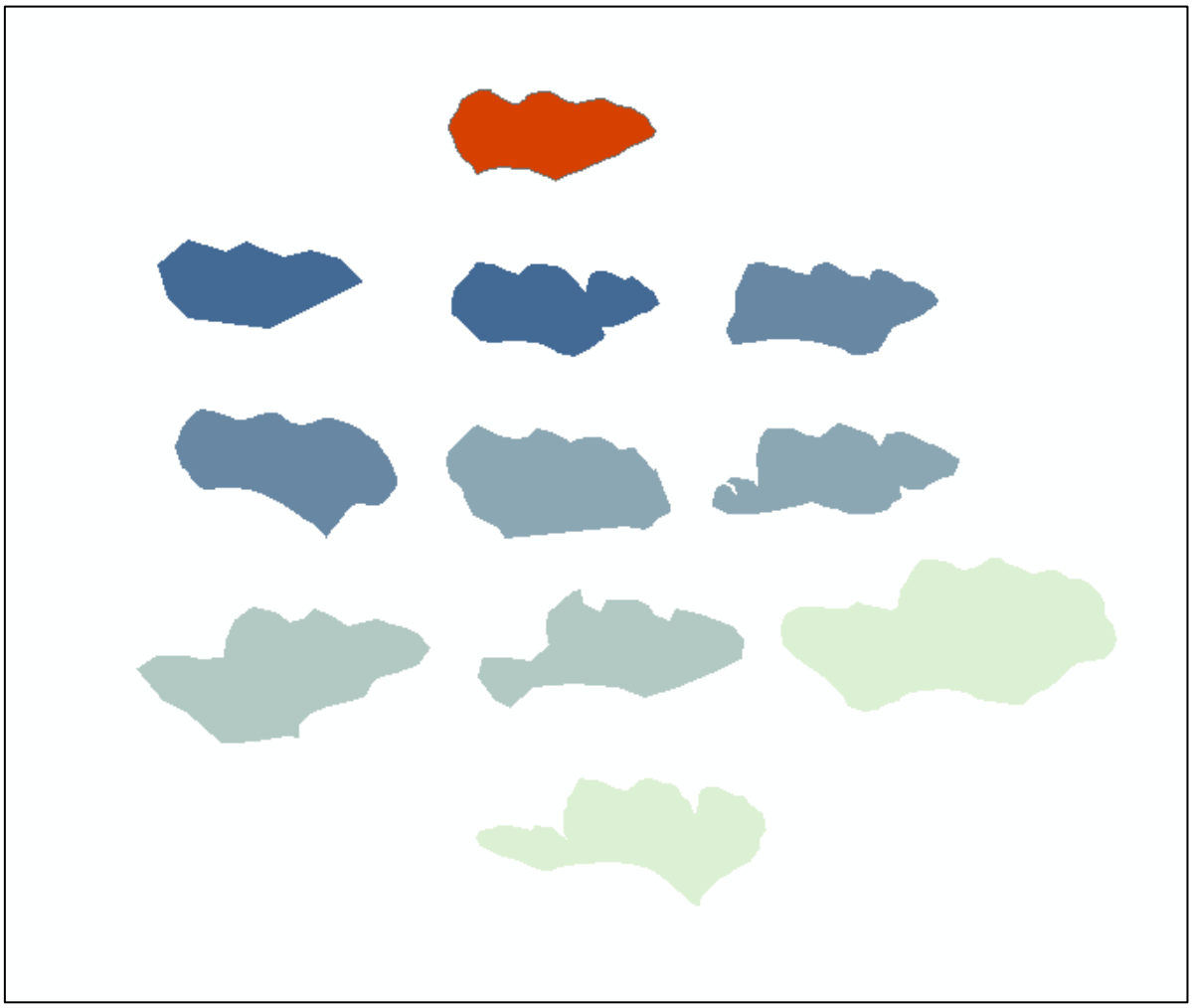

Figure 5.11 *Inter-observer polygons for donor 80a*

(Brothwell, et al. 1968; Christensen 2003; Libersa and Faber 1958; Schuller 1943). Because this study did not use any of these methods, there was a lot of variability within and between observers in how the lower boundary of the frontal sinus was determined, which in turn affected the shape of the polygons, and the area and perimeter values. This lack of standardization for determining the lower boundary contributed to the variation in polygon shape of the 1,320 polygons that I created, which affected the area and perimeter values, and subsequently affected the results of Similarity Search. It is possible that this variability is what contributed to the higher C_v values for both the inter and intra-observer polygons.

In addition to shape analysis, a standard method for determining the lower boundary of the frontal sinus needs to be employed in order to increase the accuracy and reliability of this method. A consistent method for determining the lower boundary will eliminate some of the variation in polygon shape, and variation in the area and perimeter values. Combined with shape analysis, these changes will greatly bolster the accuracy, reliability, and reproducibility of this method.

Similarity Index Value Range

Part of this study included the establishment of a similarity index value range. The purpose of this range would be to provide a reference that similarity index values of presumed matches could be compared to as a means for a practitioner to determine if the polygon Similarity Search identified as the most similar is, in fact, a potential match. The range determined for females was 0.0 – 11.56, and the range for males was 0.0 – 5.51. Both of the similarity index value ranges for all correctly identified females (0.001 – 1.557) and males (0.0 – 0.305) were well within these ranges. Based on these ranges a female index value greater than 11.56 and a male index value greater than 5.51 could not be a match. However, based on the

index ranges of the correctly identified polygons, a more conservative recommendation is that a male index value greater than 0.305 and a female index value greater than 1.557 could not be a match. However, as previously discussed, without a shape analysis component, area and perimeter are not sufficient attributes for Similarity Search to identify frontal sinus matches. Further research and development of this method, particularly the inclusion of shape analysis will greatly improve Similarity Search's ability to quantify frontal sinus morphology and provide a reproducible and accurate method for frontal sinus positive identification.

Additional Limitations

It is also important to address the issue of radiograph orientation. The sample used for this research represents the best-case scenario: cranial radiographs where the cranium was scanned in the same orientation for the AM and PM radiographs and using the same parameters for each scan. In a real forensic case, practitioners try to replicate the orientation of the skull in the AM radiograph when taking the PM radiograph. However, it is never a perfect replication because the AM radiograph would have been taken when the person was alive so flesh is present and the position of the head is a result of a living person positioning themselves for the scan, rather than the manual positioning of the skull, which is no longer attached to a body, obscured by flesh or supported by muscles.

For this study, the PM radiograph images were simulated. The PM radiographs represent true PM radiographs, as they were taken of skeletonized remains. However, the AM radiographs were not true to an AM radiograph. Instead they were simulations, also taken of the skull, but after it was removed from the pedestal and repositioned, to introduce some error and simulate a scan that was taken at a different time (Christensen 2003). This resulted in radiographs that were not exact copies, but still very similar and thus comparable, but not true to a real forensic case. In

a real forensic case, it is expected that there will be more error in terms of the skull being in a slightly different position because the practitioner will be using a true AM radiograph as a comparison and will not be able to replicate the orientation of the true AM radiograph perfectly when positioning the skull for the PM radiograph. For example, if the skull is tilted laterally, the radiograph is taken in an inferior to superior direction rather than a posterior to anterior direction, or if the distance between the machine and the frontal bone is different.

Differences in position can produce differences in the scale and skew of a radiograph that will result in distortions to the image. These distortions can result in frontal sinus polygons from the same individual that may have different area and perimeter values that would affect Similarity Search's ability to identify them as a match. If this method were to be used in a forensic case, it would be important to replicate the AM radiographs as accurately as possible when producing the PM radiograph of the skull. Two ways to ensure the radiographs are comparable and replicated as accurately as possible would be 1) check the dimensions and resolution of the AM radiograph and reproduce those dimensions for the PM radiograph or 2) find out the Standard Operating Procedure (SOP) used to obtain the AM radiograph. If a practitioner has AM cranial radiographs from five individuals who are potential matches, they could contact the hospital and find out more information about the radiograph, such as why it was taken (fractures nose, skull fracture, sinus infection, etc.) and what the SOP is for that specific type of radiograph. The practitioner could use that SOP for the PM radiograph to ensure that the PM radiograph was taken with the same parameters as the AM radiograph. Given that each AM radiograph was taken for a different reason and potentially using a different SOP, it would be necessary for the practitioner to take five sperate PM radiographs each using the SOP used for each of the AM radiographs. Adams and Maves (2002) outline a similar protocol used

for the identification of an individual killed in a helicopter crash in Vietnam. The right clavicle was determined to be the best candidate for comparison. The authors obtained an AM chest radiograph from the potential victim and used the right clavicle for comparison. The authors duplicated the SOP that would have been employed when the AM chest radiograph was taken. They also took multiple radiographs of the clavicle, each at a different rotation, and selected the radiograph that was closest in orientation to the original AM radiograph. The authors were able to establish a positive identification using this method.

Obtaining the SOP used for each AM radiograph that is available for comparison and taking multiple radiographs are steps that can ensure the PM radiograph is as close an approximation to the AM radiograph as possible. These procedures will also reduce the potential for differences in skull orientation that can lead to size and shape discrepancies between the AM and PM radiographs, and should be considered if this method is implemented in forensic casework.

Significance and Future Directions

In its current form, this method is not usable for human identification due to the issues previously discussed in this chapter. However, this thesis is a first step in the identification and implementation of this novel approach. The goal of this thesis was to determine if ArcMap is a tool that can be applied to the frontal sinus and be utilized by biological anthropologists for forensic human identification. This research shows that ArcMap can be used with frontal sinus radiographs, and that the spatial analyst tools already present in the ArcMap program have the ability to be leveraged for frontal sinus identification.

Given the issues with 2D images (different orientations and the inability to fully visualize the sinus), the use of images obtained with Computed Tomography (CT) should be explored.

Problems with different image orientation, opacity, overlapping structures, and unclear boundaries between structures would be overcome with 3D images. Also, problems comparing differently oriented radiographs, or radiographs taken at different distances could be addressed using 3D images. Facial recognition software programs that still use 2D images face similar problems as they require the face to be looking directly into the camera (Bonsor and Johnson 2018). Partial views of faces turned to either side inhibit the software's ability to identify a match. However, new systems utilize 3D images of faces that use distinct features like the curves and planes of noses, chins, and eye sockets which control for differences in orientation and lighting. The use of 3D images for frontal sinus identification would also correct for similar problems posed by 2D radiographs (Bonsor and Johnson 2018).

The use of 3D images would also allow for more robust analysis using spatial analyst tools in ArcMap. Spatial analyst tools are commonly used to analyze 3D geographic data and provide a suite of surface modeling tools that can analyze raster data by looking at contouring, profiling, slope, aspect, and volume calculations that could be applied to CT scans of the frontal sinus to calculate max height, breadth, volume, and assess the topography of the sinus (desktop.arcgis.com 2018c). This would allow for more robust metrics than just area and perimeter to be calculated, particularly volume, and allow for shape analysis that is not possible with 2-deminsional polygons.

While this method is not ready to be applied in its current state, given that further research into shape analysis algorithms and 3D images is needed, this research highlights the potential of ArcMap and Similarity Search to provide a feasible method for positive identification via the frontal sinus that can be used in conjunction with the visual comparison method. This method was not designed as a total replacement of the visual comparison method.

Instead, it may eventually serve to augment the visual comparison method by providing quantifiable results that confirm a visual match. Based on the results of this study, the similarity index values that could suggest a potential match for males and females are ≤ 5.51 and ≤ 11.56, respectively.

Any method that utilizes unique features or biological characteristics should be backed up by quantifiable results. Many of the characteristics used for human identification such as AM fractures, surgical interventions, and pathologies were found to not be as rare as previously thought and thus not reliable for establishing a positive identification, particularly in an open population scenarios such as a mass disaster (Komar and Lathrop 2006). Unlike AM fractures and pathologies, the frontal sinus is a developmental feature whose growth is influenced by genetics and environmental factors and is generally accepted as a unique biological feature. However, it is still important to develop quantifiable methods that are repeatedly tested to ensure rigorous standards are met when using biological features for positive identification. When possible, other methods such as DNA analysis and fingerprints are utilized first, but if these methods are not feasible due to the state of the remains or access to DNA analysis technology, radiographic methods can be utilized. With the addition of shape analysis algorithms and the ability to code functions in ArcMap using Python, or the use of other ArcMap tools such as Zonal Geometry, this method could be developed into a user-friendly, and quantifiable method for conducting frontal sinus matching.

Forensic Identification and Uniqueness of Biological Characteristics

This method and the visual comparison method rely on the widely held assumption amongst forensic practitioners that frontal sinus shape is unique to each individual. This assumption is based on considerable research over the last few decades into the uniqueness of the

frontal sinus (Besana and Rogers 2010; Christensen 2005b; Cox, et al. 2009; Ubelaker 1984). In addition to developmental features like the frontal sinus, skeletal characteristics such as antemortem fractures, diseases, and medical hardware are used to establish identity. However, recent research by Komar and Lathrop (2006) reevaluated the assumption of uniqueness for three morphological features commonly used in victim identification: AM fractures, evidence of surgical interventions, and pathological conditions. The comparison of features using AM and PM radiographs is a common and accepted method for victim identification. The authors used two contemporary skeletal collections housed at the Maxwell Museum of Anthropology at the University of New Mexico and the University of Tennessee Forensic Anthropology Center to determine if these morphological features are rare enough to be considered unique and usable for victim identification. The authors found that morphological features such as AM fractures and pathologies are not as rare as previously thought, and thus may not be unique enough to be used for individual identification.

While Komar and Lathrop (2006) did not specifically look at the frontal sinus, their research suggests that caution is needed when using morphological features for identification and further supports the use of multiple methods to identify human remains. Methods based on morphological features, including the frontal sinus, should be used with caution in isolation or as the first method employed to identify an individual. Other methods such as fingerprints for mummified remains or DNA analysis should be used in conjunction with or as confirmatory to radiographic methods when possible. The findings by Komar and Lathrop (2006) highlight the importance of utilizing multiple methods, the importance of continuing to improve existing methods, and the development of new, quantifiable methods.

CHAPTER 6: CONCLUSION

Comparison of frontal sinus radiographs is an established and widely accepted method for positive identification in forensic anthropology. Like many other methods, it is based on the repeatedly tested notion that certain biological features and characteristics are unique due to either their rarity within the population (fractures, diseases, medical hardware, DNA profile, etc.), or developmental processes that result in a vast amount of variation in their presentation (frontal sinus shape, skeletal morphology, fingerprint pattern) due to genetic and environmental influences.

The concept of "uniqueness" in biological characteristics has been tested and critiqued. Characteristics such as AM fractures, certain surgical procedures, and pathologies are actually more common than previously thought and thus may not be reliable for determining identity (Komar and Lathrop 2006). The uniqueness of developmental biological features, such as the frontal sinus, fingerprints, and the morphology of skeletal elements, has been critiqued, particularly the methodologies that established these features as unique and provided the basis for their use in forensic human identification (National Research Council 2009; Page, et al. 2011). Page, et al. (2011) argue that it is impossible to know with absolute certainty if a feature is unique and probabilities of a trait occurring more than once in the entire human population have been underestimated due to fallacious logic and a misunderstanding of probability statistics. However, the authors also argue that the problem with many forensic human identification methods is not the use of questionably unique features, but rather poor performance by examiners, a lack of standards and rigorous methods, and bias as these factors all contribute to misidentifications and potentially wrongful convictions (Page, et al. 2011). While the method tested in this thesis does rely on the frontal sinus being unique between individuals, more

importantly it is a method that attempts to address the need for more rigorous methods that limit observer bias, provide standards for how to approach frontal sinus identification, and provides a user-friendly method able to quantify frontal sinus morphology rather than rely on a visual pattern match by observers with variable training and experience.

This thesis shows that Similarity Search within ArcGIS has potential as a tool for frontal sinus matching. Currently, results indicate that area and perimeter are not sufficient for Similarity Search to distinguish between individuals who have sinuses that are very close in size, necessitating additional comparative values such as shape to bolster the method. ArcGIS has never been applied to frontal sinus radiographs, so starting with 2D images, and basic metrics (area and perimeter) was necessary in order to determine whether this method was even feasible and thus worth exploring further. The results of this study show that it is not only feasible, but possible. Inter-observer results indicate this method can be very accessible to those without extensive GIS experience, with the potential to provide a quantifiable, automated, and user-friendly method for frontal sinus identification. However, a shape analysis component needs to be included so that Similarity Search can truly differentiate between individuals based on shape and basic size metrics. A fully developed version of this method that incorporates metrics and shape analysis could be used in conjunction with the visual assessment method so that any determination of a frontal sinus match based on visual comparison of radiographs can be supported with the Similarity Search results.

This thesis also adds a relatively new area exploring biological anthropology and GIS, particularly how GIS can be implemented in forensic anthropology casework and methods. As previously discussed, GIS has been widely utilized by archaeologists and is beginning to be used by biological anthropologists to answer questions about human evolution, explore the effects of

diet on tooth morphology, and conduct spatial analysis of biomechanical forces on bone at the microscopic level (Rose, et al. 2012; Ungar and Williamson 2000). These studies, and the study conducted for this thesis, illustrate the potential of GIS to aid anthropological research and allow for analysis of skeletal elements that was not previously possible.

Human identification of skeletal remains will always be determined by a combination of methods dictated by the state of the remains and the elements present. No method, including frontal sinus radiograph comparison, is ever used in isolation, nor is it the first method utilized by forensic practitioners when trying to establish identity. A frontal sinus match is just another data point amongst many other data points that increase the likelihood that a set of remains belong to a specific person. This thesis is only the starting point, but with further testing, development, and creation of a protocol for practitioners to follow this method could be implemented into forensic casework and increase the rigor of frontal sinus radiograph matching, limit bias, and provide a user-friendly and quantitative method for frontal sinus identification.

REFERENCES CITED

2018 Random Number Generator, www.randomnumbergenerator.com.

Adams, Bradley J. and Robert C. Maves
2002 Radiographic identification using the clavicle of an individual missing from the Vietnam conflict. *Journal of forensic sciences* 47(2):369.

Akhlaghi, Mitra, Khadijeh Bakhtavar, Jhale Moarefdoost, Artin Kamali and Shahram Rafeifar
2016 Frontal sinus parameters in computed tomography and sex determination. *Legal Medicine* 19(C):22-27.

Aldenderfer, Mark S. and Herbert D. G. Maschner
1996 *Anthropology, space, and geographic information systems*. New York : Oxford University Press, New York.

Anemone, R. L., G. C. Conroy and C. W. Emerson
2011 GIS and paleoanthropology: Incorporating new approaches from the geospatial sciences in the analysis of primate and human evolution. *American Journal of Physical Anthropology* 146(S53):19-46.

Angyal, M. and K. Dérczy
1998 Personal identification on the basis of antemortem and postmortem radiographs. *Journal of forensic sciences* 43(5):1089.

Beckett, Sophie , Roland Wessling, Jessica I. Bolton and Jelana Bekvalac
2014 Investigation of the Potential for Use of 3D Topographical Data and Geographical Information Systems for Age-at-Death Determination From Pelvic Skeletal Remains. *Proceedings of the American Academy of Forensic Sciences*:437-438. Seattle, WA.

Benito-Calvo, Alfonso and Ignacio De la Torre
2011 Analysis of orientation patterns in Olduvai Bed I assemblages using GIS techniques: Implications for site formation processes.(Report). *Journal of Human Evolution* 61(1):50.

Besana, Joanna L. and Tracy L. Rogers
2010 Personal Identification Using the Frontal Sinus*. *Journal of Forensic Sciences* 55(3):584-589.

Bolton, Jessica I.
2013 The Pubic Symphysis Landscape - Investigating the Feasibility for a Quantitative Method of Age Determination, Using Geographical Information Systems. MSc, Cranfield Defence and Security, Cranfield University.

Bonsor, Kevin and Ryan Johnson
2018 How Facial Recognition Systems Work. HowStuffWorks, http://electronics.howstuffworks.com.

Brothwell, DR, T Molleson and C Metreweli
1968 *The Skeletal biology of earlier human populations*. Radiological aspects of normal variation in earlier skeletons: an exploratory study. Pergamon Press, New York.

Burrough, P. A.
2015 Principles of geographical information systems, edited by R. McDonnell and P. A. Burrough. Third ed. Oxford
New York : Oxford University Press, Oxford
New York.

Cameriere, Roberto, Luigi Ferrante, Dora Mirtella, Franco Ugo Rollo and Mariano Cingolani
2005 Frontal sinuses for identification: quality of classifications, possible error and potential corrections. *Journal of forensic sciences* 50(4):770.

Caplova, Zuzana, Zuzana Obertova, Daniele M. Gibelli, Danilo De Angelis, Debora Mazzarelli, Chiarella Sforza and Cristina Cattaneo
2017 Personal Identification of Deceased Persons: An Overview of the Current Methods Based on Physical Appearance. *Journal of forensic sciences*.

Carlton, Connor D., Samantha Mitchell and Patrick Lewis
2018 Preliminary application of Structure from Motion and GIS to document decomposition and taphonomic processes. *Forensic Science International* 282:41-45.

Choi, Isabela G. G., Eduardo F. Duailibi-Neto, Thiago L. Beaini, Renan L. B. Da Silva and Israel Chilvarquer
2018 The Frontal Sinus Cavity Exhibits Sexual Dimorphism in 3D Cone-beam CT Images and can be Used for Sex Determination. *Journal of forensic sciences* 63(3):692.

Christensen, Angi M.
2003 An empirical examination of frontal sinus outline variability using Elliptic Fourier Analysis : implications for identification, standardization, and legal admissibility, University of Tennessee, Knoxville.

2005a Assessing the variation in individual frontal sinus outlines. *American Journal of Physical Anthropology* 127(3):291-295.

2005b Testing the reliability of frontal sinuses in positive identification, pp. 18-22. vol. 50.

Cossellu, Gianguido, Stefano Luca, Roberto Biagi, Giampietro Farronato, Mariano Cingolani, Luigi Ferrante and Roberto Cameriere
2015 Reliability of frontal sinus by cone beam-computed tomography (CBCT) for individual identification. *La radiologia medica* 120(12):1130-1136.

Cox, Mary, Matthew Malcolm and Scott I. Fairgrieve
2009 A New Digital Method for the Objective Comparison of Frontal Sinuses for Identification*. *Journal of Forensic Sciences* 54(4):761-772.

Culbert, W. L. and F. M. Law
1927 Identification by comparison of roentgenograms: Of nasal accessory sinuses and mastoid processes. *Journal of the American Medical Association* 88(21):1634-1636.

Da Silva, Rhonan Ferreira, Felippe Bevilacqua Prado, Isamara Geandra Cavalcanti Caputo, Karina Lopes Devito, Tessa de Luscena Botelho and Eduardo Daruge Júnior
2009 The forensic importance of frontal sinus radiographs. *Journal of Forensic and Legal Medicine* 16(1):18-23.

Dawsen, Christopher J.
2011 *Geographic information systems*. New York : Nova Science Publishers, New York.

Derrick, Sharon M., Michelle H. Raxter, John A. Hipp, Priya Goel, Elaine F. Chan, Jennifer C. Love, Jason M. Wiersema and N. Shastry Akella
2015 Development of a Computer-Assisted Forensic Radiographic Identification Method Using the Lateral Cervical and Lumbar Spine. *Journal of Forensic Sciences* 60(1):5-12.

desktop.arcgis.com
2018a How Zonal Geometry works. ESRI.

2018b Methods of Creating Data. ESRI, desktop.arcgis.com.

2018c An overview of the Spatial Analyst Toolbox. ESRI, desktop.arcgis.com.

ESRI
2018 ArcGIS Desktop Release 10.5.

Gowland, R. L. and A. G. Western
2012 Morbidity in the marshes: using spatial epidemiology to investigate skeletal evidence for malaria in Anglo-Saxon England (AD 410-1050).(Author abstract)(Report). *American Journal of Physical Anthropology* 147(2):301.

Gundel, Annemarie C.
2017 Geographic Information Systems (GIS) and Predictive Modeling of Body Disposal Sites, Department of Anthropology, The University of Tennessee, Knoxville.

Hamed, Ebrahimnejad, Zarch Seyed Hosein Hoseini and Langaroodi Adineh Javadian
2016 Diagnostic Efficacy of Digital Waters' and Caldwell's Radiographic Views for Evaluation of Sinonasal Area. *Journal of Dentistry of Tehran University of Medical Sciences* 13(5):357-364.

IBM Corp
2017 Released IBM SPSS Statistics for Macintosh. vol. 25.0. IBM Corps, Armonk, NY.

Jablonski, Nina G. and Bobby S. F. Shum
1989 Identification of unknown human remains by comparison of antemortem and postmortem radiographs. *Forensic Science International* 42(3):221-230.

Jernvall, Jukka, Soile Keranen, V. E. and Irma Thesleff
2000 Evolutionary Modification of Development in Mammalian Teeth: Quantifying Gene Expression Patterns and Topography. *Proceedings of the National Academy of Sciences of the United States of America* 97(26):14444-14448.

Kahana, T., L. Goldin and J. Hiss
2002 Personal Identification Based on Radiographic Vertebral Features. *The American Journal of Forensic Medicine and Pathology* 23(1):36-41.

Kahana, T. and J. Hiss
1997 Identification of human remains: forensic radiology. *Journal of Clinical Forensic Medicine* 4(1):7-15.

Kirk, Nigel J., Robert E. Wood and Marc Goldstein
2002 Skeletal identification using the frontal sinus region: A retrospective study of 39 cases. *Journal of Forensic Sciences* 47(2):318-323.

Kolpan, Katharine E. and Michael Warren
2017 Utilizing Geographic Information Systems (GIS) to analyze geographic and demographic patterns related to forensic case recovery locations in Florida. *Forensic Science International* 281:67-74.

Komar, Debra and Sarah Lathrop
2006 Frequencies of Morphological Characteristics in Two Contemporary Forensic Collections: Implications for Identification *. *Journal of Forensic Sciences* 51(5):974-978.

Kuehn, C. M., K. M. Taylor, F. A. Mann, A. J. Wilson and R. C. Harruff
2002 Validation of chest x-ray comparisons for unknown decedent identification, pp. 725-729. vol. 47.

Libersa, C and M Faber
1958 Etude Anatomo-radiologique du Sinus Frontal Chez L'enfant. *Lille Med* 3(453).

Manhein, Mary H., Ginesse A. Listi and Michael Leitner
2006 The Application of Geographic Information Systems and Spatial Analysis to Assess Dumped and Subsequently Scattered Human Remains *. *Journal of Forensic Sciences* 51(3):469-474.

Marlin, D. C., M. A. Clark and S. M. Standish
1991 IDENTIFICATION OF HUMAN REMAINS BY COMPARISON OF FRONTAL-SINUS RADIOGRAPHS - A SERIES OF 4 CASES. *J. Forensic Sci.* 36(6):1765-1772.

Mundorff, Az, G. Vidoli and J. Melinek
2006 Anthropological and radiographic comparison of vertebrae for identification of decomposed human remains. *J. Forensic Sci.* 51(5):1002-1004.

Murphy, W. A. and G. E. Gantner
1982 Radiologic examination of anatomic parts and skeletonized remains. *Journal of Forensic Sciences* 27(1):9-18.

Nambiar, P., M. D. Naidu and K. Subramaniam
1999 Anatomical variability of the frontal sinuses and their application in forensic identification. *Clinical anatomy (New York, N.Y.)* 12(1):16.

National Research Council
2009 *Strengthening forensic science in the United States : a path forward*. Washington, D.C. : National Academies Press, Washington, D.C.

Page, Mark, Jane Taylor and Matt Blenkin
2011 Uniqueness in the forensic identification sciences--fact or fiction? *Forensic science international* 206(1-3):12.

Patil, Neha, Rohini Salvi, Freny R. Karjodkar, Subodh Sontakke and Kaustubh Sansare
2012 Uniqueness of radiographic patterns of the frontal sinus for personal identification. *Imaging Science in Dentistry* 42(4):213-217.

pro.arcgis.com
2018a How Similarity Search works. ESRI.

2018b Similarity Search. ESRI.

Quatrehomme, Gérald, Pierre Fronty, Michel Sapanet, Gilles Grévin, Paul Bailet and Amédée Ollier
1996 Identification by frontal sinus pattern in forensic anthropology. *Forensic Science International* 83(2):147-153.

Rose, David C., Amanda M. Agnew, Timothy P. Gocha, Sam D. Stout and Julie S. Field
2012 The use of geographical information systems software for the spatial analysis of bone microstructure.(Report)(Author abstract). *American Journal of Physical Anthropology* 148(4):648.

Schuller, A.
1943 A note on the identification of skulls by x-ray pictures of the frontal sinuses. *Medical Journal Australia*:554-556.

Spradley, M. Katherine, Michelle D. Hamilton and Alberto Giordano
2012 Spatial patterning of vulture scavenged human remains. *Forensic Science International* 219(1-3):57-63.

Stephan, Carl N., Allysha P. Winburn, Alexander F. Christensen and Andrew J. Tyrrell
2011 Skeletal Identification by Radiographic Comparison: Blind Tests of a Morphoscopic Method Using Antemortem Chest Radiographs*,†,‡. *Journal of Forensic Sciences* 56(2):320-332.

Tatlisumak, Ertugrul, Gulgun Yilmaz Ovali, Asim Aslan, Mahmut Asirdizer, Yildiray Zeyfeoglu and Serdar Tarhan
2007 Identification of unknown bodies by using CT images of frontal sinus. *Forensic Science International* 166(1):42-48.

Ubelaker, Douglas H.
1984 Positive Identification from the Radiographic Comparison of Frontal Sinus Patterns. In *Human identification : case studies in forensic anthropology*, edited by T. A. Rathbun and J. E. Buikstra, pp. 399-411. Springfield, Ill., U.S.A. : Thomas, Springfield, Ill., U.S.A.

Ungar, P. and M. Williamson
2000 Exploring the effects of tooth wear on functional morphology: A preliminary study using dental topographic analysis. *Palaeontologia Electronica* 3(1):XV-XVI.

Valenzuela, Aurora
1997 Radiographic Comparison of the Lumbar Sprine for Positive Identification of Human Remains: A Case Report. *The American Journal of Forensic Medicine and Pathology* 18(2):215-217.

Wilson, Re
2003 Geographic information systems as a tool for forensic science. *Forensic Sci.Int.* 136:11-12.

Yoshino, Mineo, Sachio Miyasaka, Hajime Sato and Sueshige Seta
1987 Classification system of frontal sinus patterns by radiography. Its application to identification of unknown skeletal remains. *Forensic Science International* 34(4):289-299.

APPENDIX

Appendix 1

Test Group Example

PM Radiograph

Donor 1b

AM Radiographs

Donor 2a

Donor 6a

Donor 7a

Donor 11a

Donor 18a

Donor 35a

Donor 41a

Donor 58a

Donor 66a

Donor 80a

Appendix 2

Inter-observer Polygons

Donor 1b

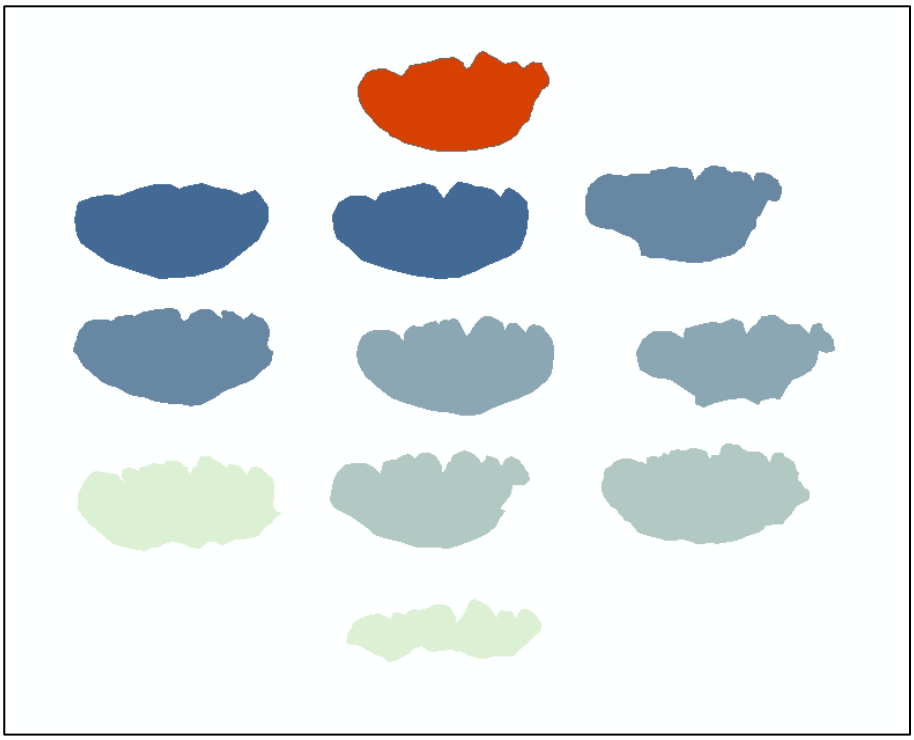

Donor 2a

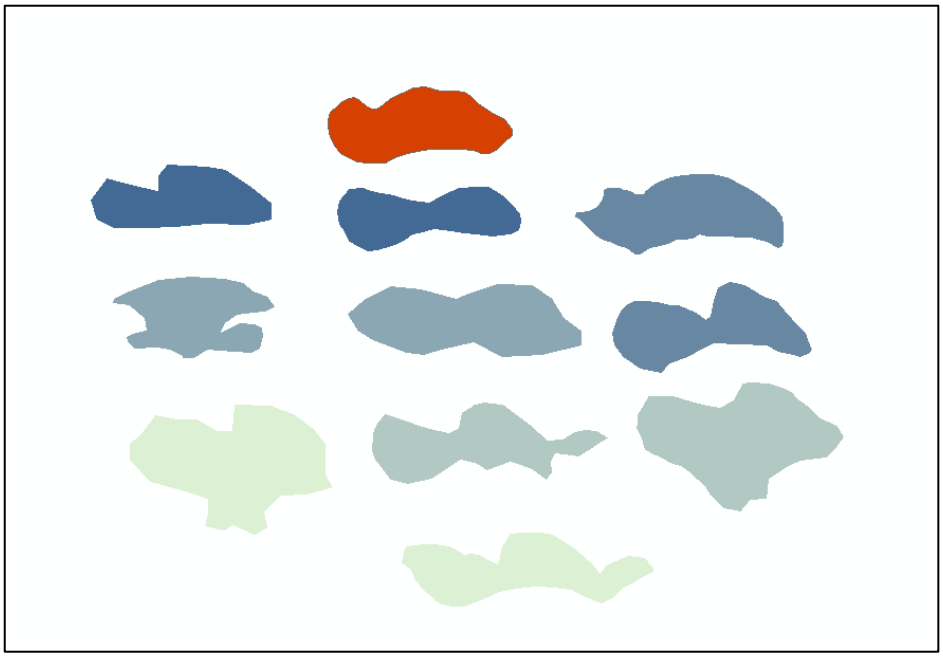

Donor 6a

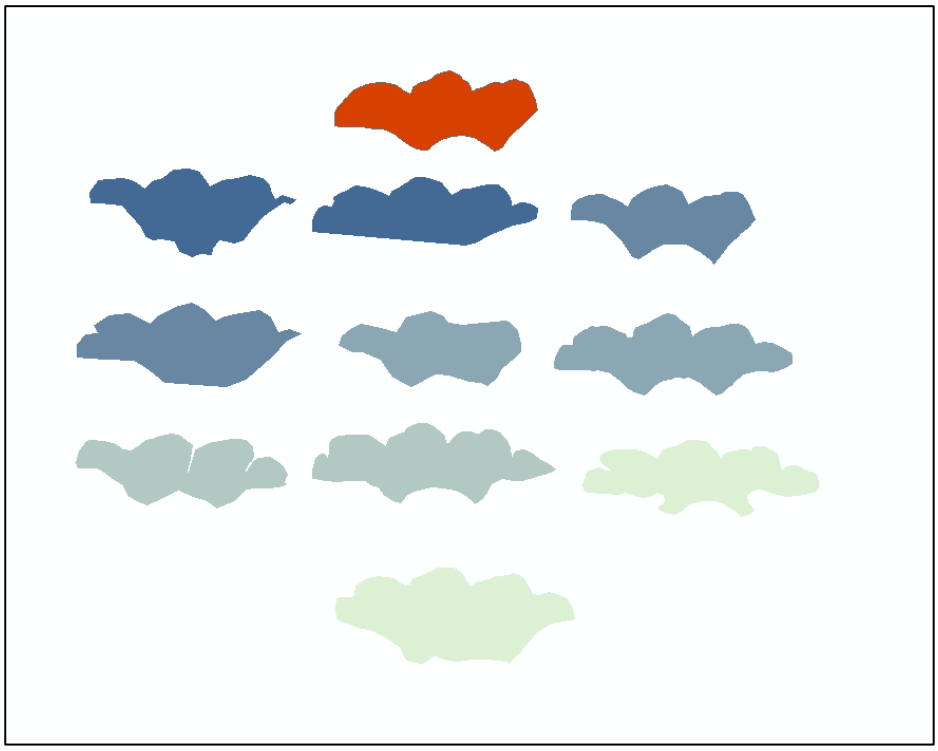

Donor 7a

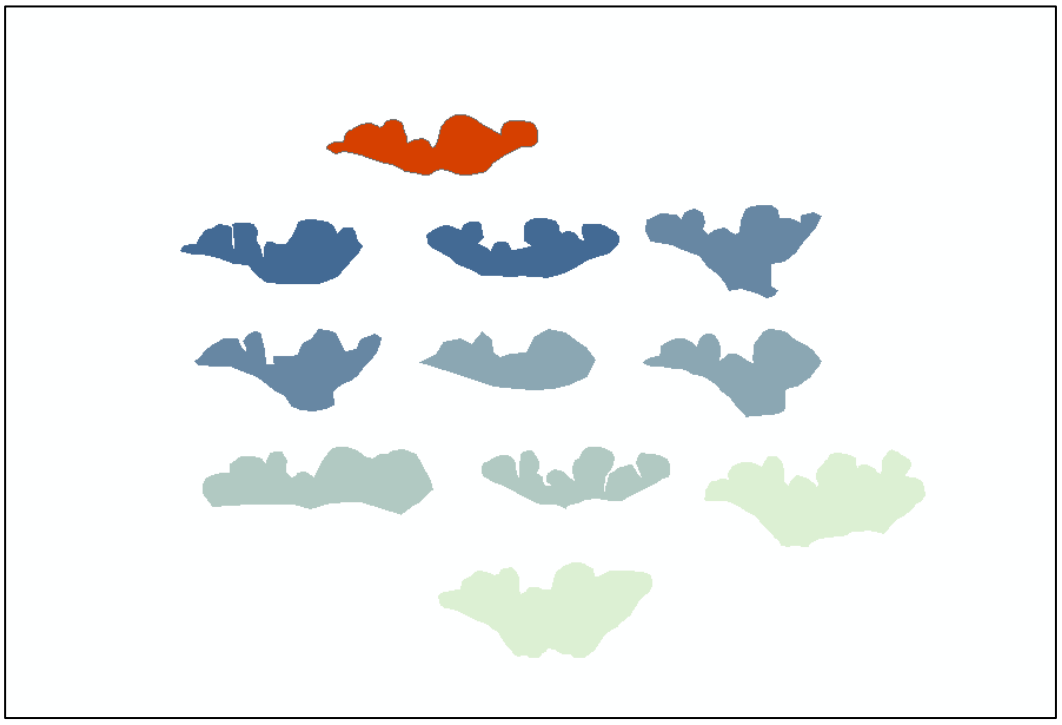

Donor 11a

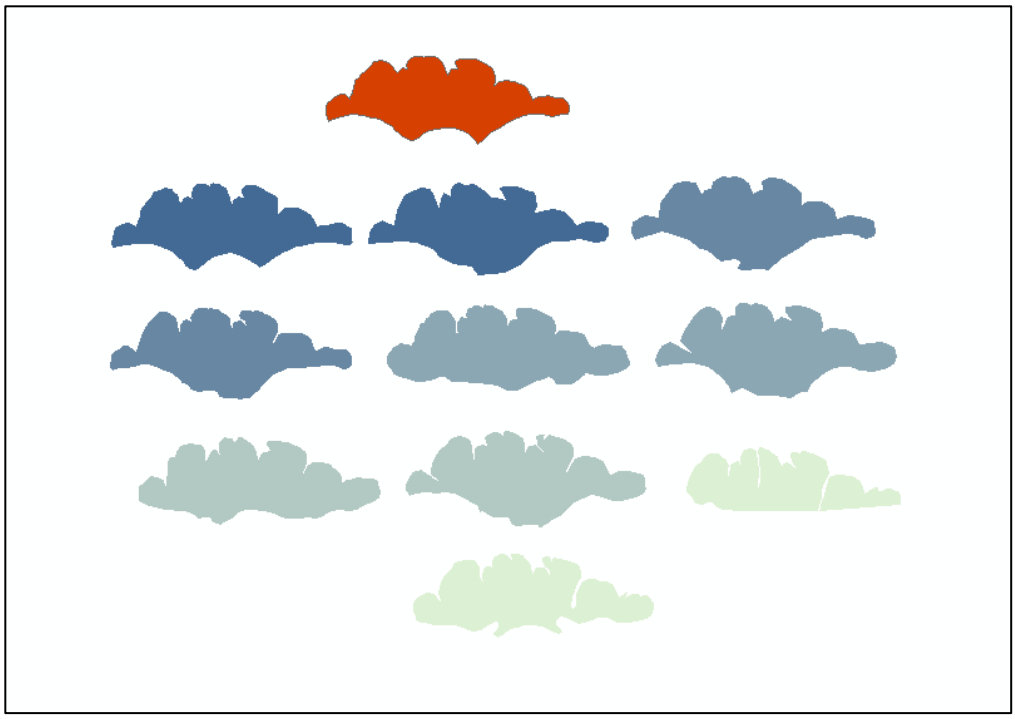

Donor 18a

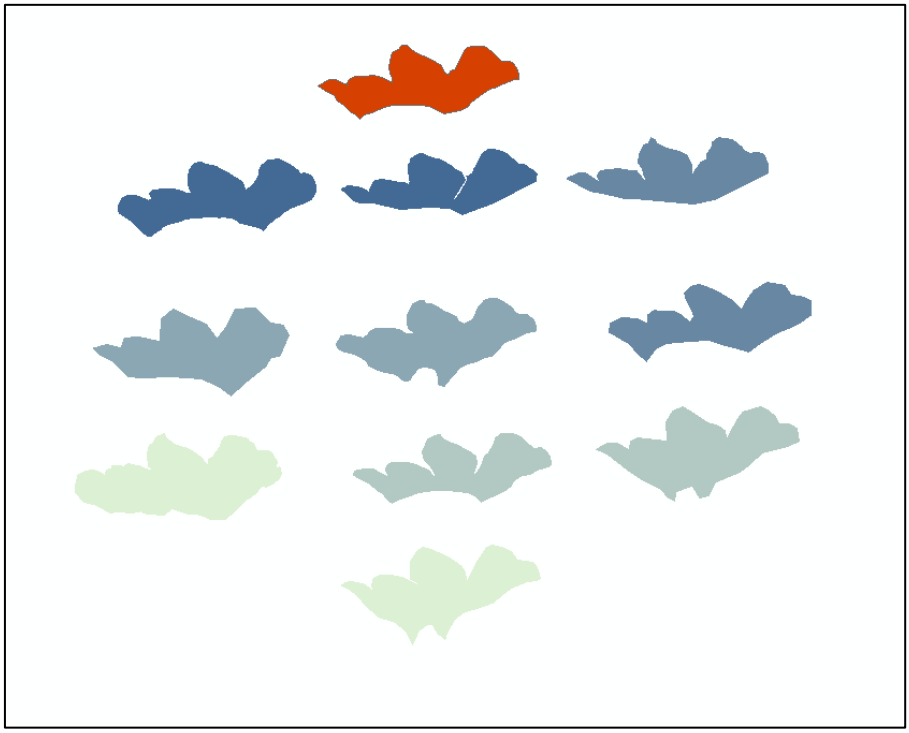

Donor 35a

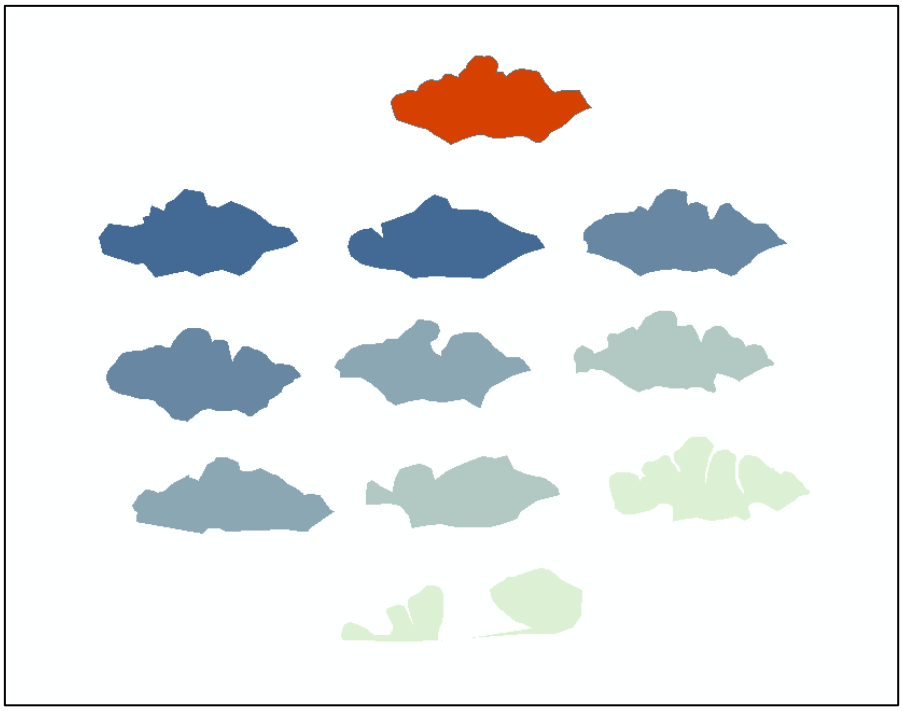

Donor 41a

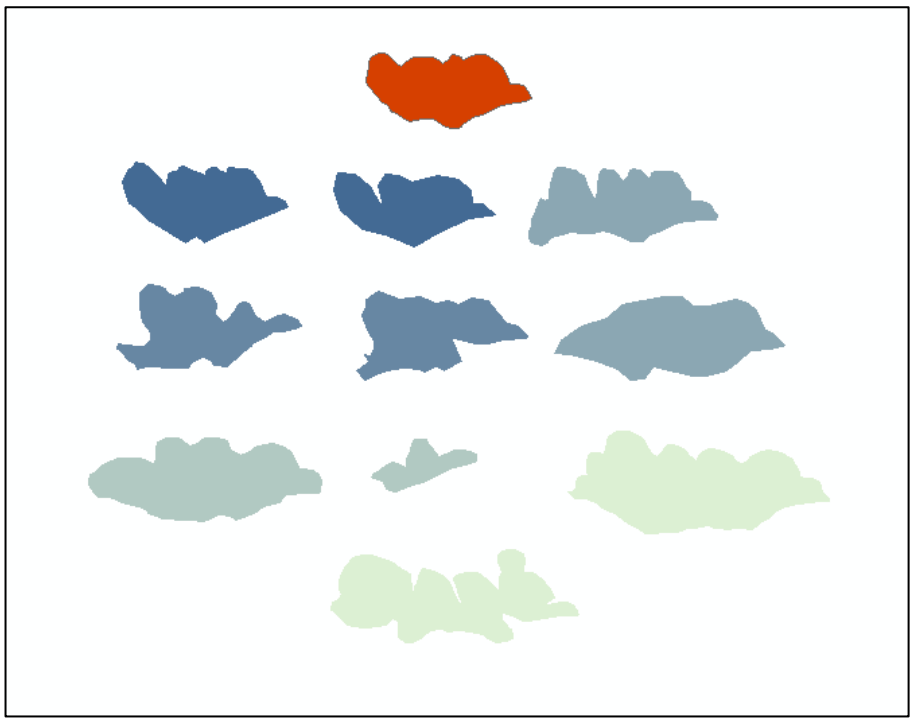

Donor 58a

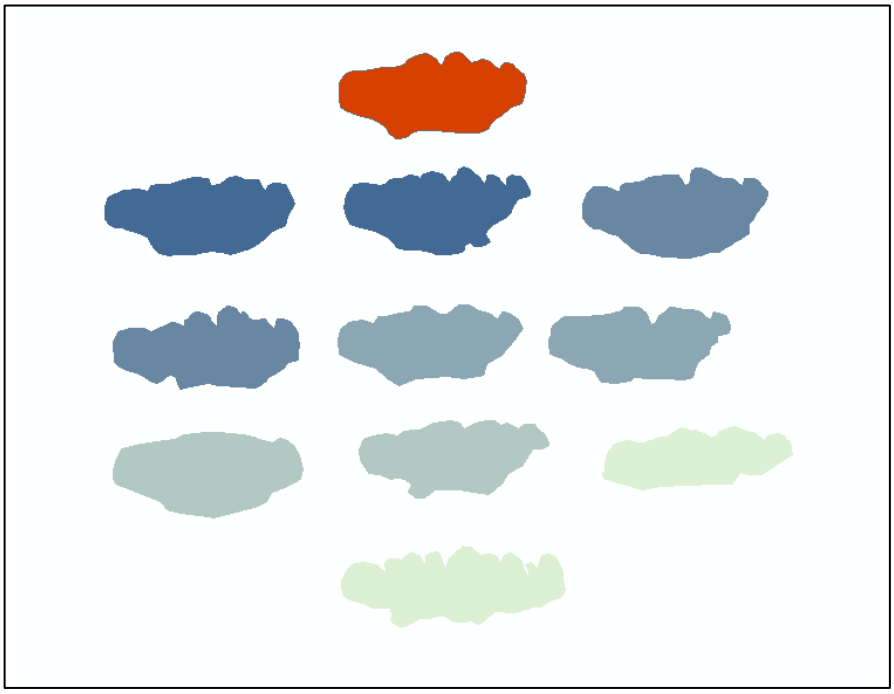

Donor 66a

Donor 80a

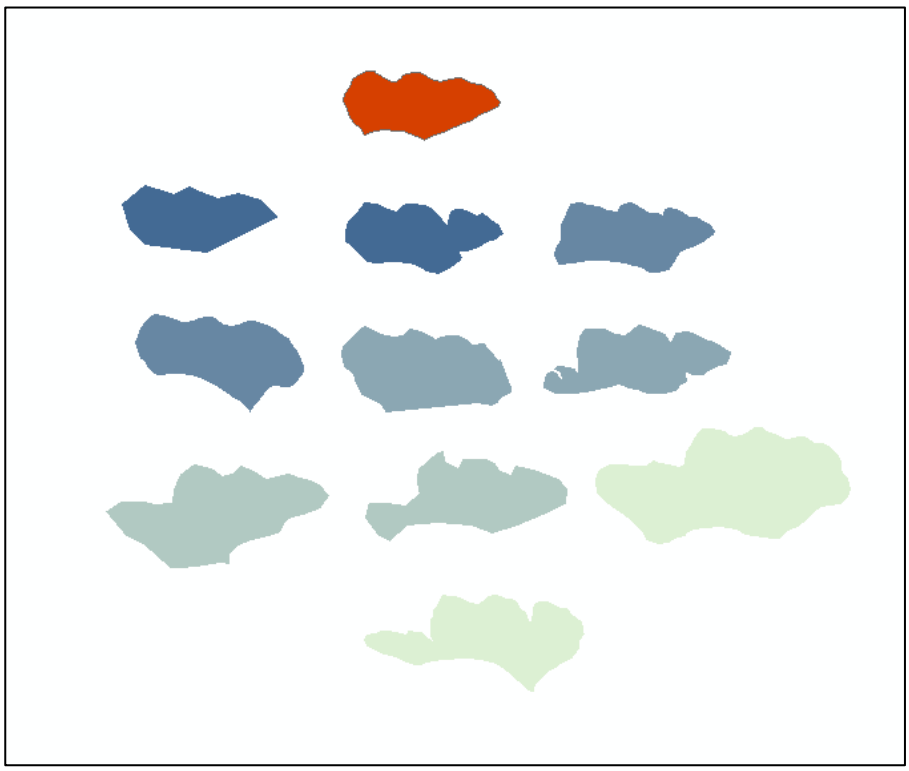

VITA

Jenna Watson was born in Tucson, Arizona and grew up in Vancouver, Washington. She attended Wellesley College in Boston, Massachusetts where she obtained her Bachelor of Arts degree in anthropology in 2013. As an undergraduate, Jenna traveled to Albania and Romania for the Utica College Forensic Anthropology Field School and attended the Public Archaeology Field school at Historic Fort Vancouver National Historic Site in Vancouver, Washington. After graduating, she served as a Corps Member with AmeriCorps National Civilian Community Corps – FEMA Corps where she provided administrative support for FEMA's disaster preparedness, response, and recovery projects. For her service she received the Congressional Award and the President's Volunteer Service Award. After completing her service with AmeriCorps, Jenna accepted a position with Physicians for Human Rights (PHR) in New York City as the Executive Assistant and Office Manager. After two years with PHR, she moved to Knoxville, Tennessee to pursue her Master of Arts degree in biological anthropology at the University of Tennessee with Dr. Amy Mundorff. She accepted a one-year graduate research assistantship with Dr. Mundorff working with plant isotope analysis. The following year she accepted a graduate assistantship position with the Forensic Anthropology Center managing communications and correspondence for the Body Donation Program. Jenna graduated with a Master of Arts in anthropology in August 2018 and continued on to pursue her PhD in anthropology with Dr. Mundorff at the University of Tennessee.